UNIVERSITY MICROFILMS, INC., ANN ARBOR, MICH.

L. C. Card no. Mic 59- 2132

HICKMAN, George Daniel.

DIRECTIONAL CORRELATION OF THE GAMMA RAYS IN Gd^{154} AND W^{182}.

University of Michigan, Ph. D., 1959

Physics, nuclear

Negative microfilm received from university.

DIRECTIONAL CORRELATION OF THE GAMMA RAYS IN Gd^{154} AND W^{182}

George Daniel Hickman

A dissertation submitted in partial fulfillment
of the requirements for the degree of
Doctor of Philosophy in the
University of Michigan
1958

Doctoral Committee:

Professor Marcellus L. Wiedenbeck, Chairman
Assistant Professor Karl T. Hecht
Associate Professor Hazel M. Losh
Associate Professor Robert W. Pidd
Professor George E. Uhlenbeck

Dedicated To

My parents, Mrs. J. R. Hickman, the late Professor Jennings R. Hickman; my wife and daughter, Joanne and Gail Ann.

ACKNOWLEDGEMENTS

The author wishes to express his sincere appreciation to Professor M. L. Wiedenbeck for his friendly guidance and encouragement given throughout the course of this work.

The many helpful discussions with Dr. T. Hecht, Dr. E. Funk, and Mr. R. L. Lide have been invaluable.

Mr. R. G. Arns is acknowledged for the results of the collimated beam experiment.

The author wishes to thank Eastman Kodak Company for the Eastman Kodak Predoctoral Fellowship granted during the year 1957-1958, and to express his appreciation to Professor D. M. Dennison and Professor M. L. Wiedenbeck for making this fellowship available to him.

The College of Engineering Industry Program is acknowledged for the printing of this manuscript.

Sincere appreciation is extended to my wife, Joanne, for her constant encouragement, and for her assistance in the preparation of this manuscript.

The author also wishes to express his appreciation to the Office of Naval Research for the partial support of this work under Contract NONR-1224(13).

TABLE OF CONTENTS

	Page
ACKNOWLEDGEMENTS	iii
LIST OF TABLES	vi
LIST OF FIGURES	viii
BASIC CONCEPTS OF NUCLEAR PHYSICS	1
Angular Momentum, Spin	1
Parity	2
Beta Decay	3
Photon, Gamma Emission	4
Internal Conversion	6
THEORY OF ANGULAR CORRELATION	9
Results from General Theory Applied to γ-γ Directional Correlation	18
γ-γ Directional Correlation for Mixed Multipole Radiation	21
1--3 Directional Correlation	22
Assumptions	25
TECHNIQUES - EQUIPMENT	26
Corrected Counting Rates	28
Accidental Coincidences	29
Correction for Finite Resolution	30
Annihilation Radiation Method	32
Absorption Coefficient Method	32
Collimated Beam Method	32
Resolving Time and Source Strength	33
"Fast - Slow" Coincidence Circuit	33
Detector Assembly	35
Fast Channels	36
Limiting Amplifier	36
Blocking Oscillators and Coincidence Circuits	37
Slow Channels	37
SPHEROIDAL NUCLEI	41
Transition Probabilities	44
Vibration	47
Octupole Vibrations	50
Interactions	55
"Rotation-Vibration" Interaction	55
Rotation - Particle Coupling	56

TABLE OF CONTENTS (CONT'D)

	Page
DIRECTIONAL CORRELATION OF THE GAMMA RAYS IN Gd^{154}	58
Introduction	58
Procedure	58
Results	61
Directional Correlation of 0.123 Mev - 0.248 Mev Gamma Rays	61
Directional Correlation of 0.725 Mev - 0.998 Mev Gamma Rays	63
Directional Correlation of 0.725 Mev - 0.875 Mev Gamma Rays	69
Directional Correlation of 1.277 Mev - 0.123 Mev Gamma Rays	71
Directional Correlation of 0.593 Mev - 1.007 Mev Gamma Rays	76
Discussion	78
DIRECTIONAL CORRELATION OF THE GAMMA RAYS IN W^{182}	87
Introduction	87
Results	92
Directional Correlation of 1.222 Mev - 0.068 Mev Gamma Rays	92
Interference	98
Directional Correlation of 0.152 Mev - 1.222 Mev Gamma Rays	100
Directional Correlation of 0.152 Mev - (1.122 - 1.222) Mev Gamma Rays	102
Directional Correlation of 0.264 Mev - 1.222 Mev Gamma Rays	104
Directional Correlation of 1.231 Mev - 0.222 Mev Gamma Rays	109
Directional Correlation of 1.231 Mev - 0.100 Mev Gamma Rays	109
Directional Correlation of 0.222 Mev - 0.100 Mev Gamma Rays	113
Discussion	114
Considerations of Reduced Transition Probabilities	115
Conclusions	119
BIBLIOGRAPHY	123

LIST OF TABLES

Table		Page
I	Lowest Multipole Order for Given Spin and Parity Change.....	6
II	"Pure" Correlation Functions.....	64
III	Mixture Content of Higher Order Pole Radiation for the 0.725 Mev Gamma Ray for Various Spin Sequences.....	68
IV	Mixture Content of Higher Order Pole Radiation for the 1.277 Mev Gamma Ray for Various Spin Sequences.....	76
V	Comparison of the Intensities of the Transitions from the Third Excited State to the Second and First Excited States, $B(2\rightarrow I_F)$, with the Intensity of the Transition from the Third Excited State to the Ground State, $(B(2\rightarrow 0)$, for Various Values of K_i...	79
VI	Gamma-Ray Abundances, Conversion Coefficients, and Multipolarity Assignments.....	80
VII	Comparison of the Intensity of the Transition from the Fourth Excited State to the Second Excited State, $B(3\rightarrow 4)$, with the Intensity of the Transition from the Fourth Excited State to the First Excited State, $B(3\rightarrow 2)$, for Various Values of K_i...	81
VIII	Comparison of the Intensity of the Radiation from the 1.723 Mev Level to the 0.998 Mev Level with That to the 1.130 Mev Level, Assuming Various Values of K and I for the 1.723 Mev Level. The Transitions were Assumed to be Either Both Dipole or Both Quadrupole Radiation.....	84
IX	Data for Transitions in W^{182}.....	88
X	Directional Correlation Results.....	95
XI	"Pure" Cascades Connecting States F, D, and A - D is Considered as Spin 1.....	97
XII	Values of A_2 and A_4, or the Quadrupole Content of the 0.264 Mev Gamma Ray, Obtained for Various Spin Assignments to State K.....	108

LIST OF TABLES (CONT'D)

Table		Page
XIII	Comparison of the Intensities of Transitions from the Third Excited State to the Second and First Excited States, $[B(2\rightarrow I_f)]$, with the Intensity of the Transition from the Third Excited State to the Ground State, $[B(2\rightarrow 0)]$, for Various Values of K_1 - E2 Radiations Have Been Assumed for All the Transitions.....	115
XIV	Comparison of the Intensity of the Transition from Level G to Level C, $[B(3\rightarrow 4)]$, with the Intensity of the Transition from Level G to Level B, $[B(3\rightarrow 2)]$, for Various Values of K_1. E2 Radiations Have Been Assumed for All the Transitions....	116
XV	Comparison of the Intensity of the Transition from Level G to Level C, $[B(2\rightarrow 4)]$, with the Intensity of the Transition from Level G to Level B, $[B(2\rightarrow 2)]$, for Various Values of K_1. E2 Radiations Have Been Assumed for All the Transitions....	117

LIST OF FIGURES

Figure		Page
1	Schematic Diagram Representing Beta Decay.....	4
2	Schematic Diagram Representing Electron Capture and Positron Emission.....	4
3	Energy Level Diagram Showing the Quantum Numbers Associated with the Initial State, Emitted Radiation, and Final State.....	5
4	Energy Level Diagram of Two Gamma Transitions in Cascade.....	9
5	Energy Level Diagram Showing Splitting of the Levels Into Magnetic Substates.....	11
6	Energy Level Diagram Showing Splitting of the Levels Into Magnetic Substates. The Initial and Final States Have Spin 0, Intermediate State Spin 1.....	11
7	Energy Level Diagram Showing Three Gamma Transitions in Cascade.....	23
8	Detector Arrangement.....	26
9	Finite Solid Angle Subtended by Detectors.....	31
10	Block Diagram of the Fast-Slow Coincidence System.....	34
11	Pulse Shapes at Various Locations in the Fast-Slow Coincidence System.....	38
12	Schematic Diagram of a Spheroidal Nuclear Equilibrium Shape Showing the Quantum Numbers Involved when the Nuclear Motion Can Be Separated Into Rotational and Intrinsic Modes.....	42
13	Energy Level Diagram Showing the Ground State Rotational Band and the Rotational Bands Associated with the First Quadrupole Vibrational Excitation of the Two Modes ($\eta_\beta = 1$ and $\eta_\gamma = 1$); Respectively.....	49
14A	Decay Scheme of Tb^{160}.....	51
14B	Decay Scheme of N_p^{238}.....	52

LIST OF FIGURES (CONT'D)

Figure		Page
15	Schematic Diagram of a Spheroidal Nuclear Equilibrium Shape Showing the Quantum Numbers Involved when the Intrinsic Motion of the Nucleus Can Be Separated Into a Purely Single-Particle Motion and a Rotational-Vibrational Motion.....	54
16	Decay Scheme of Eu^{154}.....	59
17	Scintillation Spectrum of Eu^{154}.....	60
18	0.248 Mev - 0.123 Mev Correlation in Gd^{154}.....	62
19	0.725 Mev - 0.998 Mev Correlation in Gd^{154}.....	65
20	A_2 and A_4 Vs. Q for a 2(D,Q)2(Q)0 Sequence.....	66
21	A_2 and A_4 Vs. Q for a 3(D,Q)2(Q)0 Sequence.....	67
22	0.725 Mev - 0.875 Mev Correlation in Gd^{154}.....	70
23	1.277 Mev - 0.123 Mev Correlation in Gd^{154}.....	72
24	A_2 and A_4 Vs. Q for a 2(D,Q)2(Q)0 Sequence.....	73
25	A_2 and A_4 Vs. Q for a 3(D,Q)2(Q)0 Sequence.....	74
26	A_2 and A_4 Vs. Q for a 4(Q,0)2(Q)0 Sequence.....	75
27	0.592 Mev - 1.007 Mev Correlation in Gd^{154} - Uncorrected for Background.....	77
28	Decay Scheme of Ta^{182}.....	88
29	Comparison of Theoretical (Curves) and Experimental K-Shell Internal Conversion Coefficients for E1, E2,E3,M1,M2 and M3 Transitions in W^{182} (Crosses)....	89
30	Comparison of Theoretical (Curves) and Experimental K-Shell Internal Conversion Coefficients for E1, E2,E3,M1,M2 and M3 Transitions in W^{182} (Crosses)....	90
31	Scintillation Spectrum of Gamma Rays in W^{182}.....	93
32	1.222 Mev - 0.068 Mev Correlation in W^{182}.....	94
33	A_2 and A_4 Vs. Q for a 3(D,Q)2(Q)0 Sequence.....	96
34	0.152 Mev - 1.222 Mev Correlation in W^{182}.....	99

LIST OF FIGURES (CONT'D)

Figure		Page
35	A_2 and A_4 Vs. Q for a 3(D,Q)2(Q)0 Sequence.....	101
36	A_2 and A_4 Vs. Q for a 3(D)2(D,Q)2 Sequence.....	103
37	0.264 Mev - 1.222 Mev Correlation in W^{182}.....	105
38	A_2 and A_4 Vs. Q for a 3(D,Q)2(.99D, .01Q)2(Q)0 Sequence.....	107
39	1.231 Mev - 0.100 Mev Correlation in W^{182}.....	111
40	A_2 and A_4 Vs. Q for a 3(D,Q)2(Q)0 Sequence.....	112

CHAPTER I

BASIC CONCEPTS OF NUCLEAR PHYSICS

Angular Momentum, Spin

Just as the electron possesses an intrinsic angular momentum $1/2\hbar$, it has been found that both the neutron and proton possess an intrinsic angular momentum $1/2\hbar$. If the selection rules which are imposed by quantum mechanics are considered, the results show only two orientations in space which an angular momentum of $1/2\hbar$ can assume. It must either be parallel or anti-parallel to any given direction. Thus, the component of angular momentum along a given direction is either $\pm 1/2\hbar$.

There have been many proofs showing that the nucleus is made up of neutrons and protons, and does not include electrons as had been previously postulated. The nucleus then possesses an angular momentum $\vec{I} = [I(I+1)]^{1/2}\hbar$ which is the combined effect of the intrinsic angular momentum of the nucleus and the orbital motion within the nucleus. The orbital motion within the nucleus must be an integral multiple of $\hbar$. The intrinsic angular momentum of the nucleus can add or subtract $\hbar/2$ depending on its orientation relative to the reference axis. Thus, it is obvious that the total angular momentum of a nucleus is an even multiple of $1/2\hbar$ for nuclei with even number of nucleons (A) and is an odd multiple of $1/2\hbar$ for nuclei with odd A.

In nuclear physics the terminology "spin" is usually reserved for the total angular momentum of the nucleus. This includes the intrinsic angular momentum of the nucleus and the angular momentum of the individual nucleons. This terminology will be used throughout this paper.

Nuclei, like atoms, can exist in excited quantum states. The angular momentum, as well as other properties for nuclei in these excited states, may differ from their ground state values. The contribution of the orbital angular momenta and the relative orientation of the intrinsic spins of the nucleons differ, in general, from state to state in one nucleus. Either effect changes the total angular momentum by an integral multiple of $\hbar$. Thus, the spins of the excited states may differ from the spin of the ground state by integral multiples of $\hbar$.

Nuclear angular momentum vectors, like atomic angular momentum vectors, exhibit "space quantization." Any angular momentum I can be orientated in space with respect to a given axis in only (2I+1) directions. The component of the angular momentum along the axis of reference in any of these states has the magnitude $m\hbar$, where the integer or half-integer m, called the magnetic quantum number, is any member of the sequence -I, -I+1,..., I. These 2I+1 orientations are degenerate in the absence of a magnetic field.

Parity

Another quantum number which is needed in any discussion of nuclear physics is parity. Parity is a property possessed by wave functions; it has no classical analog. This discussion will be restricted to problems in which the potential energy function V(x,y,z) remains unchanged if the signs of all the space coordinates are changed. For such problems it can be shown that the wave functions have the property that such a transformation can either (1) leave ψ unchanged, or (2) change ψ to its negative. In case (1), where

$$\psi(x, y, z) = +\psi(-x, -y, -z) \qquad 1.1$$

ψ is said to have "even" parity. In case (2), where

$$\psi(x,y,z) = -\psi(-x,-y,-z) \qquad 1.2$$

ψ is said to have "odd" parity.

For example, in the case of the photon, the parity of the radiation field is $(-1)^L$ for 2^L electric multipoles, and $(-1)^{L+1}$ for magnetic 2^L multipoles.

Beta Decay

In beta decay, the excited nucleus ejects either a negative particle (electron), a positron, or captures an orbital electron (electron capture). However, it was stated previously that the nucleus is composed of only neutrons and protons. How then does one reconcile beta decay? A solution to this apparent conflict is to imagine that the electrons are created at the time of emission, just as photons from excited atoms. Beta decay corresponds to the following processes within the nucleus.

$$\begin{aligned} n &\longrightarrow p + e^- + \nu \qquad (a) \\ p &\longrightarrow n + e^+ + \nu \qquad (b) \\ p + e^- &\longrightarrow n + \nu \qquad (c) \end{aligned} \qquad 1.3$$

ν = neutrino.

The neutrino, which must be added to Equations (1.3), was initially hypothesized in order that beta decay conform to several conservation laws. Very recently the definite existence of the neutrino has been verified[1]. Upon the emission of a negative particle from an excited nucleus, the element is changed to the next higher element in the periodic table, Equation (1.3a). However, in the case of the other

two processes, there is the decay of a proton changing the element to the next lower one in the periodic table. These can be represented schematically by the following.

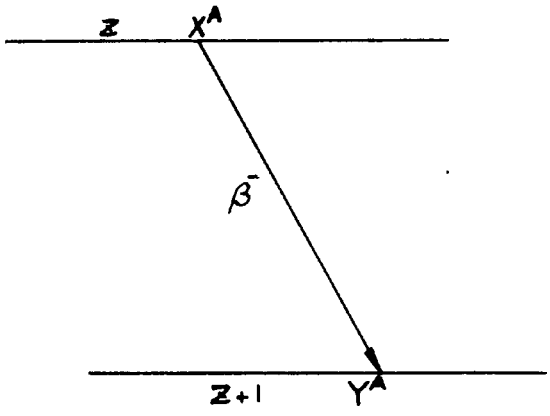


Figure 1. Schematic Diagram Representing Beta Decay.

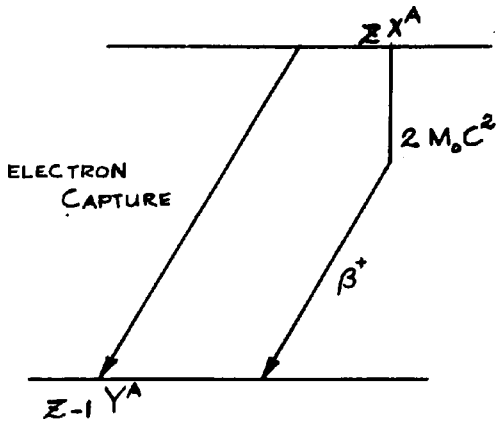


Figure 2. Schematic Diagram Representing Electron Capture and Position Emission.

Photon, Gamma Emission

In many cases after one of the beta decay processes has taken place, the resulting nucleus is left in an excited state. The nucleus can then emit photons (gamma rays), or the excited nucleus may interact directly with an orbital electron, transferring its excitation energy to it (internal conversion). In gamma emission, the initial and final states differ in energy by $E_f - E_i$, and therefore conservation of energy restricts the emission of photons to ones whose energy $\hbar\omega$ is given by this difference. Since the spin of the photon is 1, in units of $\hbar$, the multipolarity of the emitted radiation has to be integral values of $\hbar$. Conservation of charge requires that the final state must have the same charge as the initial state, since none is carried away by the photons. These rules could also be called selection rules. Selection rules are restrictions placed on the matrix elements relating the

states involved such that they are non-zero. The matrix elements are made up of the quantum numbers of the initial and final states, and the interaction energy causing the transition. Besides the energy and charge conservation, there are other selection rules relating other properties of the nucleus.

The parity selection rules governing electric and magnetic radiation have already been given. The selection rules on rotational quantum numbers are most easily stated as a conservation law for angular momentum in terms of the vector model for the addition of angular momenta. If the total angular momentum and Z-component for the initial state, emitted radiation, and final state, are represented by I, m; L, M_L; and I', m', the conservation laws take the form

$$\vec{I} + \vec{L} = \vec{I}' \qquad \text{(a)}$$
$$m + M_L = m' \qquad \text{(b)} \qquad (1.4)$$

This is shown in Figure 3.

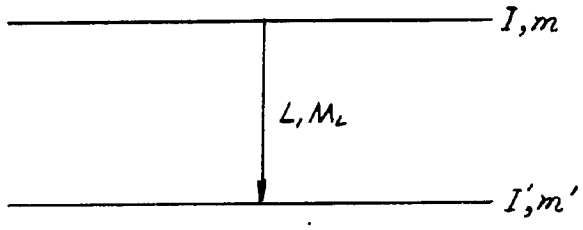


Figure 3. Energy Level Diagram Showing the Quantum Numbers Associated with the Initial State, Emitted Radiation, and Final State.

The permissible types of radiation are given by the selection rule

$$|I - I'| \leqq L \leqq |I + I'| \qquad (1.5)$$

When these selection rules are met, the matrix element connecting the initial and final states will be non-zero. When the matrix elements

are evaluated in terms of these rules the following table for determining the type of radiation emitted can be given.

TABLE I

LOWEST MULTIPOLE ORDER FOR GIVEN SPIN AND PARITY CHANGE

Parity Change	$\Delta I=0,1$	$\Delta I=2$	$\Delta I=3$	
No	M1	E2	M3	Preferred*
	E2	M3	E4	
Yes	E1	M2	E3	Preferred*
	M2	E3	M4	

* Preferred means that the transition probability is greater.

Internal Conversion

As was stated previously, a nucleus in an excited state can perform a transition to a lower state not only by emitting a quantum but also by internal conversion. In this case, the energy of the ejected electron is equal to the energy lost by the nucleus less the binding energy of the electron in the atom. This can be expressed simply as

$$E_{\gamma} = E_e + E_B \tag{1.6}$$

where

E_e = energy of the ejected electron

E_B = binding energy of the electron

The total transition probability from a nuclear state a to a nuclear state b is the sum of two terms $T(a,b)$ and $T^{(i)}(a,b)$

$$\overline{T}(a,b) = T(a,b) + T^{(i)}(a,b) \tag{1.7}$$

where

$T(a,b)$ = transition probability due to photon emission

$T^{(i)}(a,b)$ = transition probability of internal conversion

The internal conversion coefficient α is defined by

$$T^{(i)}(a,b) \equiv \alpha T(a,b) \tag{1.8}$$

Equation (1.7) becomes

$$\overline{T}(a,b) = (1+\alpha)\, T(a,b) \tag{1.9}$$

α is equal to the ratio of number of electrons that come from an atom to the number of accompanying nuclear photons. If a particular shell χ of the atom is considered, α_χ is defined as

$$\alpha_\chi = \frac{N_\chi}{N_\gamma} \tag{1.10}$$

In some cases, especially for higher multipole radiation, the conversion coefficients may be so large that it is difficult to observe any γ radiation. In such cases, the relative conversion coefficients for different shells or subshells furnish information on the multipolarities of the transitions. Thus, one refers to the K/L ratio which is defined as

$$\frac{K}{L} = \frac{N_e(K)}{N_e(L)} \tag{1.11}$$

where

$$N_e(L) = N_e(L_I) + N_e(L_{II}) + N_e(L_{III}) \tag{1.12}$$

N_e denotes the number of electrons from a particular shell.

Designating the conversion coefficients by $\alpha(K)$, etc., this is obtained from theory as

$$\frac{K}{L} = \frac{\alpha(K)}{\alpha(L_I)+\alpha(L_{II})+\alpha(L_{III})} \tag{1.13}$$

In actual experiments, one attempts to make a comparison between theoretical and experimental K/L, L_I/L_I, etc., ratios in order to determine the type of radiation involved. The particular ratio of greatest interest to the investigator depends on the resolution of the measurement and therefore, to some extent on Z. These conversion ratios also depend on the value of L and the parity of the transition.

Angular correlation is another important tool of nuclear spectroscopy. It is this topic which will be the subject of the remainder of this dissertation.

CHAPTER II

THEORY OF ANGULAR CORRELATION

Angular correlation is a comparitively young field. The first theoretical work was carried out by Hamilton in 1940[2]. In the next few years that followed there were no successful attempts at the verification of this theory. Brady and Deutsch[3] performed the first successful experiments using Geiger counters in 1947. In 1948, a great advancement was made when Brady, Deutsch and Metzger[4-7] introduced scintillation counter techniques into the field of angular correlation. A great number of correlations which have been carried out would have been virtually impossible using Geiger counters.

As will be seen later, the correlation function $W(\theta)$ depends on the angular momentum quantum numbers of the nuclear states, Figure 4, and the angular momenta L_1 and L_2 of the successive radiations.

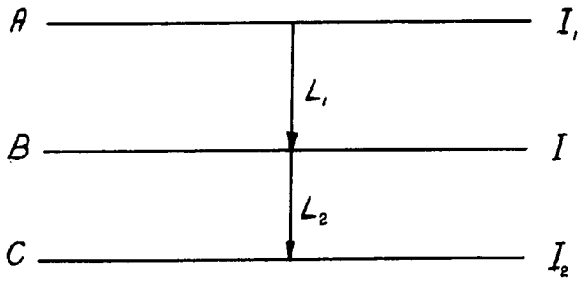


Figure 4. Energy Level Diagram of Two Gamma Transitions in Cascade.

It is therefore, just these quantities which angular correlation measurements help to determine. In γ-γ directional correlation measurements, which are the only type considered in this paper, the parity of the radiation and that of the nuclear states is indeterminable. Other measurements such as conversion coefficients,.

lifetimes of excited states, shapes of beta spectra, etc., must be relied upon to help make unique assignments. In cases where the gamma transitions are not of pure multipole character, angular correlation measurements can be used to determine mixing ratios.

The probability of emission of a particle or quantum by a radioactive nucleus depends, in general, on the angle between the nuclear spin axis and the direction of emission. Under ordinary circumstances, however, the total radiation from a radioactive sample is isotropic because the nuclei are randomly oriented in space. An anisotropic radiation pattern can be observed only from an ensemble of nuclei which are not randomly oriented. If the case of a cascade of gamma rays, see Figure 4, is considered, and only one transition is observed, either the first or the second, then the angular distribution of the emitted radiation is isotropic. No direction in space has been singled out and there is no reason to expect an anisotropic distribution. If, however, a system can be devised whereby a certain direction in space can be singled out, then one might expect to observe an angular distribution, characteristic of the type of radiation emitted.

The general problem which is to be investigated is the following: a nucleus with spin I_a emits a γ-ray with multipolarity L_1 and magnetic quantum number M_1 and decays to a state with spin I_b, whereupon a γ-ray of multipolarity L_2 and magnetic quantum number M_2 is emitted with the nucleus going to a state I_c, see Figure 5.

From the conservation of angular momentum we have Equations(1.4). The splitting of each level into the magnetic substates can be represented in Figure 5.

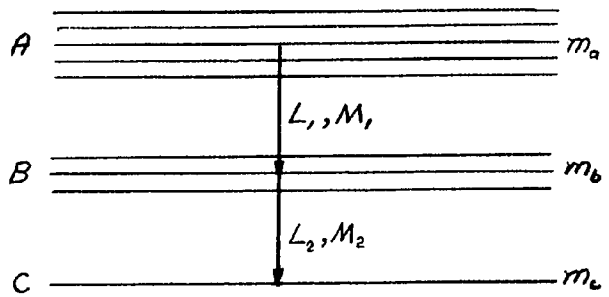


Figure 5. Energy Level Diagram Showing Splitting of the Levels Into Magnetic Substates.

Each component $m_b \rightarrow m_c$ between specified magnetic sub-levels possesses a characteristic distribution $F_L^M(\theta)$ which is independent of I_B and I_C. θ represents the angle between the γ-ray and the Z-axis. For gamma rays, the function $F_L^M(\theta)$ is just the energy flow (Poynting vector) as a function of θ for multipole radiation with quantum numbers L and M.

The following will be given as an example of angular correlation. The initial state will be given the spin value of 0, the intermediate state 1, and the final state 0, see Figure 6. States A and C have even parity, while state B is considered to have odd parity. From the selection rules, Chapter 1, Table 1, one would expect electric dipole radiation for both γ_1 and γ_2

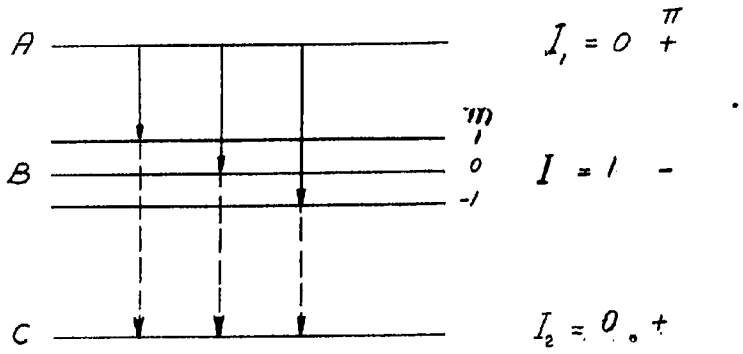


Figure 6. Energy Level Diagram Showing Splitting of the Levels Into Magnetic Substates. The Initial and Final States Have Spin 0, Intermediate State Spin 1.

As is seen from the above figure there are three transitions equally possible, $\Delta M = +1, 0, -1$ in the transition A $\rightarrow$ B. The figure shows the transition $\Delta M = 0$ must be followed by the transition $\Delta M = 0$ in B $\rightarrow$ C; $\Delta M = \pm 1$ is followed by $\Delta M = \mp 1$.

The directional distribution in each of these transitions is given by $F_L^M(\theta)$. For electric dipole transitions (L=1, change of parity)[8,9].

$$F_1^0(\theta)\,d\Omega = C\,(1-\cos^2\theta)\,d\Omega$$
$$F_1^{\pm 1}(\theta)\,d\Omega = \frac{C}{2}\,(1+\cos^2\theta)\,d\Omega \qquad (2.1)$$

where

C = constant independent of the angles.

The sum over the above equations gives a constant, and therefore, the first quantum of energy is isotropically distributed.

The choice of the Z-direction is quite arbitrary. It determines a polar coordinate system, and it also defines the substates $m = 1, 0, -1$ of state B. Without any loss of generality the Z-direction may be chosen parallel to the direction of the first quantum. Then the first transition cannot lead to state B with magnetic quantum number $m = 0$ since a dipole emission with $\Delta M = 0$ does not give rise to any radiation in the Z-direction. The first transition A $\rightarrow$ B is therefore of the type $\Delta M = \pm 1$. The second transition B $\rightarrow$ C must then be of the type $\Delta M = \mp 1$ respectively. Either of these gives rise to the second directional distribution in Equations (2.1). Hence, the direction of the second quantum is not arbitrary, but is

distributed according to

$$W(\theta_{1,2})\,d\Omega = \frac{3}{16\pi}(1+\cos^2\theta_{1,2})\,d\Omega \qquad (2.2)$$

Here $W(\theta_{1,2})\,d\Omega$ is the probability that the direction of the second quantum lies within the solid angle element $d\Omega$ at an angle $\theta_{1,2}$ with respect to the first quantum (Z-axis). It is seen, therefore, that the probability is twice as great that the two photons be emitted in the same (or opposite) direction than that they be emitted at right angles to each other. A directional correlation measurement performed upon this cascade would yield a correlation curve that would increase by a factor of 2 from 90° to 180°.

The splitting of excited states in a magnetic field can be observed in atomic spectroscopy (Zeeman effect). The directional distribution associated with the various m substates of various states can be observed as the longitudinal and transverse effects. In nuclear spectroscopy the Zeeman effect is unobservable, because the splitting of the nuclear energy levels even in very strong magnetic fields is of the order of 10^{-8} ev. In nuclear physics, it is thus impossible to separate the components, and the unresolved transition is always observed.

To calculate $F_L(\theta)$ [10], the directional distribution, the function $F_L^M(\theta)$, the relative population $P(m_b)$ for each sublevel m_b, and the relative transition probability $G(m_b m_c)$ for each component $m_b \rightarrow m_c$ must be known.

Then

$$F_L(\theta) \longrightarrow \sum_{m_b, m_c} P(m_b)\, G(m_b m_c)\, F_L^M(\theta) \qquad (2.3)$$

The case of radiation from a dipole oriented along the Z-axis will be considered. The matrix element for this case is

$$Z_{cb} = \int \psi_c^* Z \psi_b \, d\tau \qquad (2.4)$$

Let the wave functions ψ be assumed

$$\psi = R(r)\, Y_I^M(\theta, \phi)$$

where

$$Y_I^M(\theta, \phi)$$

denotes a normalized spherical harmonic.

Since $Z = r\cos\theta$,

$$Z_{cb} = \left[\int_0^\infty R_c(r) r^3 R_b(r)\, dr\right]\left[\int Y_{I_c}^{*m_c} Y_{I_b}^{m_b} \cos\theta \, d\Omega\right] \qquad (2.5)$$

If the substitution

$$r\cos\theta = r\left(\frac{4\pi}{3}\right)^{1/2} Y_1^{*0} \qquad \text{is made,} \qquad (2.6)$$

Z_{cb} then becomes

$$Z_{cb} = (\text{const. x radial integral}) \int Y_{I_c}^{*m_c} Y_1^{*0} Y_{I_b}^{m_b} \, d\Omega \qquad (2.7)$$

Since Y_1^{*0}, $Y_{I_b}^{m_b}$, and $Y_{I_c}^{m_c}$ are eigenfunctions of the operators I^2 and I_z, and $I_b = I_c + L$ (where $L = 1$), the product $Y_{I_c}^{*m_c} Y_1^{*0}$ can be expanded in terms of $Y_{I_b'}^{*m_b'}$ using the theorems of vector addition.

Thus,

$$Y_{I_c}^{*m_c} Y_1^{*0} = \sum_{I_b' m_b'} Y_{I_b'}^{m_b'} \langle I_c L m_c M | I_b' m_b' \rangle \qquad (2.8)$$

where $\langle I_c L m_c M | I_b' m_b' \rangle$ is the Clebsch-Gordan coefficient. When Equation (2.8) is inserted into Equation (2.7), the following expression is obtained

$$Z_{cb} = A \int \sum_{I_b' m_b'} Y_{I_b'}^{m_b'} Y_{I_b}^{m_b} \langle I_c L m_c M | I_b' m_b' \rangle d\tau \qquad (2.9)$$

Because of the orthogonality of spherical harmonics, all integrals vanish except that with $I_b = I_b'$ and $m_b = m_b'$

For the special case which has been chosen, $L = 1$ $m = 0$, Equation (2.9) reduces to

$$Z_{cb} \sim \langle I_c 1 m_c 0 | I_b m_b \rangle \qquad (2.10)$$

The relative transition probability is proportional to the square of Z_{cb}, and therefore proportional to the square of the Clebsch-Gordan coefficient.

The above calculations were based on the assumption of single particle wave functions and for electric dipole radiation only. It can be shown that the results are independent of the first assumption, and can be generalized for higher multipole radiation.

The relative transition probability can therefore be defined as

$$G(m_b m_c) = \langle I_c\, L\, m_c\, M | I_b\, m_b \rangle^2 \qquad (2.11)$$

Equations (2.10) and (2.3) are the expressions by which $F_L(\theta)$ can be calculated, once the relative population of state m_β is known $P(m_\beta)$. If the Z-axis is made identical to the direction of γ_1, $F_{L_2}(\theta)$ becomes identical with $W(\theta)$, the directional correlation of γ_1 with respect to γ_2.

$P(m_\beta)$ is the sum of all the allowed transition probabilities originating from state m_a and ending in state m_b. Assuming all m_a states equally populated, $M_1 = m_a - m_b$

$$P(m_b) \sim \sum_{m_a} G(m_a m_b) F_{L_1}^{M_1}(\theta=0) \qquad (2.12)$$

When the Z-direction is chosen as the direction of the first gamma ray, definite restrictions are seen to exist. The result is that M_1 can only be ± 1. With this simplification, only $F_{L_1}^{+1}(\theta)$ and $F_{L_1}^{-1}(\theta)$ appear in Equation (2.12). When Equation (2.3) is written for the second transition B $\rightarrow$ C, the result is

$$F_{L_2}(\theta) \sim \sum_{m_b, m_c} P(m_b) G(m_b m_c) F_L^{M_2}(\theta) \qquad (2.13)$$

Equations (2.12) and (2.11) yield the following expressions for the first transition.

$$P(m_b) \sim \sum_{m_a}{}' G(m_a m_b) F_{L_1}^{\pm 1}(\theta=0) \tag{2.14}$$

$$G(m_a m_b) = \langle I_b L_1 m_b \pm 1 | I_a m_b \rangle^2 \tag{2.15}$$

Equation (2.13) then becomes

(2.16)

$$F_{L_2}(\theta) = W(\theta) \sim \sum \langle I_b L_1 m_b \pm 1 | I_a m_a \rangle^2 F_{L_1}^{\pm 1}(0) \langle I_c L_2 m_c M_2 | I_b m_b \rangle^2 F_{L_2}^{M_2}(\theta)$$

Each substate (magnetic sublevel of an isolated nucleus) emits anisotropically but on summing over these substates with equal populations and random (relative) phases, so that the sum is incoherent, the total intensity is independent of angle. However, in the case of the angular correlation process, the angular distribution of one of radiation is observed when it is known that the other has a fixed direction. This prescription of a fixed direction singles out a direction in space. The observation of the gamma ray in this case acts as a kind of a projection operator in giving different weights to the various substates[11]. In other words, it gives information about the substates of the nuclear level formed after the emission of the radiation. In particular, it asserts that these sublevels are not uniformly

populated. Consequently, the radiation subsequently emitted will not be isotropic. This is, therefore, the principle of angular correlation.

Hamilton, as the pioneer in the field of angular correlation, was the first to derive Equation (2.3). For many years investigators used his results which are fairly simple for pure dipole and quadrupole radiation. However, for cases of higher pole and/or mixed radiation, Hamilton's method becomes extremely cumbersome.

In the further developments of angular correlation theory, not only was this difficulty overcome[15-26], but the theory was generalized and extended to radiation other than gamma rays[11-14] and to cases where the nucleus is disturbed in the intermediate state[10,15,27-31]. The progress in the theory of angular correlation after Hamilton's work was due to the use of three tools: group theory, Racah algebra, and density matrices. This is not an elementary formalism and will not be presented here.

Results from General Theory Applied to γ-γ Directional Correlation[10]

Pure Multipole Radiation

The cascade given in Figure 4 will be considered to represent a cascade A $\rightarrow$ B $\rightarrow$ C in which both γ rays of multipole order L_1 and L_2, respectively, are pure. Such a cascade will be denoted by $I_1(L_1)I\ (L_2)I_2$. This notation will be used throughout the remainder of this paper.

The directional correlation function between γ_1 and γ_2 can be expressed as

$$W(\theta) = 1 + A_2 P_2(\cos\theta) + \cdots A_{k_{max}} P_{k_{max}}(\cos\theta) \quad (2.17)$$

The highest term in the expansion is determined by

$$k_{max} = \min(2I, 2L_1, 2L_2) \quad (2.18)$$

A_k can be broken up into two factors, each factor depending on only one transition of the cascade

$$A_k = F_k(L_1 I I) F_k(L_2 I_2 I) \quad (2.19)$$

The F_k's can then be expressed in terms of Racah coefficients and radiation parameters. When use is made of the fact that the detectors to be used are polarization independent, and also that the only allowed values of M are ± 1, the coefficient F_k is then, apart from a normalization factor, given by

$$F_k(L I I') \sim (-1)^{L-1}(2L+1)\langle LL1-1|k0\rangle W(I'I k L; L I') \quad (2.20)$$

where $W(I'I k L; L I')$ are the Racah coefficients.

The Clebsch-Gordan[32] and Racah W coefficients[33] are tabulated for many cases, and hence the coefficients F_k can be obtained. The F_k coefficients have been tabulated by Biedenharn and Rose[34] for many cases. To form the directional correlation for a

γ-γ cascade the appropriate F_k's are located from the table and A_k computed. $W(\theta)$ is then found from Equation (2.17).

Rather recently, tables on the F coefficients have been published by Ferentz and Rosenzweig[35]. These tables are particularly useful when mixtures are of concern. Experimentally, the coefficients A_k are determined by assuming an appropriate value for k_{max} (usually not greater than 4) and then making a least squares fit of Equation (2.17) to the values of $W_{exp}(\theta)$ measured at several angles. All the experimental points in this investigation were taken from 90°→180°→270° in intervals of 15°. The anisotropy is, therefore, also determined. This quantity is defined as

$$A \equiv \frac{W(180°) - W(90°)}{W(90°)} \tag{2.21}$$

The evaluation of Equation (2.21) for a maximum coefficient of A_4 in the expansion of $W(\theta)$ yields

$$A = \frac{1 + A_2 + A_4}{1 - (1/2)A_2 + (3/8)A_4} - 1 \tag{2.22}$$

A very useful fact when making calculations is that the correlation function for the two cascades $I_1(L_1)I(L_2)I_2$ and $I_2(L_2)I(L_1)I_1$ are identical.

The directional correlation function $W(\theta)$ being independent of the parities of the transition is not surprising when it is noted that classically electric and magnetic radiation of order L are related by the transformations E→H, and H→-E. Since these transformations leave the Poynting vector unaltered, the angular distribution of the radiation is unchanged.

γ-γ Directional Correlation for Mixed Multipole Radiation

In many instances, one finds that the radiation emitted is not of pure multipole order L, but rather must be described by more than one value L of angular momentum. Ling and Falkoff[17] were the first to treat mixtures theoretically, but since then the theory has been extended by others. For mixture in any one transition, a mixing ratio can be defined as

$$\delta^2 = \frac{I(L')}{I(L)} \tag{2.23}$$

where $I(L')$ and $I(L)$ refer to the intensities of the $2^{L'}$ and 2^{L} radiations respectively (usually $L'=L+1$).

Denote I_1, I, I_2 as the initial, intermediate, and final momenta of a cascade in the gamma decay of a nucleus. Let the transition between I_1, and I be a mixture of 2^{L_1} and 2^{L_1+1} poles. Similarly describe the second transition as a mixture of 2^{L_2} and 2^{L_2+1} poles. The theoretical directional correlation function has been expressed by Coester[36] in the form

$$W(\theta) = \sum_{\substack{k=0 \\ \text{even}}}^{k_{max}} A_k^{(1)} A_k^{(2)} P_k(\cos\theta) \tag{2.24}$$

$A_k^{(1)}$ is dependent only on the spins and multipolarities involved in the first transition. $A_k^{(2)}$ is dependent only on the spins and multipolarities involved in the second transition. $A_k^{(\nu)}$ can be written as

$$A_k^{(\nu)} = F_k(L_\nu L_\nu I_\nu I) + 2\delta_\nu F_k(L_\nu L_\nu+1\ I_\nu I) + \delta_\nu^2 F_k(L_\nu+1\ L_\nu+1\ I_\nu I) \tag{2.25}$$

The summation over k in Equation (2.24) runs from zero to the least of $2I$, $2(L_1+1)$ or $2(L_2+1)$. The $F_k(LL'I'I)$ are the F-coefficients as defined and tabulated by Ferentz and Rosenzweig[35].

However, instead of plotting δ, the mixing parameter, as a function of the coefficients, a much more convenient form is obtained if the substitution

$$Q_\nu = \frac{\delta_\nu^2}{1+\delta_\nu^2} \tag{2.26}$$

is made. In this form, Q_ν represents the amount of quadrupole radiation present. $1-Q_\nu$ then represents the amount of dipole radiation.

When Equation (2.25) is substituted in Equation (2.24), can be written in the following form.

$$A_k = A_k^{(1)} A_k^{(2)} = [F_k(L_1,L_1,I_1,I)(1-Q_1) + 2F_k(L_1,L_1+1,I_1,I)\sqrt{Q_1(1-Q_1)} + F_k(L_1+1,L_1+1,I_1,I)Q_1][F_k(L_2,L_2,I_2,I)(1-Q_2) + 2F_k(L_2,L_2+1,I_2,I)\sqrt{Q_2(1-Q_2)} + F_k(L_2+1,L_2+1,I_2,I)Q_2] \tag{2.27}$$

1--3 Directional Correlation

In many decay schemes it is possible to measure a correlation function of two gamma transitions which are only in coincidence through a third (unobserved) transition. This is shown in Figure 7.

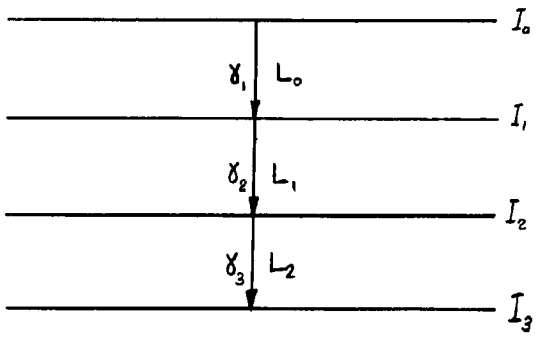


Figure 7. Energy Level Diagram Showing Three Gamma Transitions in Cascade.

Such a measurement is called a 1-3 correlation. The theory of angular correlation has been extended to the 1-3 correlation $W(\gamma_1 \gamma_3)$ by Biedenharn, Arfken and Rose[37,38], and later generalized by Satchler[39] to be valid for arbitrary particles from an arbitrary cascade.

For the case in which all transitions are "pure," the 1-3 gamma-gamma directional correlation function is given by

$$W(\theta) = (-1)^{L_1 - I_1 - I_2} \left[(2I_1+1)(2I_2+1)\right]^{1/2} \sum_k F_k(L_0 L_0 I_0 I_1) \times F_k(L_2 L_2 I_3 I_2) \times W(I_1 I_1 I_2 I_2; k L_1) \times P_k(\cos\theta) \quad (2.28)$$

where k_{max} is 2 min (L_0, L_2, I_1, I_2)

For the case of a mixture in the first transition δ_1, the correlation function can be written

$$W(\theta) = W(L_0) + \delta_0^2 W(L_0') + 2\delta_0 W(L_0 L_0') \tag{2.29}$$

Expanding this equation

$$W(\theta) = (-1)^{L_1 - I_1 - I_2} [(2I_1+1)(2I_2+1)]^{1/2} \times \sum A_k^0(L_0 L_0') A_k^2(L_2) \times W(I, I_1 I_2 I_2; k L_1) P_k(\cos\theta) \tag{2.30}$$

where

$$A_k^0(L_0, L_0') = F_k(L_0 L_0 I_0 I_1) + 2\delta_0 F_k(L_0 L_0' I_0 I_1) + \delta_0^2 F_k(L_0' L_0' I_0 I_1) \tag{2.31}$$

$$A_k^2(L_2) = F_k(I_2 I_3 L_2 L_2) \tag{2.32}$$

These expressions are applicable to the case where the mixture is in the third transition instead of the first transition, if the roles of L_0, L_0' and L_2, L_2' are interchanged.

When a mixture occurs in the unobserved transition the correlation function is given by

$$W(\theta) = W(L_1) + \delta_1^2 W(L_1') \tag{2.33}$$

Expanding this equation

$$W(\theta) = \left[(2I_1+1)(2I_2+1)\right]^{1/2} \sum A_k^0 (L_0 L_0') A_k^2 (L_2) \times \left[W(I_1 I_1 I_2 I_2; k L_1)(-1)^{L_1 - I_1 - I_2} + \delta_1^2 (-1)^{L_1' - I_1 - I_2} \times W(I_1 I_1 I_2 I_2; k L_1')\right] P_k(\cos\theta) \tag{2.34}$$

Assumptions

It was assumed that the substates belonging to a particular level were equally populated for any choice of the Z-axis. This is a valid assumption unless the radioactive nuclei are in a strong field at low temperatures. This is just the case of "oriented nuclei" and will not be discussed here. In this case, the population of the various states and substates follow a Maxwell-Boltzmann distribution.

The second assumption which was made was that the nuclei were free. This is just the statement that the nuclei are not disturbed by extranuclear fields. This assumption is justified if the mean life of the intermediate nuclear state is much shorter than the interaction time. It is generally assumed that if the lifetime of the intermediate state is less than 10^{-9} seconds this condition is fulfilled. For states with longer lifetimes, perturbations are possible. To minimize the chance of perturbations an environment where the extranuclear fields are very small must be utilized. This is realized in cubic crystals where the time average effect of the fields vanishes. The extranuclear fields are also small in certain liquids. All the correlations carried out in this research were performed in acidic solutions.

CHAPTER III

TECHNIQUES - EQUIPMENT

In Chapter II the directional correlation function was written as

$$W(\theta) = \sum_{k=0\ even}^{k_{max}} A_k P_k(\cos\theta) \qquad (3.1)$$

The experimental problem is that of determining the coincidence counting rate N_c between two gamma rays in cascade (γ_1 and γ_2) as a function of the angle θ. θ is the angle between the direction of emission of the first gamma ray γ_1 and the direction of emission of the second gamma ray γ_2.

A schematic diagram of the experimental arrangement of the detector assembly is shown in Figure 8.

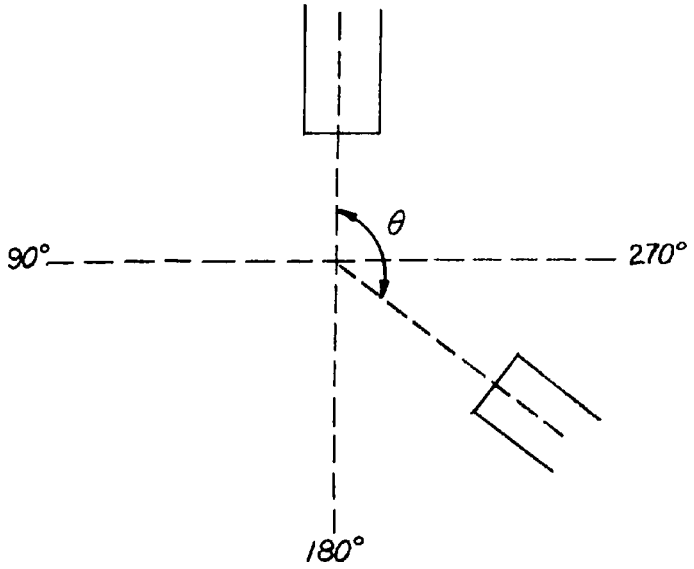


Figure 8. Detector Arrangement.

All the desired information could be obtained by observing the coincidence counting rate $N_c(\theta)$ from 90° to 180°. However, in practice $N_c(\theta)$ is observed from 90° to 180° and 180° to 270°, in most cases at intervals of 15°. The data at 90° and 270° are added together, the data at 105° and 255° are added together, etc. In general, the data at $(90°+\theta)$ is added to the data obtained at $(270°-\theta)$. This corrects for any false asymmetries which might be produced due to scattering from surrounding objects, and to source misalignment.

After $N_c(\theta)$ is recorded, a least squares fit[40] of the data is made to the function

$$F(\theta) = A_0 P_0 + A_2 P_2(\cos\theta) + A_4 P_4(\cos\theta) \tag{3.2}$$

The experimental values of A_0, A_2 and A_4 are determined by this procedure. It is a standard procedure to normalize the value of the coefficients which have been determined so that $A_0 = 1$. Carrying this normalization out results in the following values for the coefficients

$$A_2' \pm \epsilon_2' = \frac{A_2 \pm \epsilon_2}{A_0 \pm \epsilon_0} \quad ; \quad A_4' \pm \epsilon_4' = \frac{A_4 \pm \epsilon_4}{A_0 \pm \epsilon_0} \tag{3.3}$$

The experimental directional correlation function is then written as

$$W_{exp}(\theta) = 1 + (A_2' \pm \epsilon_2') P_2(\cos\theta) + (A_4' \pm \epsilon_4') P_4(\cos\theta) \tag{3.4}$$

The experimental points can be placed on the least squares curve by dividing the observed counting rates, or "corrected counting rates,"

by $W_{exp.}(90°)$. The meaning of the expression "corrected counting rates" will now be examined.

Corrected Counting Rates

The observed coincidence rate $N_c^{ob.}(\theta)$ is proportional to the efficiencies $(\varepsilon_1, \varepsilon_2)$ for the detection of the gamma rays of each counter, the solid angles (Ω_1, Ω_2) which the source subtends at each counter, and the directional correlation function $W(\theta)$. When energy discrimination is employed, the proportionality constant is N, where N is the source strength.

$$N_c^{ob.}(\theta) = N\varepsilon_1\varepsilon_2\Omega_1\Omega_2 W(\theta) \tag{3.5}$$

The individual singles counting rates for each counter are given by

$$\begin{aligned} N_1 &= N\varepsilon_1\Omega_1 \\ N_2 &= N\varepsilon_2\Omega_2 \end{aligned} \tag{3.6}$$

If Equation (3.5) is divided by Equations (3.6), the following expression is obtained

$$\frac{N_c^{ob.}(\theta)}{N_1 N_2} = N_c'(\theta) = \frac{W(\theta)}{N} \tag{3.7}$$

The corrected counting rates will now be independent of variations in the solid angle of the counters, and fluctuations in the efficiencies of the counters. $N_c'(\theta)$ depends only on $W(\theta)$ and the source strength N. Since the isotopes used in this study had long halflives, there was no need for correcting for decay of the source.

Accidental Coincidences

In the expressions previously given, $N_c^{ob.}(\theta)$ has been used to stand for the real coincidence rate as a function of θ These coincidences arise from the simultaneous detection of two quanta originating from the same nucleus. In addition to these, accidental coincidence counts, $N_c^{Acc}(\theta)$, which are due to simultaneous detection of two quanta from different nuclei, will be registered. Simultaneous used in this sense means within the resolving time τ of the coincidence circuit. If two counts arrive at the coincidence circuit less than τ seconds apart, they will be recorded as being in coincidence. The accidentals must be subtracted from the total coincidence rate to find the real coincidence rate

$$N_c^{R}(\theta) = N_c^{ob.}(\theta) - N_c^{Acc.}(\theta) \tag{3.8}$$

The number of accidentals can be determined from the expression[41]

$$N_c^{Acc.} = 2\tau N_1 N_2 \tag{3.9}$$

if the counting rates N_1, N_2 and the resolving time τ of the circuit are known. In practice $N_c^{Acc.}$, N_1 and N_2 are measured to determine the resolving time of the circuit. When Equations (3.6) are substituted into Equation (3.9), the expression

$$N_c^{Acc.} = 2\tau N^2 \varepsilon_1 \varepsilon_2 \Omega_1 \Omega_2 \tag{3.10}$$

is obtained. When Equation (3.5) is now divided by Equation (3.10), the following expression is obtained expressing the real to accidental ratio.

$$\frac{N_c^{ob.}}{N_c^{Acc}} = \frac{1}{2\tau N} \tag{3.11}$$

The accidental coincidence counting rate was determined by using two independent sources. Each counter was isolated from the other by lead shielding. The observed coincidence rates were then normalized by the singles rates

$$N_c^{Acc}(\theta) = \frac{N_1 N_2 N_c^{Acc.}(\theta)_{OBSERVED}}{N_1' N_2'} \tag{3.12}$$

N_1 and N_2 refer to the single counting rates observed in counters 1 and 2 when the counter assemblies are set up to observe $N_c^{ob.}(\theta)$ as shown in Figure 1. N_1' and N_2' refer to the singles counting rates observed in counters 1 and 2 when the counter assemblies were set up to observe $N_c^{Acc.}(\theta)$ as described above.

Correction for Finite Resolution

It has been stated that in angular correlation measurements the coincidence rate between two gamma transitions in cascade is recorded as a function of the angle θ between the two counters. However, since the detector assemblies have finite resolution, this angle θ is not a unique angle but rather a range of angles θ_1 to θ_2. This spread in the angle θ is shown in Figure 9. This $\Delta\theta$ has the effect of smearing out, or attenuating the correlation[42]. The measured correlation function can be expressed as the true correlation function

with attenuation coefficients B_k [40,42-44].

$$W'(\theta) = \sum_{k=0\ \text{even}}^{k_{max}} B_k A_k P_k(\cos\theta) \tag{3.13}$$

A_k are the coefficients which depend only on the cascade parameters. There are three general methods by which the attenuation coefficients are determined.

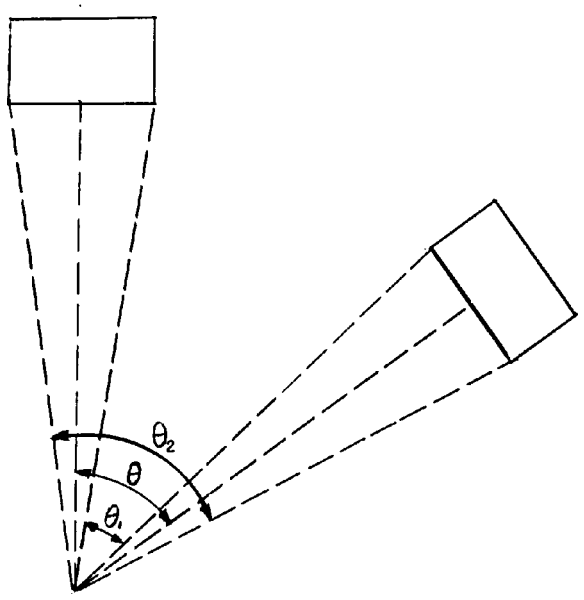


Figure 9. Finite Solid Angle Subtended by Detectors.

Annihilation Radiation Method

If the energies of the gamma rays are of the order of 0.51 Mev, the annihilation radiation method may be used to determine the resolution of the counters[43]. The attenuation coefficients are found by a numerical integration over the resolution curve.

Absorption Coefficient Method

The attenuation coefficients B_k can be calculated if the shape of the scintillation crystals and distances between the source and crystals are known. The absorption coefficient μ of the crystal is a function of the energy of the radiation. Rose has tabulated the attenuation coefficients B_2 and B_4 for μ ranging from $(0.12 - 40)cm^{-1}$ and for source to crystal distances of 7 and 10 cm[40]. The absorption coefficients may be found in articles by Howland and Kreger[45] and Davisson and Evans[46]. All the attenuation coefficients used in the Eu^{154} directional correlation measurements were obtained by the absorption coefficient method.

Collimated Beam Method

In this method, a collimated beam of mono-energetic gamma rays is used to measure the resolution of the counters[44]. A resolution curve is obtained and the attenuation coefficients are found by numerical integration. This is essentially the Church-Kraushaar method[43] where the experimental resolution curve is measured for each energy separately. The B_k's used in the directional correlation measurements in Ta^{182} were based on the collimated beam experiments of Arns[47].

Resolving Time and Source Strength

Since the real to accidental ratio is inversely proportional to both the resolving time of the circuit and the source strength, Equation (3.11), it is desirable to use as large a source strength as possible. If a good real to accidental ratio is to be maintained, a resolving time as short as possible must be employed. The method which was used to obtain a short resolving time is essentially using the first few photoelectrons from the cathode of the photomultiplier tube, caused by the detection of a gamma ray, to trigger a coincidence or "summing" network. Morton[48] has shown that much more precise timing is possible using the first few electrons than using the mean time of the photomultiplier pulse as would be done if the whole pulse were used. The resolving time that was obtained was approximately 3.5×10^{-8} seconds for energies down to approximately 50 kev. It should be pointed out that this method destroys the identification of the pulse as far as energy is concerned.

A block diagram of the experimental arrangement is shown in Figure 10.

"Fast - Slow" Coincidence Circuit

It was noted in the previous section that the method of obtaining a fast resolving time destroys the information about the energy of the gamma rays. However, when complicated decay schemes are to be investigated, energy selection of the gamma rays must be employed. At first glance this seems to be a contradictory situation. This seemingly hopeless situation is overcome by the application of a "fast - slow"

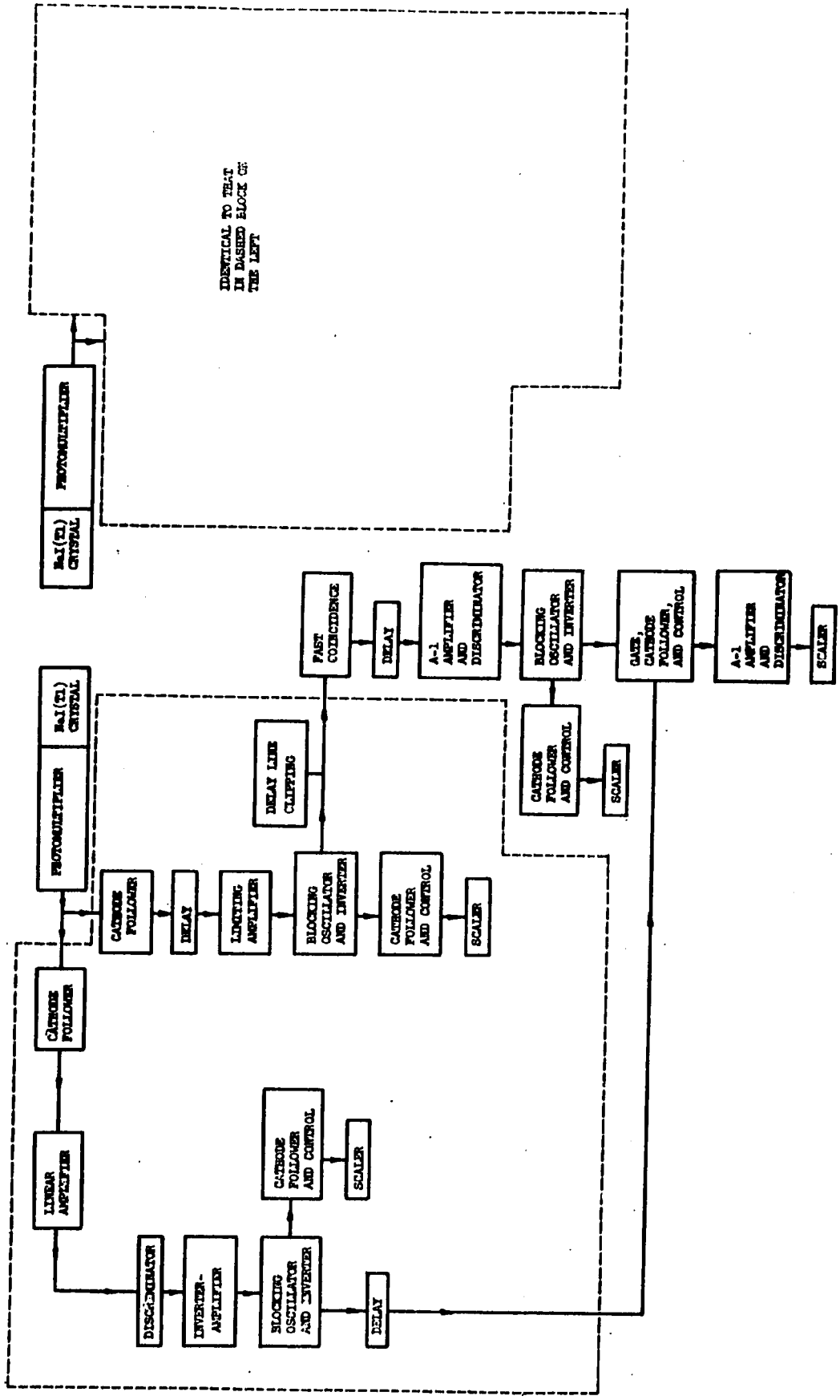


Figure 10. Block Diagram of the Fast-Slow Coincidence System.

coincidence circuit. As is shown in Figure 10, parallel channels are constructed, one a fast channel for the production of a fast resolving time, and a slow channel where energy selection is obtained.

The fast coincidence circuit records a count each time two detected gamma rays are in coincidence. The resolving time of this circuit is approximately 3.5×10^{-8} seconds. The output of this coincidence circuit and the output from the slow coincidence circuit are brought together into a triple coincidence circuit whose resolving time is approximately 2×10^{-7} seconds. This triple coincidence, or gate circuit, then records a count only when the detected gamma rays from each detector are in fast coincidence and have energies within certain preselected limits.

Detector Assembly

Thallium activated sodium iodine [Na I(Tl)] scintillation crystals, were coupled to Dumont 6292 photomultiplier tubes by means of Dow-Corning (200) silicone oil. The crystals were of two types. Crystals 1-1/2 inches in diameter and 1-inch thick were used in the Gd^{154} measurements. In the W^{182} measurements, 2-in. x 2-in. crystals were used. Lead shielding 1/2-inch thick surrounded the sides of the crystals to reduce crystal to crystal scattering. One-eighth inch aluminum was placed in the front of the crystals as a beta shield. The electric field in the photocathode to first dynode space is weak necessitating the use of mu-metal shields to reduce the effect of the earths magnetic field. A 2-1/2-inch soft iron pipe was mounted surrounding the phototube and shield.

The sources used in this investigation were in HCL solution and placed in lucite holders 1/2 inches in length and 1/8-inch in diameter. These holders were mounted centrally between the two photomultiplier - crystal assemblies at distances of either 7 or 10 centimeters.

The output of the photomultiplier tubes is sent to the grids of two cathode followers. The pulses coming out of this arrangement had a rise time of 2.0×10^{-7} seconds with amplitudes up to 0.5 volts for a 1 Mev gamma ray.

Fast Channels

The output of the fast cathode follower is sent to the limiting amplifier. The limiting amplifier - blocking oscillator combination is designed to produce fast rising uniform pulses from slow rising varying amplitude pulses. These uniform pulses which reach the coincidence circuit have the effect of producing good stability.

Limiting Amplifier

In this amplifier the pulses are amplified to a large value and then the tops of the pulses are clipped off. This produces a fast rising pulse from a slow rising pulse. The rise time which is obtainable is determined by the band width of the amplifier. The result is that all the limited pulses have approximately the same rise time. The circuit, which was devised by Kelly[49], had a band width of 2 megacycles. The output is a positive 20-volt flat-topped pulse with a rise time of approximately 0.04 microseconds for all energies down to approximately 50 kev. The duration of this pulse is approximately two microseconds. Figure 11 A is a picture of the limited pulses of Eu^{154}.

The high voltage which is applied to the photomultiplier tubes can be adjusted to change the amplitude of the output pulses from the photomultiplier tubes. In this way the lowest energy gamma rays, x-rays, or noise can be adjusted to be either limited or discarded.

The principle difficulty in this method of using amplifiers of such small band widths is that there is an apparent delay introduced by each stage[50]. This delay time is, to a small extent, dependent upon the pulse amplitude. This introduces a so-called jitter, i.e., pulses of different amplitude arrive at different times. Ideally, this can be compensated for by adding delay to the appropriate channel. However, it is difficult to add the proper amount of delay because of the low coincidence rates and so this is done approximately.

Blocking Oscillators and Coincidence Circuits

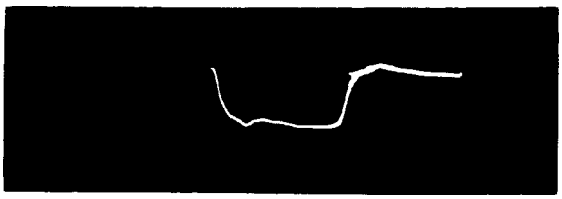
The output from the limiting amplifier is fed into the blocking oscillator circuit. The blocking oscillators produce uniform positive output pulses. The rise time of these pulses is about 0.05 microseconds and a duration of approximately 0.2 microseconds. A picture of these pulses is given in Figure 11 B. The pulse is then shortened to 0.05 microseconds., Figure 11 C, by the use of delay line clipping. The resultant negative triangular-shaped pulses are then applied to the grids of a Garwin type coincidence circuit[51,52]. These circuits have been described by Stewart[53], Scharenberg[54], and Kelly[49], and will not be given here.

Slow Channels

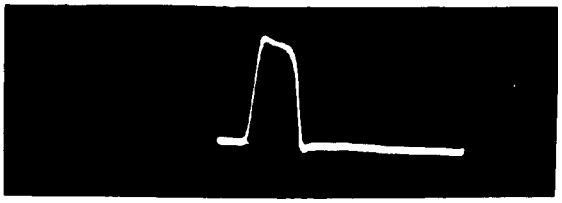
The output from the slow cathode followers is sent into a linear amplifier. The maximum pulse height that can be obtained from



Output Pulse From the Limiting Amplifier.



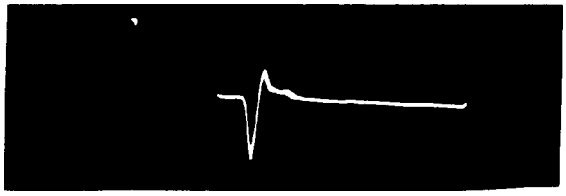
Output Pulses From the Pulse Height Analyzer After Going Through Delay Line.



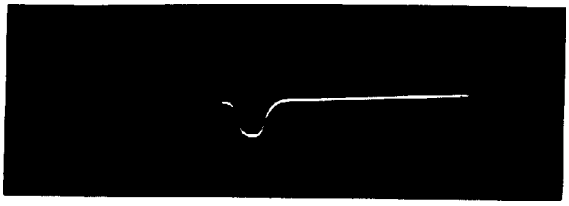
Output Pulse From the Fast Blocking Oscillator.



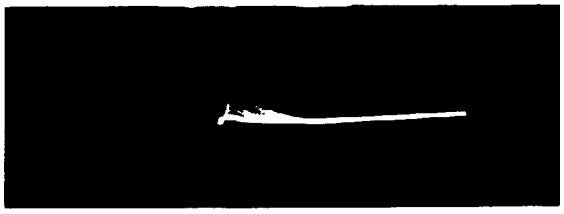
Output Pulse From the Slow Blocking Oscillator.



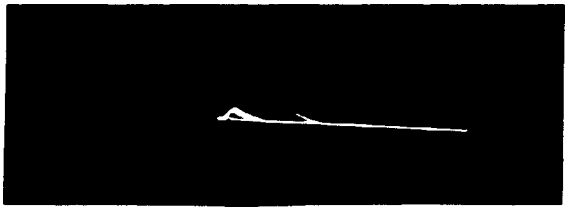
Fast Blocking Oscillator Pulse After It Is Inverted and Shortened By the Use of Delay Line Clipping.



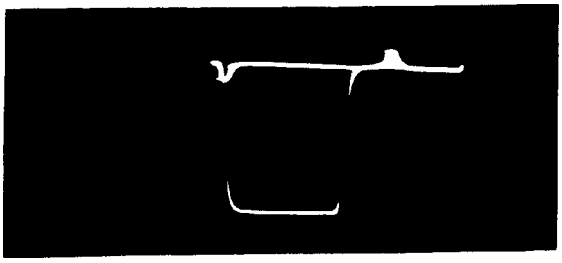
Slow Blocking Oscillator Pulse After Being Inverted.



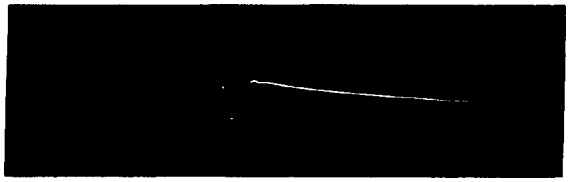
Output Pulses From the Linear Amplifier.



Output Pulses From Triple Coincidence Circuit.



Output Pulses From the Pulse Height Analyzer.



Input Pulse to Scaling Circuit.

Figure 11. Pulse Shapes at Various Locations In the Fast-Slow Coincidence System.

these amplifiers is approximately 150 volts. Figure 11 D shows the positive output pulses from the linear amplifier from an Eu^{154} source.

The output from the linear amplifier is fed into a pulse height analyzer. The output of the pulse height analyzer is a negative flat-topped pulse of approximately 20 volts and a duration of approximately 1.5 microseconds. Figure 11 E shows the output from the pulse height analyzer. The small blips appearing at the beginning and end of the pulse are the firing and blocking pulses of the two circuits which form the differential discriminator action. If the discriminator is set integrally instead of differentially, these blips do not occur. Figure 11 F shows the same pulse as is shown in Figure 11 E after going through a variable delay line. The pulse has been attenuated to approximately 8 volts.

At the cathode of the blocking oscillator, the pulses are positive and uniform. These pulses are approximately 30 volts. This is shown in Figure 11 G. A potential divider attenuates this pulse to 5 volts. This smaller pulse is sent to a scaler via a cathode follower to monitor the singles counting rate. The plate of the inverter tube shows a negative pulse of 40 volts in size and a duration of approximately 0.25 microseconds. This is shown in Figure 11 H. This is the place in the circuit where the pulses are lined up for maximum coincidence by the use of delay line.

The output of the slow coincidence circuit is put into coincidence with the output from the fast coincidence circuit. The action of this circuit is that of producing a large pulse when a triple coincidence pulse is formed and a much smaller pulse when a double coincidence

pulse is formed. This action is shown in Figure 11 I. (The triple coincidence pulses in this picture are approximately 30 volts, while the double coincidence pulses are approximately 10 volts). A discriminator is then adjusted to cut out the lower amplitude pulses and, therefore, only the triple coincidence pulses are passed on to the scaling circuits.

The pulses which are sent into the scalers are approximately 1.5 volts in amplitude. A typical pulse is shown in Figure 11 J.

The scalers that record the counts are shown on the block diagram. Only those recorded in the triple coincidence scaler, and those monitoring the slow channels are used in the calculations. The fast channel single counting rates and the fast coincidence counting rates are used only to monitor the equipment for stability.

The instrument as a whole was fairly stable. The fast singles counting rates were stable to within $\pm$ 0.1%, the energy selected singles counting rates to within $\pm$ 0.2%.

CHAPTER IV

SPHEROIDAL NUCLEI

There have been fairly recent studies on the level structure of a number of even-even nuclei which have a spheriodal equilibrium shape. These have given increasing experimental support for the existance of rotational and collective vibrational states in such nuclei as predicted by the unified model. The evidence consists mainly in the systematic occurence and decay properties , which in most cases agree with the predictions of the theory.

The present study of the level structure of Eu^{154} and Ta^{182} has been undertaken to extend the systematic picture of rotational and vibrational states further in the region of the rare earths where the experimental material in support of such states is still meager. It should be noted that tantalum is not a rare earth, but does border the rare earth region.

Nuclei whose equilibrium shape deviates strongly from spherical symmetry can be distinguished by two types of excitation[55-59]. The first is associated with a collective motion of the nucleons. This affects only the orientation of the nucleus in space while preserving the internal structure of the nucleus. The second mode of excitation can be associated with the excitation of individual particles or with collective excitations. This latter type corresponds to vibrations about the equilibrium shape.

The rotational spectrum depends on the nuclear equilibrium shape, and is especially simple for axially symmetric nuclei. The rotational motion can then be characterized by the quantum numbers I,K,M,

representing the total angular momentum, its projection on the nuclear symmetry axis, and its projection on the space fixed axis, respectively. This is shown schematically in Figure 12.

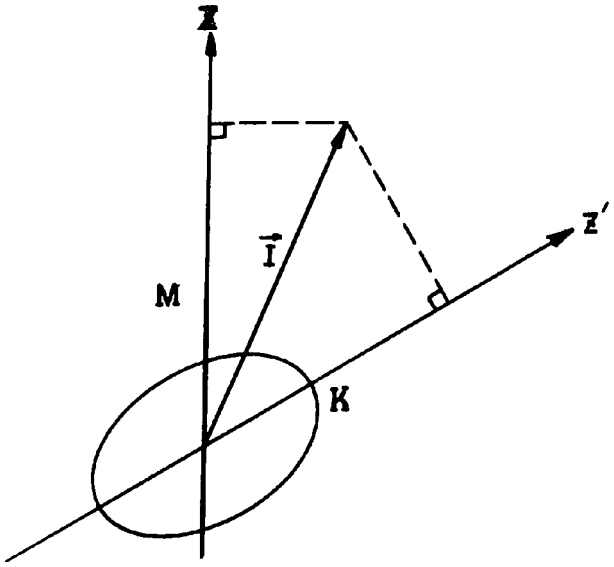


Figure 12. Schematic Diagram of a Spheroidal Nuclear Equilibrium Shape Showing the Quantum Numbers Involved when the Nuclear Motion Can Be Separated Into Rotational and Intrinsic.

The separation of the nuclear motion into rotational and intrinsic modes corresponds to the existence of approximate solutions of the nuclear wave equation of the type

$$\psi = \sqrt{\frac{2I+1}{8\pi^2}}\, \varphi_{\tau K}\, \mathcal{D}^{I}_{MK}(\theta_i) \qquad (4.1)$$

where φ represents the intrinsic structure characterized by K, and the additional set of intrinsic quantum numbers, τ . Since the intensity rules which are discussed below are independent of the intrinsic quantum numbers, they will be omitted.

The rotational wave functions $\mathcal{D}(\theta_i)$ depending on the Eulerian angles θ_i of the nuclear coordinate system are the proper functions for the symmetric top.

The states in a rotational band are characterized by the same intrinsic wave functions $\varphi_{\tau K}$ and are labeled by different values of I. In an odd-A nucleus, where K is a positive half integer number, I may take on the values

$$I = K,\ K+1,\ K+2,\ \cdots \qquad \text{all the same parity as the intrinsic structure} \tag{4.2}$$

In an even-even nucleus, the ground state has $K=0$ and the symmetrization of the wave function limits the rotational band to

$$I = 0, 2, 4, 6, \cdots \qquad \text{even parity} \tag{4.3}$$

In an odd-odd nucleus or in excited states of even-even nuclei with $K \neq 0$, the rotational sequence is again given in expression (4.2).

The energies in a rotational band are given by

$$E_{ROT} = \frac{\hbar^2}{2\tau}\left[I(I+1) + a(-)^{I+\frac{1}{2}}(I+\tfrac{1}{2})\delta_{K,\frac{1}{2}}\right] \tag{4.4}$$

τ = moment of inertia, which depends on the deformation. This parameter varies fairly smoothly with the atomic number, increasing with the number of nucleons outside of closed shells.

The rotational model which has been described here has proven extremely successful in accounting for many features of the spectra of nuclei in the range of $155 \leqq A \leqq 185$, and $A \geqq 225$. Nuclei with $A \approx 25$ also appear to have rotational spectra.

The two nuclei which will be treated in greater detail in this paper are Eu^{154} and Ta^{182}, therefore, falling into region one. The tantalum isotope falls in the upper part of region one, but within the region. The europium isotope is on the lower edge of the range of A, but out of the region, which had formerly been given for A. It now appears that this range should be lowered to include A of 154.

Using Equation (4.4), the following theoretical energy ratios for the spacing of the energy levels have been calculated

$$\frac{E_4}{E_2} = \frac{10}{3} \quad ; \quad \frac{E_6}{E_2} = 7 \quad ; \quad \frac{E_8}{E_2} = 12$$

where the number $E_{2,4,6,8\cdots}$ is interpreted to mean the energy of the state above ground state with spin 2, etc.

Whatever small deviation there are from these ratios, well away from closed shells can be attributed to "rotation-vibration" interaction. This will be discussed in greater detail later in the chapter.

Transition Probabilities

Gamma-ray emission is a simple kind of electromagnetic process with a transition probability given by

$$T = \frac{8\pi(L+1)}{L[(2L+1)!!]^2\hbar}\left(\frac{\Delta E}{\hbar c}\right)^{2L+1} B(L) \qquad (4.5)$$

where L denotes the multipole order, ΔE the energy difference between initial and final states, and $B(L)$ the "reduced-transition" probability. Only $B(L)$ depends upon the details of the nuclear structure.

The "reduced-transition" probability can be written as a product of a geometrical factor, depending only on the angular momenta I,K, and L, and a factor involving integrations over the intrinsic wave function of the initial and final states, and thus, depending only on τ , K, and L. For transitions within a rotational band the initial and final states have the same intrinsic wave function, and therefore, the absolute transition probabilities can be expressed directly in terms of the intrinsic nuclear moments.

In transitions involving a change of the intrinsic nuclear state, the absolute value of the matrix elements depends on more specific features of the intrinsic nuclear structure. However, when a comparison of the reduced transition probability for the emission of a given multipole radiation from a state, i, to different members f, f'... of a rotational family is made, the factor involving the intrinsic wave functions is the same. The result is a ratio which depends only on the geometrical factors. This can be written

$$\frac{B(L, I_i \to I_f)}{B(L, I_i \to I_{f'})} = \frac{\langle I_i L K_i K_f - K_i | I_i L I_f K_f \rangle^2}{\langle I_i L K_i K_f - K_i | I_i L I_{f'} K_f \rangle^2} \qquad (4.6)$$

The factor $\langle I_i L K_i \nu | I_i L I_f K_f \rangle$ is the Clebsch-Gordan coefficient for the addition of angular momenta I_i and L to form the resultant I_f. This relation also holds where the states i, f, and f' belong to the same rotational family.

If the nuclear wave function can be expressed as a simple product of an intrinsic and a rotational function as in Equation (4.1) i.e., if the simple rotational coupling scheme is applicable, then the quantity K is a constant of the motion.

For the transition probability to be non-vanishing, it is necessary that not only the angular momentum selection rule

$$|I_i - I_f| < L < |I_i + I_f| \tag{4.7}$$

and the parity rule

$$\pi = \pi_i \pi_f \tag{4.8}$$

be satisfied, but also

$$|K_i - K_f| \equiv \Delta K \leq L \tag{4.9}$$

This selection rule on K would hold rigorously if Equation (4.1) were an exact representation of the problem. This is only realized in the limit of large deformations where the rotational motion is so slow that it does not disturb the nuclear shape. With decreasing deformation, and increasing rotational frequency, the intrinsic nuclear structure is excited by the rotational motion, and the quantum numbers K and τ are no longer constants of the motion. When this is the case, a strict adherance to the rotational spectrum is not expected. A modification in the spectrum proportional to $I^2(I+1)^2$ is expected. This is due to "rotation-vibration" interaction. The magnitude of this term provides a measure of the adequacy of the rotational description.

In the regions which are being considered, the magnitude of this correction term in the energy amounts to one percent or less for the lowest rotational excitation.

All known electromagnetic transitions within a rotational band are of multipolarity M1 and E2 or a mixture of these two. Because of the angular momentum selection rules, such transitions can occur

only between states with $|\Delta I| \leq 2$. If $|\Delta I| = 2$ the radiation is pure E2. For $|\Delta I| = 1$, both M1 and E2 can contribute. On the basis of a single particle model, the radiation of lower multipole order is expected, i.e., M1 to predominate. However, the strong E2 transitions within a rotational band must involve the collective effects of many nucleons, combining their individual matrix elements coherently. This effect is also responsible for the sizable nuclear deformation necessary for the existence of rotational spectra. Although M1 transitions can also involve a large number of nucleons, their individual magnetic moments do not add coherently, and no significant increase of the M1 transition strengths over the single particle values occur.

Vibration

While the lowest collective excitations of the strongly deformed nuclei correspond to rotations with preservation of shape, one may also expect these nuclei to exhibit collective excitations which correspond to vibrations about the equilibrium shape.

For a non-spherical nucleus, the angular momentum of a vibrational quantum is not a constant of the motion due to the coupling of the nuclear rotation. Still, the symmetry of the vibrations may be characterized by a quantum number λ. This quantum number represents the number of nodal surfaces and in the limit of small nuclear eccentricities, corresponds to the multipole order. The parity of the vibrations is $(-1)^{\lambda}$. For axially symmetric nuclei, the vibrations may in addition be characterized by the quantum number ν , representing the component of vibrational angular momentum about the symmetry axis.

For given λ , the component ν may take on the values $0, \pm 1, \cdots \pm \lambda$ In the special case of $\nu = 0$, the vibrations preserve the axial symmetry of the nuclear shape.

The quadrupole vibrations $(\lambda = 2)$ of the nucleus about a spheroidal equilibrium shape separate into two modes of which one has $\nu = 0$ (β vibrations) and the other $|\nu| = 2$ (γ vibrations).

The shape of an ellipsoid which deviates from a spherical shape can be characterized by two shape parameters. The quantity β measures the deviation from sphericity and the value of the parameter γ determines the specific shape of the nucleus. Thus, $\gamma = 0$ describes a prolate (football shape) spheroid whose symmetry axis coincides with the Z'-axis, while $\gamma = \pi$ corresponds to an oblate (disk shaped) spheroid, again with a symmetry axis along the Z'-direction. An axially symmetric (say prolate) nucleus may perform two kinds of quadrupole vibrations. There may be oscillations of the eccentricity about its equilibrium value, but with preservation of axial symmetry; vibrations of β about β_0 (γ fixed at 0). These vibrations carry no angular momentum about the symmetry axis. The other kind of vibration involves oscillations of the nuclear shape about axial symmetry; β is fixed at β_0 while γ oscillates about 0. The "γ-vibrations" carry two units of angular momentum parallel to the symmetry axis.

Superimposed upon each vibrational state one expects to find a rotational band. Thus, in even-even nuclei the rotational band associated with the lowest mode of β vibration $(n_\beta = 1, n_\gamma = 0)$ is expected to have the same form as the ground state band K=0, I=0,2,4... The band corresponding to the first excited state of γ-vibration

$(n_\beta = 0, n_\gamma = 1)$ should have K=2, I=2,3... Since any ellipsoidal shape is in variant under reflection through the origin, and the intrinsic structure in even-even nuclei has even parity, it can be shown that all quadrupole vibrations as well as rotational excitations in even-even nuclei have even parity.

The following figure illustrates the ground state rotational band as well as the rotational bands associated with the first quadrupole vibrational excitation of the two modes $(n_\beta = 1$ and $n_\gamma = 1)$; respectively.

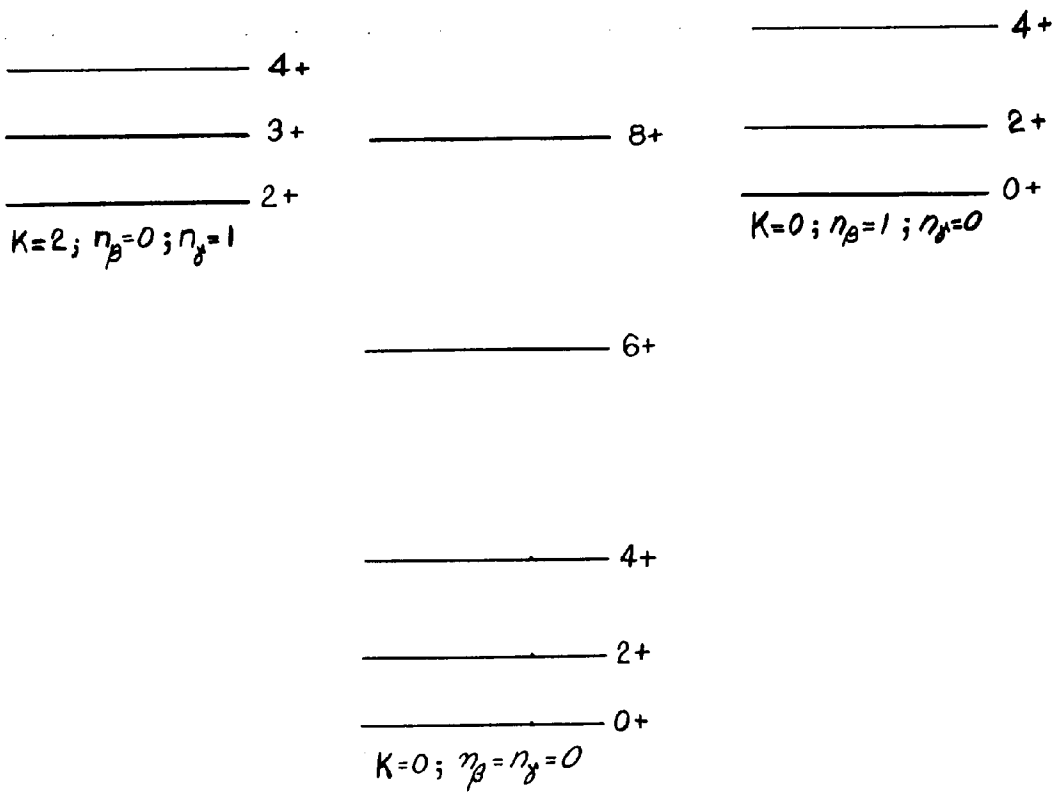


Figure 13. Energy Level Diagram Showing the Ground State Rotational Band and the Rotational Bands Associated with the First Quadrupole Vibrational Excitation of the Two Modes (η_β = 1 and η_γ = 1), Respectively.

It is expected that coulomb excitation will strongly excite the two states $n_\beta = 1, I = 2+$ and $n_\gamma = 1, I = 2+$ These states decay by means of E2 radiation to the I=0,2,4 members of the ground state band with relative reduced transition probabilities 1:10/7:18/7 for the β -vibrations, and 1:10/7:1/14 for the γ-vibrations.

Octupole Vibrations

The lowest odd parity modes (λ =3) should resemble octupole vibrations, and have $\nu = 0, \pm 1, \pm 2, \pm 3$. For the cases where low-lying states (0, 1 -) have been observed, they are interpreted as follows: the lower energy of the $\nu = 0$ mode as compared with the vibrations having $|\nu|$ = 1, 2, 3 may be characterized with a prolate nuclear shape. The state with I=1, can have a K value of either 0 or 1. Equation (4.6) must be evaluated in order to establish the correct assignment.

In the two problems which are to be discussed in Chapters V and VI, it will be seen that octupole vibrations with K=0 and 1 do not appear. However, octupole vibrations with K=2 or 3 may possibly be present. The reason why these states rather than the ones with K=0 or 1 occur will be given in Chapter VI.

Figure 14 A is the decay scheme of Tb^{160}. The values of (K, I, π) have been assigned by Nathan[60]. This isotope is in the same rotational region as Eu^{154} and Ta^{182} which are discussed in greater detail in Chapter V and VI respectively. Figure 14 B is the main portion of the decay scheme of Np^{238}. The values of (K, I, π) have been assigned by Rasmussen, et al[61]. This element is in the rotational region $A \geqq 225$. In both Figures 14 A and 14 B, the log ft

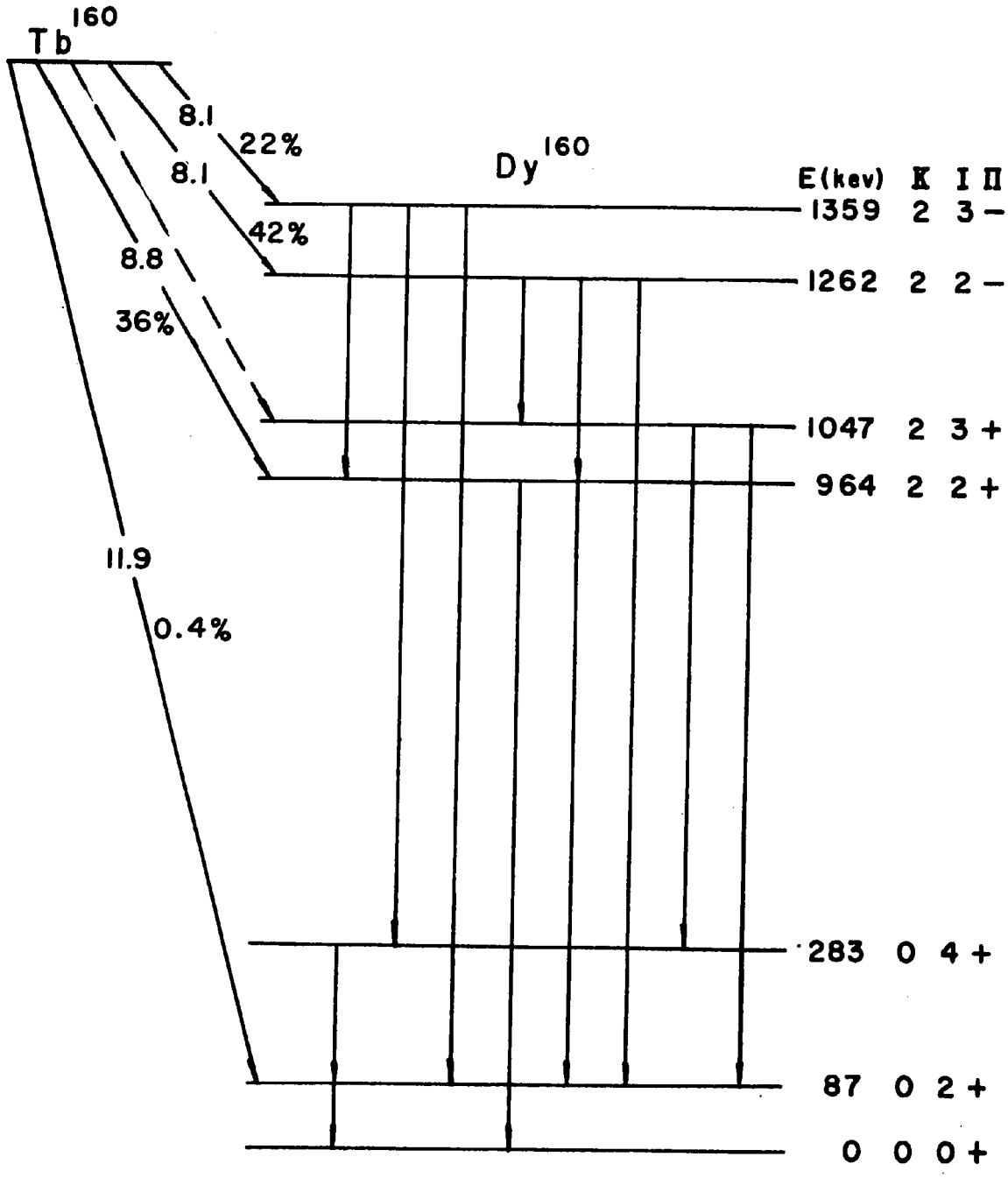


Figure 14A. Decay Scheme of Tb^{160}.

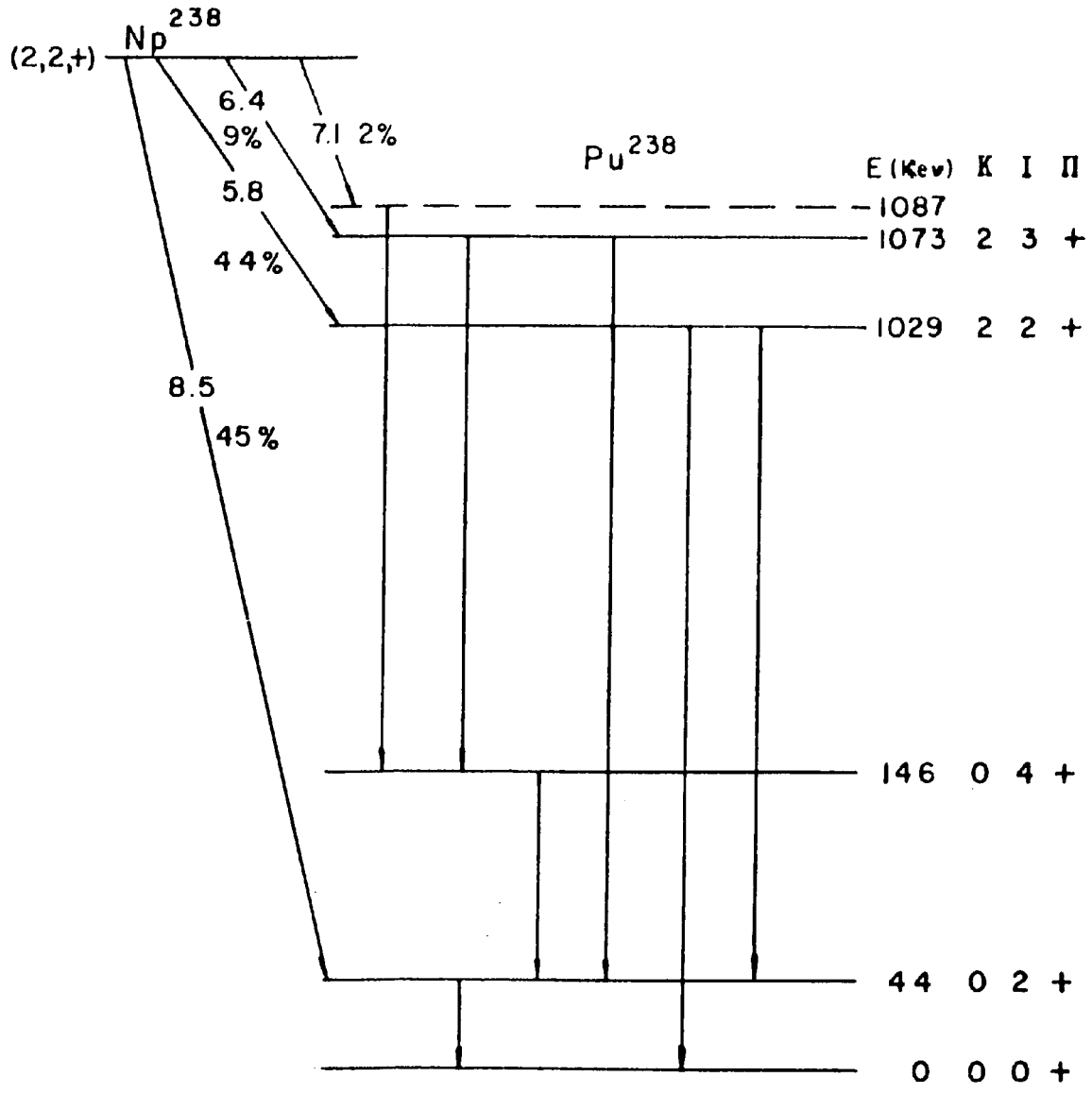


Figure 14B. Decay Scheme of Np^{238}.

values and percentages of the beta transitions are given. In Dy^{160} there is evidence for both the even parity "gamma-vibrational" band, and the odd parity "octupole-vibrational" band. Only the "gamma-vibrational" band is seen in Pu^{238}. In both cases, the ground state rotational band is also observed. The assignment of the quantum numbers (K, I, π) in both Dy^{160} and Pu^{238} has been made on the basis of conversion coefficients and reduced transition probabilities. These are the only isotopes which will be mentioned, although similar rotational and vibrational bands have been seen in other isotopes.

If the intrinsic motion of the system can be separated into a purely "single-particle" motion and a collective vibrational motion, another quantum number Ω is considered. Ω is the component of total individual particle angular momentum along the nuclear symmetry axis. If the excited states of the spheroidal nuclei are examined and found to be of vibrational character, this means that the individual nucleons remain in paired configurations, and Ω is a good quantum number. If, however, the separation of the deformed nucleus into vibrational and individual particle motion is just partially valid, this could lead to a state with partial vibrational character giving enhanced E2 transition rates, but with Ω not a very good quantum number.

Figure 12 can now be expanded to include this quantum number. This is shown in Figure 15.

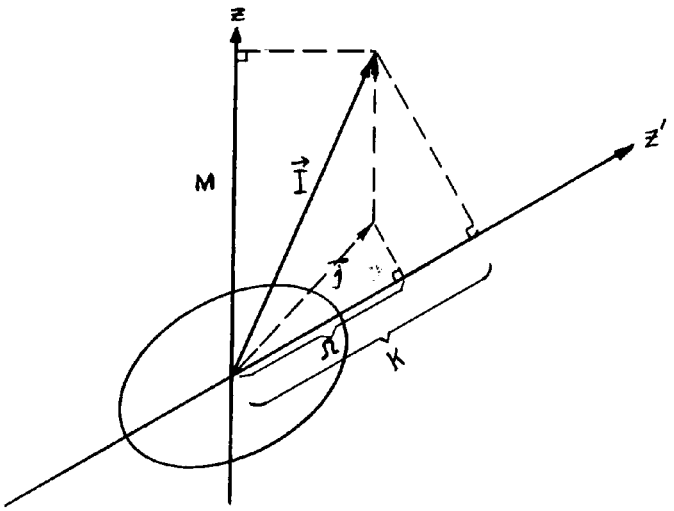


Figure 15. Schematic Diagram of a Spheroidal Nuclear Equilibrium Shape Showing the Quantum Numbers Involved when the Intrinsic Motion of the Nucleus Can Be Separated Into a Purely Single-Particle Motion and a Rotational-Vibrational Motion.

The angular momentum $\vec{j}$ of the particle precesses around the nuclear axis with a constant projection Ω. The total angular momentum $\vec{I}$ is the sum of $\vec{j}$ and the angular momentum $\vec{R}$ of the surface. The angular system of particles and surface rotates like a symmetric top with quantum number I, K (projection of I on the nuclear axis), and M (projection of I on space fixed axis).

For even-even nuclei all the nucleons are in a paired configuration and $K = \Omega = 0$ for the ground state rotational band. For excited states, the existence of axial symmetry implies that the nuclear wave function must be invariant with respect to arbitrary rotation of the body-fixed reference frame about the symmetry axis. Such an invariance condition force the requirement

$$K = \Omega \qquad (4.10)$$

If the deviation from axial symmetry is small so that there is still an approximate symmetry axis, the condition on K and Ω is $K - \Omega$ = even.

Interactions

It was mentioned earlier that in the limit of large deformations where the rotational motion is so slow compared with the more rapid internal motion that it does not disturb the nuclear shape, Equation (4.4) is expected to be in good agreement with most rotational spectra. As the rotational frequency increases, both distortion of the nuclear shape due to centrifugal forces (rotation-vibration interaction) and non-adiabatic perturbations of the particle-structure due to Coriolis forces (rotation-particle coupling) can become important. Either of these interactions can cause a modification in the spectrum which is proportional to $I^2(I+1)^2$

"Rotation-Vibration" Interaction

The nuclear rotation-vibration interaction is analogous to the effect of the same name occuring in molecular spectra, and is associated in both cases with an increase of the moment of inertia with angular momentum. It can be shown that if a nucleus vibrates about equilibrium value of β, the rotational energy spectrum deviates from the I(I+1) law, Equation (4.4). The result is

$$E'_{ROT} = \left(\frac{\hbar^2}{2\mathcal{I}}\right) I(I+1) + E_\beta^{(2)} I^2(I+1)^2 \qquad (4.11)$$

where

$$E_\beta^{(2)} = \frac{-12}{(\hbar\omega_\beta)^2}\left(\frac{\hbar^2}{2\mathcal{I}_0}\right)^3 \qquad (4.12)$$

When the rotational motion is perturbed by γ-vibrations, the result is

$$E_\gamma^{(2)} = \frac{-4}{(\hbar\omega_\gamma)^2}\left(\frac{\hbar^2}{2\mathcal{I}_0}\right)^3 \qquad (4.13)$$

The perturbation of the rotational spectrum is small if the rotational energies are small compared to the vibrational energies. Substituting Equations (4.12) and (4.13) into Equation (4.11)[62], the following expression is obtained.

$$\frac{\Delta E}{E_{ROT}} = -\frac{1}{I(I+1)}\left[\frac{12}{(\hbar\omega_\beta)^2}+\frac{4}{(\hbar\omega_\gamma)^2}\right]E_{ROT}^2 \quad ; \quad \Delta E = E_{ROT} - E'_{ROT} \qquad (4.14)$$

If ω_β is assumed to be equal to ω_γ, $\hbar\omega$ can then be found. In most cases, $\hbar\omega$ turns out to be approximately 1 Mev, which agrees quite well with the empirical average vibrational energy of 1 Mev. The corrections to the energies due to "rotation-vibration" interaction are always negative.

Rotation - Particle Coupling

In the previous discussion of the rotational spectrum, the separation of the wave equation into a rotational motion and an intrinsic motion of the nucleus was assumed. The coupling term between $\vec{I}$ and $\vec{j}$ was neglected.

If the rotation now becomes sufficiently rapid, $\vec{I}$ and $\vec{j}$ become coupled and K is no longer a good quantum number. Thus, there will be at least a partial breakdown of the K selection rules and intensity rules, and deviations from the simple I(I+1) law will occur. This interaction term is also proportional to $I^2(I+1)^2$, but in general is larger than that for the "rotation-vibration" interaction case. The sign of the term can be either positive or negative in the "rotation-particle coupling," whereas, it is only negative for the latter case.

Often it is difficult to tell to what extent the deviations from the I(I+1) law are due to "rotation-particle coupling" or to the "rotation-vibration" interaction. However, the latter effect is believed to predominate in even-even nuclei; excited intrinsic states usually occur here at higher energy than vibrational states.

CHAPTER V

DIRECTIONAL CORRELATION OF THE GAMMA RAYS IN Gd^{154}

Introduction

Until rather recently, the exact nature of the decay of Eu^{154} has been obscured by the activity of Eu^{152}. Since the half-life of Eu^{154} (16 $\pm$ 4 years) is of the same magnitude as that of Eu^{152} (13 years), separation of the two isotopes on the basis of their half-lives is virtually impossible. An investigation of the mode of decay of both of these isotopes has been carried out by Cork, et al[63], using sources obtained by neutron bombardment of the enriched isotopes of europium. Juliano and Stephens[64] have also studied the decay of Eu^{154} using a very pure source of Eu^{154} which was obtained from fission products. The proposed level scheme of Juliano and Stephens for Eu^{154} is shown in Figure 16. Except for a few minor discrepancies, the decay schemes which have been proposed by Cork, et al, and Juliano and Stephens for the decay of Eu^{154} are in excellent agreement. A starting point is, therefore, established for the measurement of other properties of this interesting nucleus by angular correlation techniques.

The directional correlation of the 0.123 Mev gamma ray with the 0.248 Mev gamma ray kas been reported by Grodzins[65] and supports a spin sequence of 4 (Q)2(Q)0 for the low-lying levels.

Procedure

The sources were prepared by dissolving Eu_2O_3 in a dilute solution of HCl. Although the europium was enriched in Eu^{154}, some Eu^{152} was present and prevented several of the possible correlations from being carried out. The gamma spectrum is shown in Figure 17.

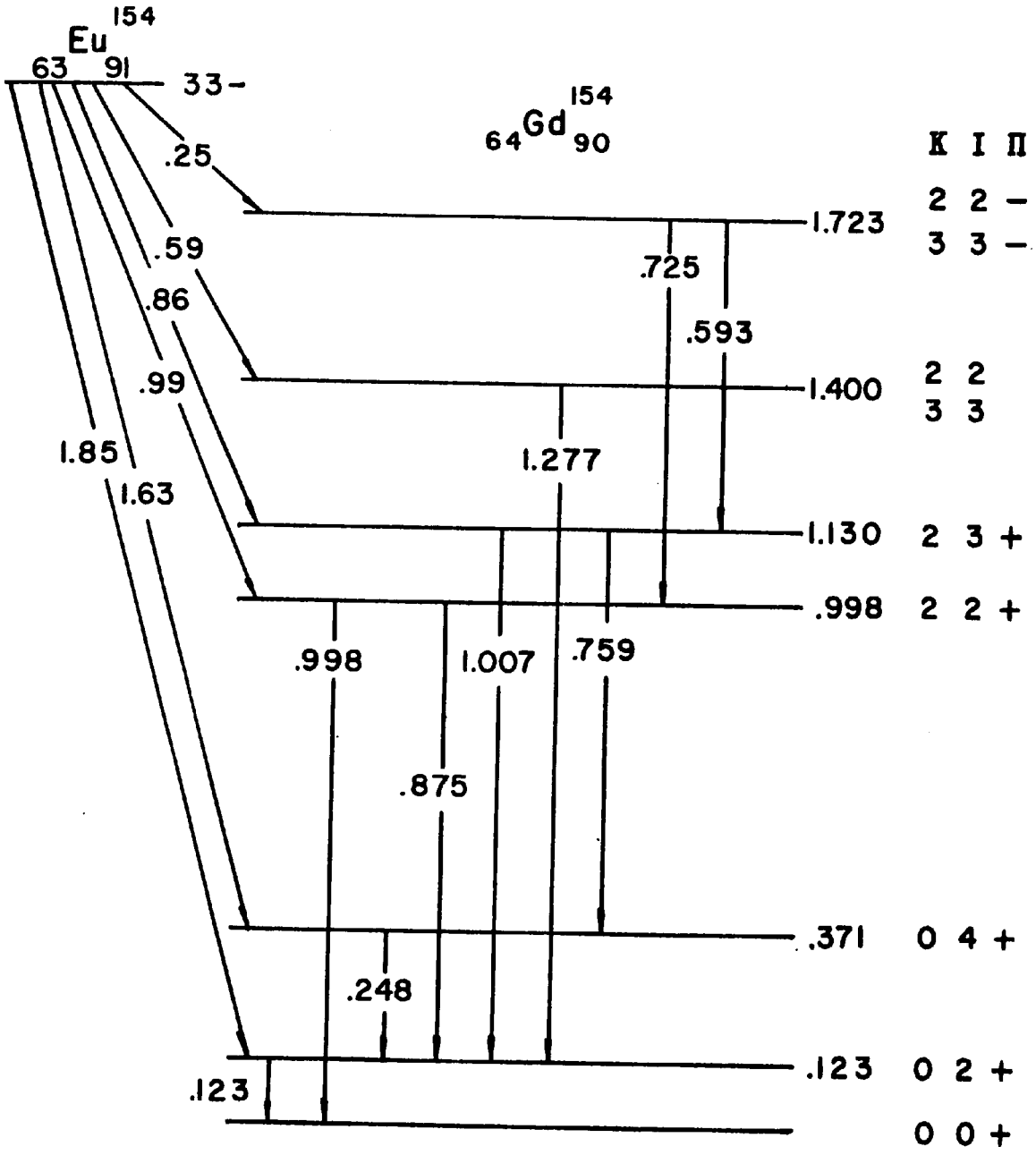


Figure 16. Decay Scheme of Eu^{154}.

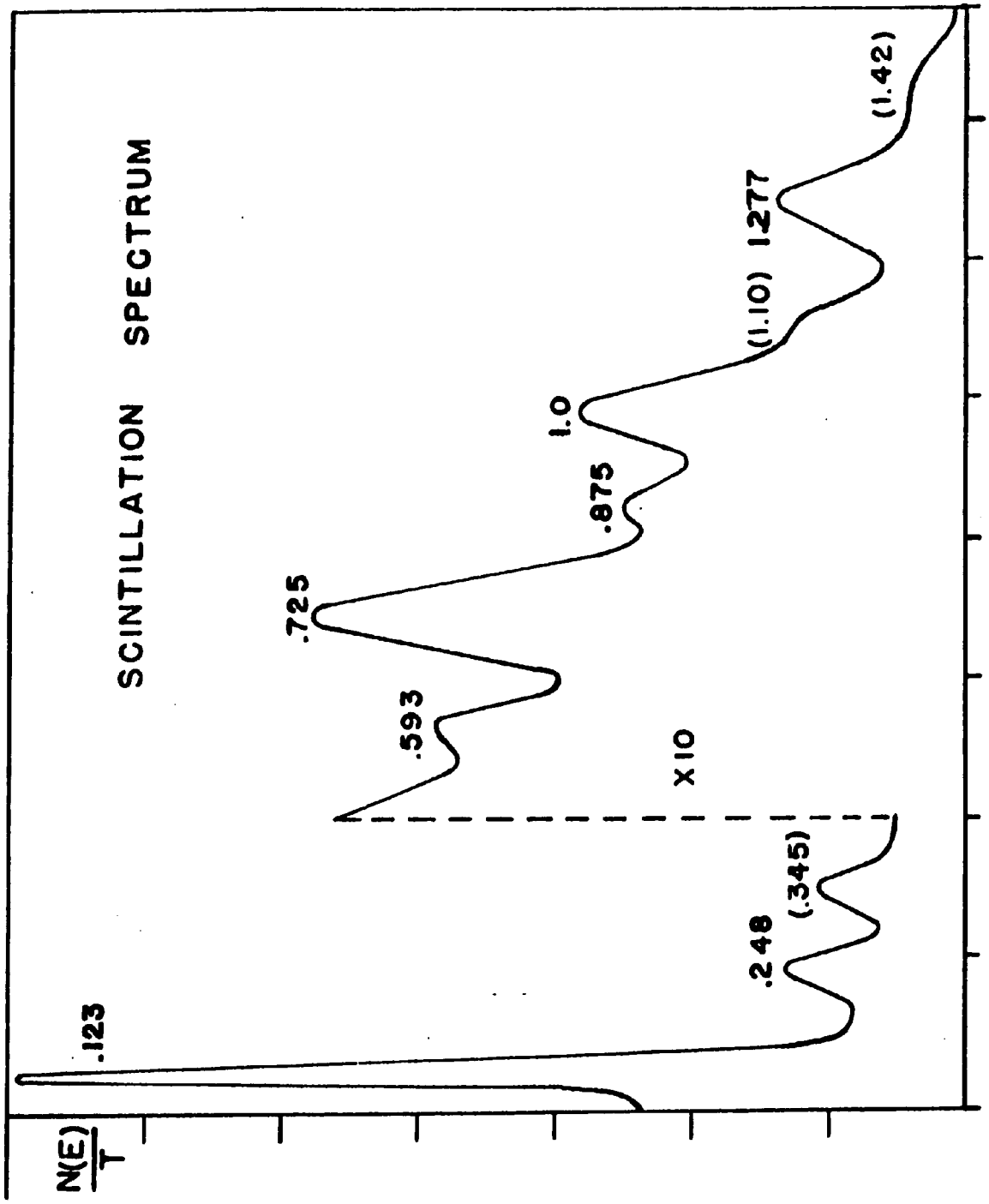


Figure 17. Scintillation Spectrum of Eu^{154}.

In all cases, a least squares fit of the correlation data was made to the function

$$F(\theta) = A_0' + A_2' P_2(\cos\theta) + A_4' P_4(\cos\theta)$$

The error flags on the experimental points represent the root mean square statistical errors. The effect of finite angular resolution was computed by the Rose[40] method.

Data were obtained on five cascades and the results have been interpreted, with the aid of conversion data, in terms of the model for spheroidal nuclei which was proposed by Alaga, et al.

Results

Directional Correlation of 0.123 Mev-0.248 Mev Gamma Rays

Discriminator (1) was set with a narrow window on the 0.123 Mev peak, while discriminator (2) was set with a narrow window on the 0.248 Mev peak. A least squares fit of the data to the function $F(\theta)$ corrected for solid angle gives

$$W(\theta) = 1 + (0.059 \pm 0.007)P_2 + (0.001 \pm 0.011)P_4$$

This is shown by the dashed curve in Figure 18. Nearly all the other gamma rays are in coincidence with the 0.123 Mev gamma ray, and, therefore, the Compton radiation which is produced from these gamma rays will also be counted as real coincidences, and must be subtracted in order to give the true correlation function for this cascade.

This was carried out in the following manner. Discriminator (1) was kept on the 0.123 Mev peak while discriminator (2) was moved

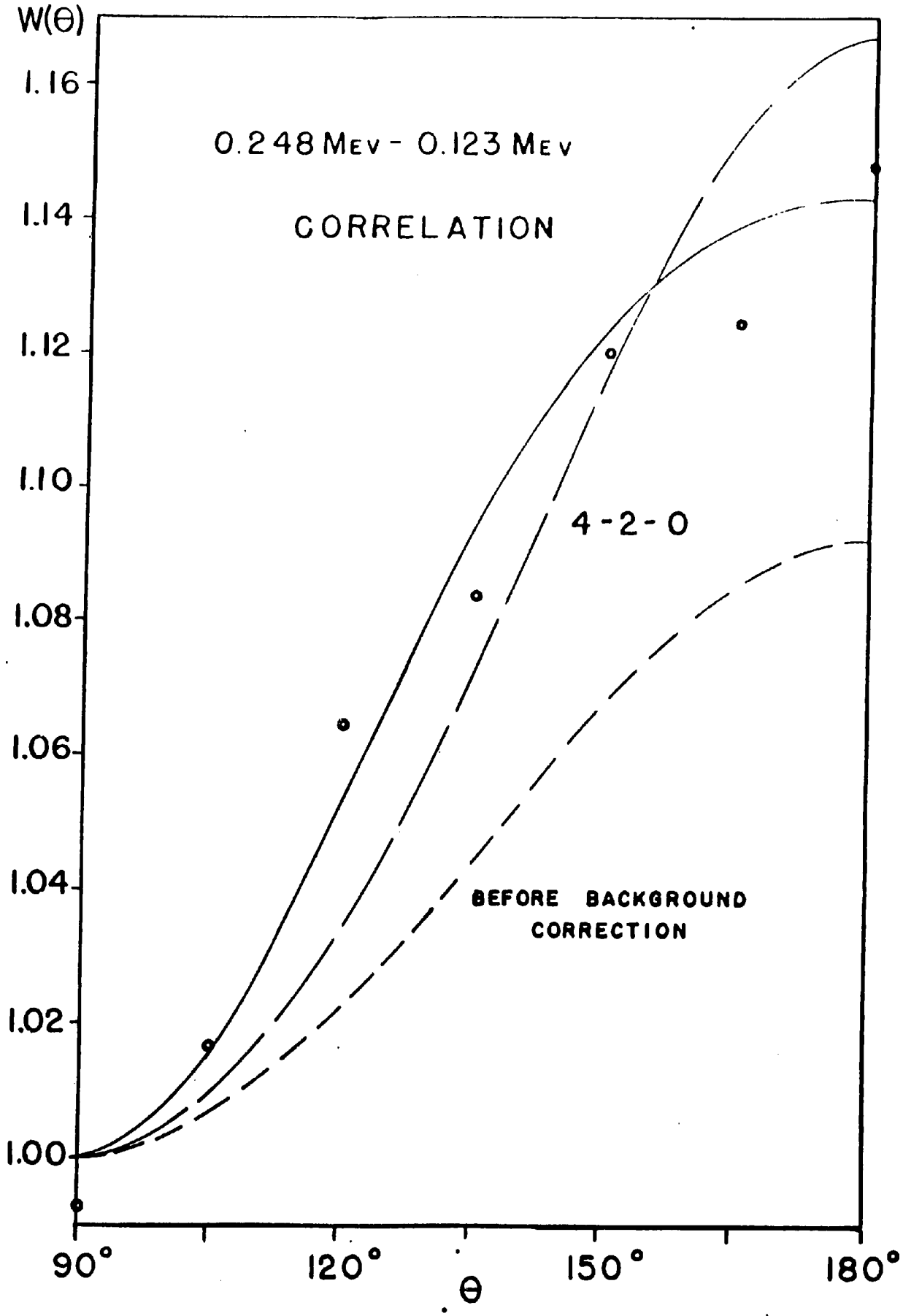


Figure 18. 0.248 Mev - 0.123 Mev Correlation in Gd^{154}.

to the high side of the 0.344 Mev peak, which belongs exclusively to Gd^{152}. The correlation was obtained for this arrangement. The coincidences were due entirely to the Comptons from the high energy gammas in coincidence with the 0.123 Mev gamma. This correlation function was nearly isotropic.

$$W(\theta) = 1 + (0.010 \pm 0.011)P_2 + (0.023 \pm 0.014)P_4$$

The result of this subtraction yields the corrected correlation function

$$W(\theta) = 1 + (0.098 \pm 0.018)P_2 - (0.020 \pm 0.024)P_4$$

shown as the solid curve in Figure 18, along with the corrected experimental points. The theoretical values for a 4(Q)2(Q)0 cascade are $A_2 = + 0.102$ and $A_4 = + 0.009$. Within the experimental accuracy, the data are in good agreement with 4(Q)2(Q)0 assignment for the second and first excited states respectively. (All even-even nuclei have a ground state spin of 0). The conversion data[64] also support the E2 character for both of these transitions. There is little doubt that this cascade is truly a 4(Q)2(Q)0 cascade, all with even parity.

It should be noted that nearly all the gamma radiation goes through the 0.123 Mev gamma transition, while the 0.371 Mev level is fed very weakly by the other gamma rays. Therefore, no correction was made for Compton gamma rays from higher energy radiations being in coincidence with the 0.248 Mev gamma ray.

Directional Correlation of 0.725 Mev-0.998 Mev Gamma Rays

One discriminator was set on the peak of the 0.725 Mev gamma with a narrow window, while the second discriminator was set with an

equally narrow window to include only the 1 Mev peak. There are two gammas at this energy, but only one is in coincidence with the 0.725 Mev gamma. The result of the 0.725 Mev-0.998 Mev correlation is

$$W(\theta) = 1 + (0.213 \pm 0.025)P_2 - (0.013 \pm 0.037)P_4$$

The experimental points and least squares curve are shown in Figure 19. Theoretical 6-2-0 and 5-2-0 curves are also shown in this figure. The coefficients for these two sequences are listed in Table II, along with those for 2(D)2(Q)0 sequence which is also in agreement with the experimental results.

TABLE II

"PURE" CORRELATION FUNCTIONS

Sequence	A_2	A_4
5-2-0	+0.179	-.004
6-2-0	+0.221	-.018
2(D)2(Q)0	+0.250	0

The values of A_2 and A_4 obtained in this experiment are plotted on a mixture curve for a 2(D,Q)2(Q)0 cascade in Figure 20. The required mixture, which is in agreement with both the A_2 and A_4 data, is found to be Q = 0.3 $\pm$ 0.3%. The 0.725 Mev gamma ray would be a mixture of 0.3% quadrupole and 99.7% dipole radiation.

The experimental data also support a 3(D,Q)2(Q)0 sequence as shown in Figure 21, with a mixture of 21.5 $\pm$ 6% Q. (It can also be fit with approximately 60% Q, but it is felt that with better statistics on the A_4 this would not be the case).

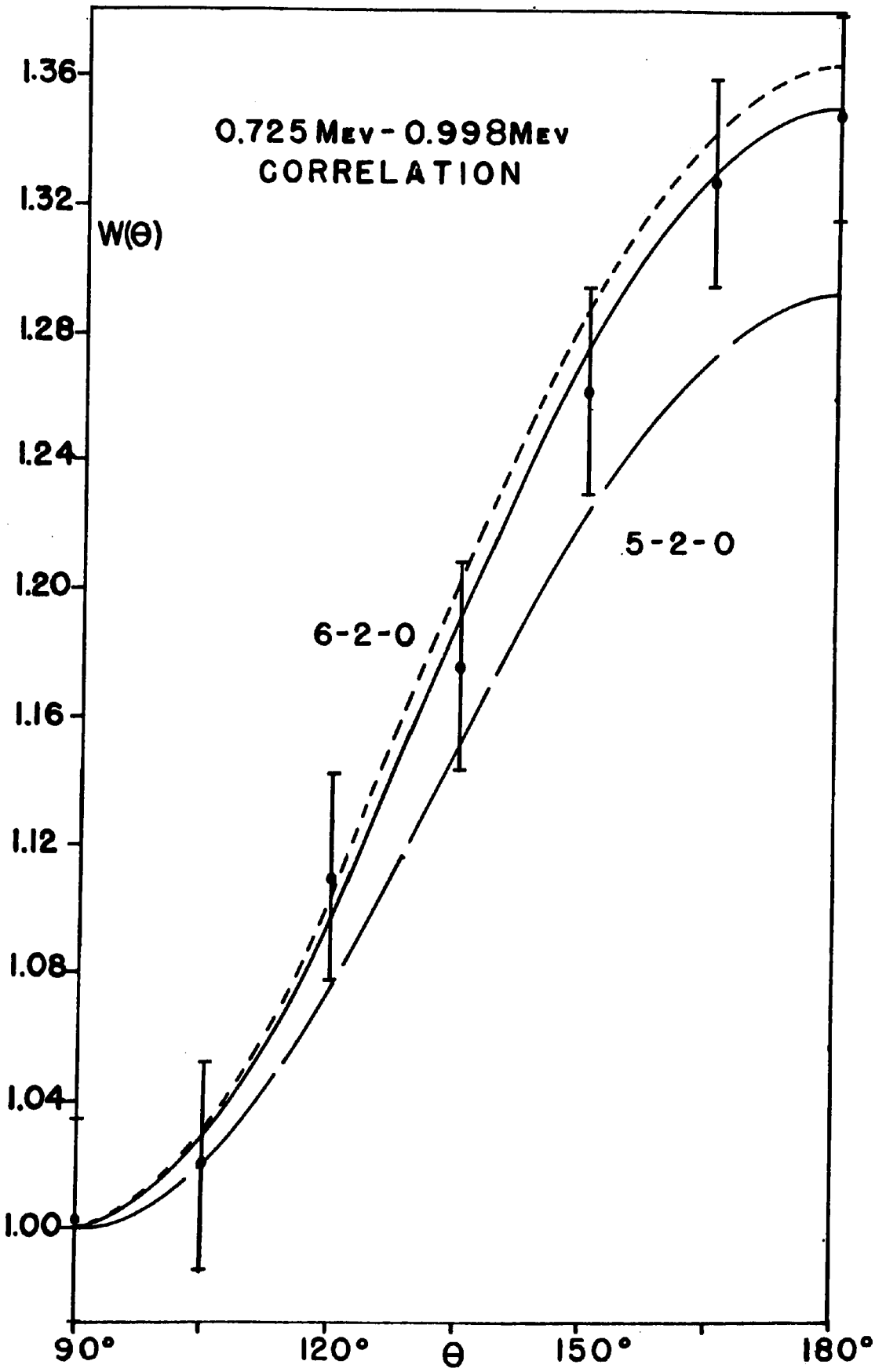


Figure 19. 0.725 Mev - 0.998 Mev Correlation in Gd^{154}.

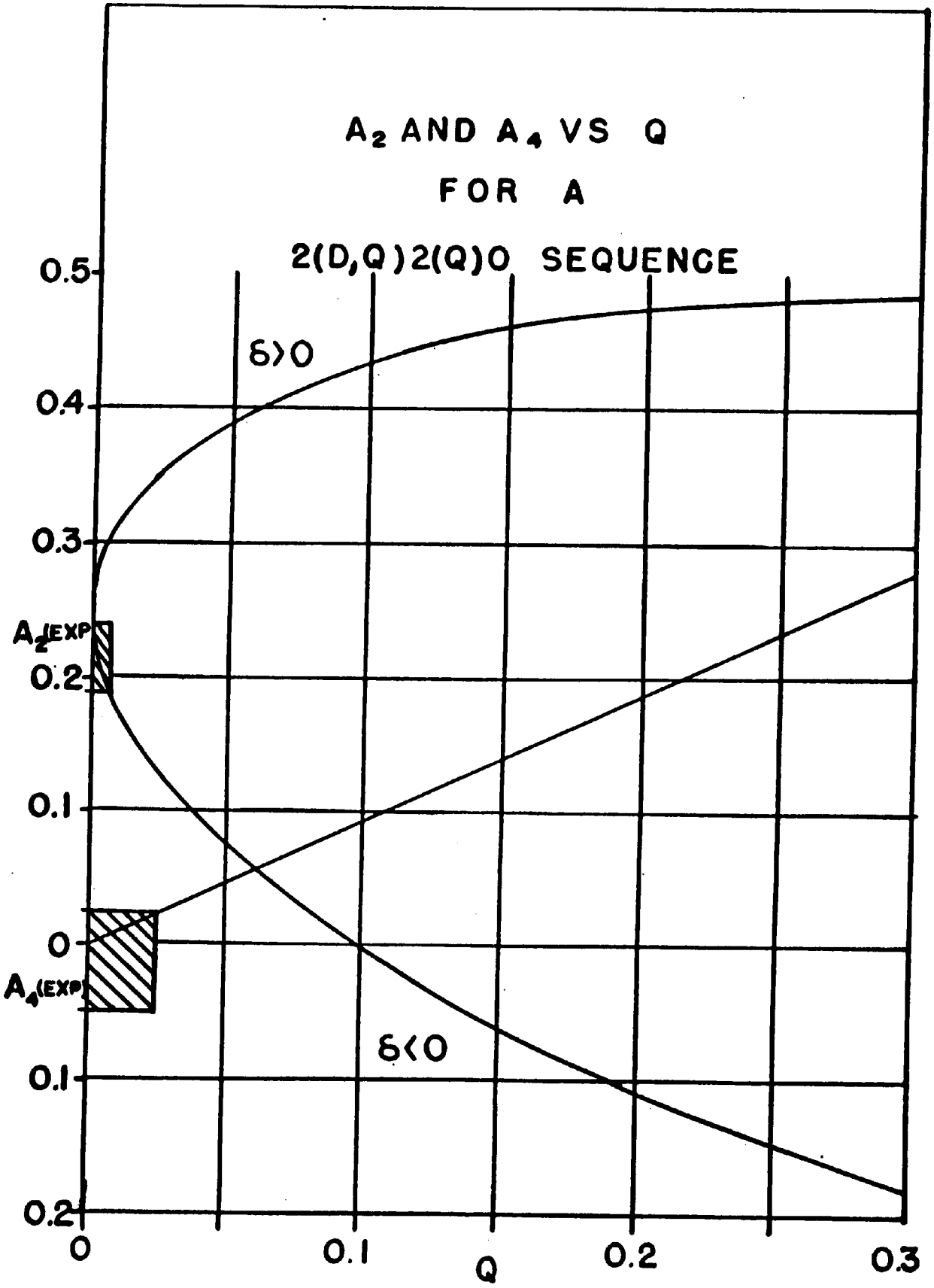


Figure 20. A_2 and A_4 Vs. Q for a 2(D,Q)2(Q)0 Sequence.

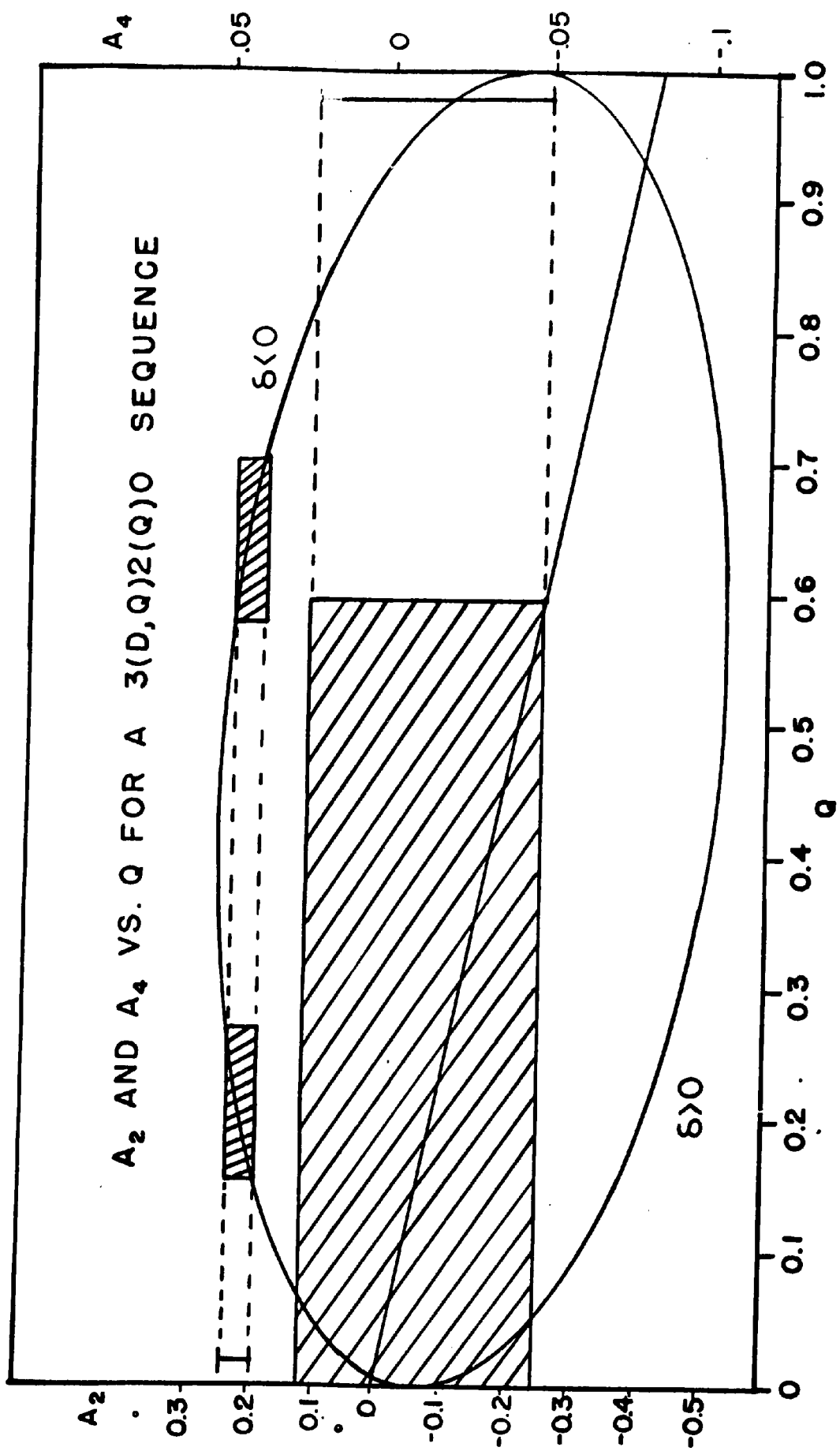


Figure 21. A_2 and A_4 Vs. Q for a 3(D,Q)2(Q)O Sequence.

If a spin of 4 is considered for the 1.723 Mev level, the 0.723 Mev gamma ray is required to have an octupole content of 6 ± 3% or 52 ± 6%. These results are summarized in Table III.

TABLE III

MIXTURE CONTENT OF HIGHER ORDER POLE RADIATION FOR THE 0.725 MEV GAMMA RAY FOR VARIOUS SPIN SEQUENCES

Spin Sequence	Higher Order Content	Percentage of Higher Order Content
2(D,Q)2(Q)0	Q	.3 ± .3%
3(D,Q)2(Q)0	Q	21.5 ± 6% 60% (?)
4(Q,0)2(Q)0	0	6 ± 3% 52 ± 6%

If a spin of 2 is assumed for the 0.998 Mev level, from the correlation data alone, spins of 2, 3, 4, 5, and 6 can be assigned to the 1.723 Mev level. Spins of 5 and 6 are precluded on the basis of the conversion data, and will not be given further consideration. The only other assignment of spin for the 0.998 Mev level which was given consideration was a spin of 1. If this level is assumed to have a spin of 1, then the correlation data can be fit by spins of 1 or 2 for the 1.723 Mev level with mixture in the .725 Mev gamma transition. A spin of 3 to the 0.998 Mev level was not given consideration as this requires the 0.998 Mev radiation to be pure octupole. This is in disagreement with the conversion data. In addition, if a spin 3 is assigned to the 0.998 Mev level, the transition to the 0.371 Mev (4+)

level would be expected to compete with the 0.998 Mev radiation to the ground state (0+). The transition from the 0.998 Mev level to the 0.371 Mev level is not observed.

Directional Correlation of 0.725 Mev-0.875 Mev Gamma Rays

One discriminator was set on the 0.725 Mev peak, while the second discriminator was set on the 0.875 Mev peak. As in the other correlations, narrow windows were used in order to keep interferring radiations to a minimum. This correlation yields

$$W(\theta) = 1 - (0.029 \pm 0.016)P_2 - (0.031 \pm 0.024)P_4$$

These data must be corrected for Compton radiation from the 0.998 Mev gamma being counted with the 0.875 Mev peak. This radiation is in coincidence with the 0.725 Mev radiation and yields the 0.725 Mev-0.998 Mev correlation. It is estimated that this interference is 30 $\pm$ 10%. When a value of 30% interference is considered, the resulting correlation function for the 0.725 Mev-0.875 Mev correlation is

$$W(\theta) = 1 - (0.133 \pm 0.024)P_2 - (0.039 \pm 0.037)P_4$$

These correlation results along with 20% and 40% subtractions are shown in Figure 22. It is seen that the interference which is caused by the 0.725 Mev-0.998 Mev coincidences changes the correlation function which is calculated for the 0.725 Mev-0.875 Mev correlation quite drastically. Although this is the case, it has been determined that the 0.875 Mev gamma ray requires an appreciable amount of quadrupole mixture, and possibly could be nearly 100% quadrupole which would be expected if a K value of 2 is assigned to the 0.998 Mev level.

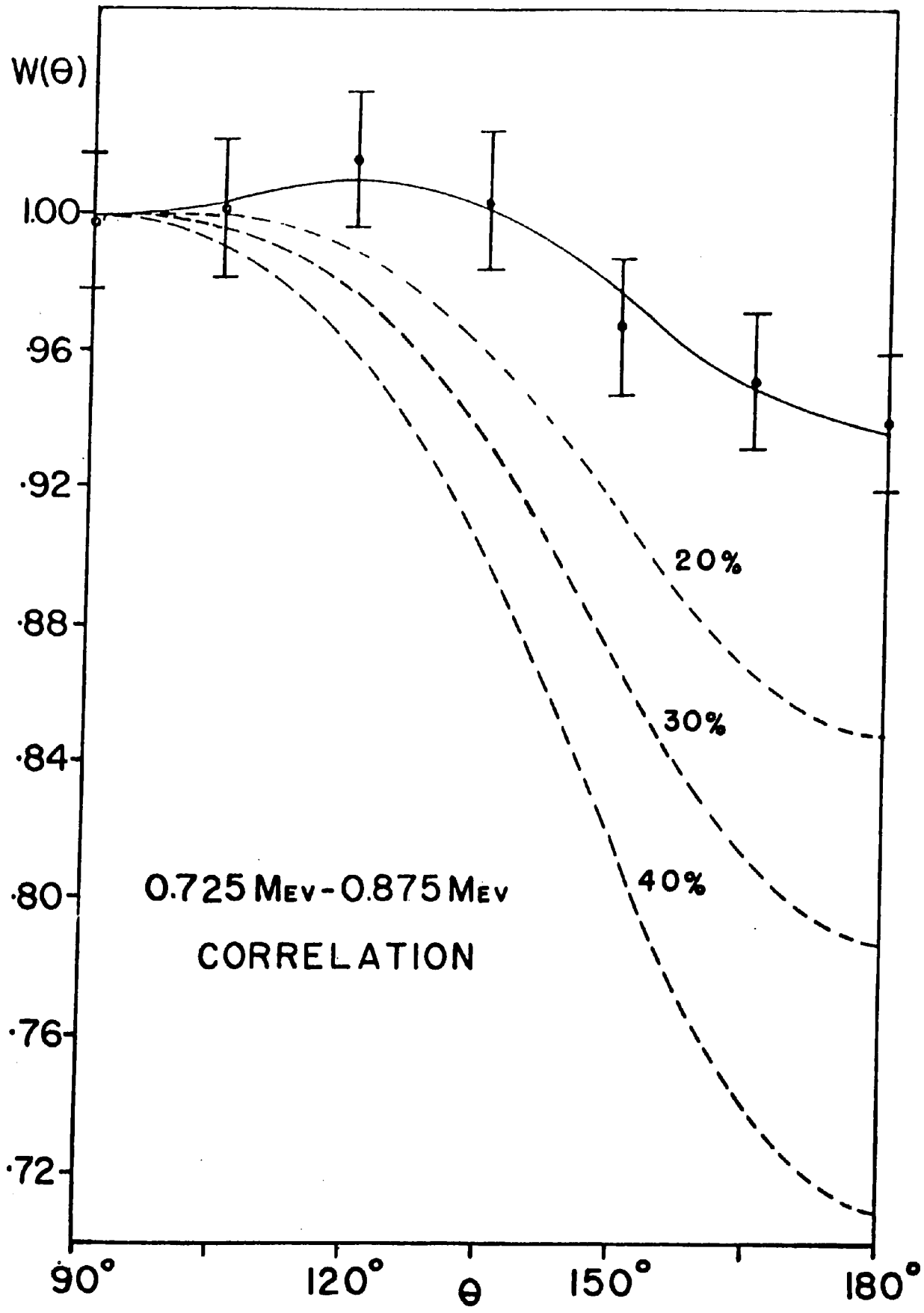


Figure 22. 0.725 Mev - 0.875 Mev Correlation in Gd^{154}.

Directional Correlation of 1.277 Mev-0.123 Mev Gamma Rays

One discriminator was set to detect the 0.123 Mev radiation with a narrow window, while the other discriminator was set on the 1.277 Mev peak, also with a narrow window. This was done in order to minimize the amount of 1.415 Mev radiation, arising from the contamination of Eu^{152}. This interference was estimated to be small and, therefore, no correction was made. In addition, this correlation gave approximately the same correlation function as has been reported for the 1.415 Mev-0.123 Mev correlation[66,67] in Sm^{152}, and, therefore, a small contamination could not change the results to an appreciable extent. The correlation function was found to be

$$W(\theta) = 1 + (0.191 \pm 0.010)P_2 - (0.007 \pm 0.015)P_4$$

The experimental points along with the least squares curve are shown in Figure 23. The theoretical 6-2-0 and 5-2-0 curves are shown on the same figure. Reference should be made at this time to Table II. As with the correlation between the 0.998 Mev-0.725 Mev gammas, the data can also be fit by 2(D,Q)2(Q)0, 3(D,Q)2(Q)0 and 4(Q,0)2(Q)0 sequences. These are shown in Figures 24, 25 and 26 respectively. The results are summarized in Table IV. According to the directional correlation measurements, therefore, the various spin assignments to the 1.400 Mev level can be given as 2, 3, 4, 5 and possibly 6. These are based on a spin of 2 for the 0.123 Mev level. Spins of 5 and 6 are precluded on the basis of the conversion data, and will not be given further consideration.

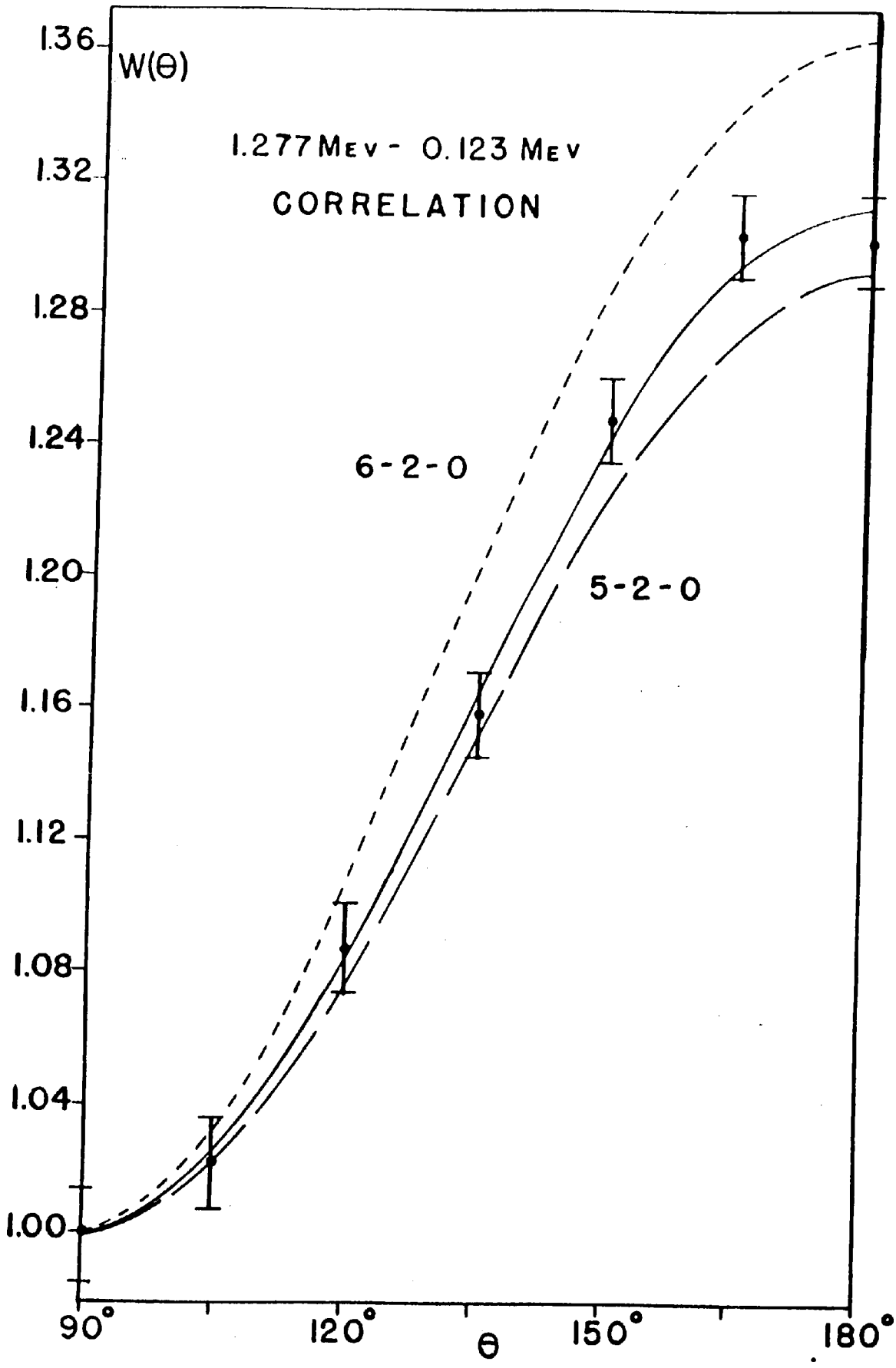


Figure 23. 1.277 Mev - 0.123 Mev Correlation in Gd^{154}.

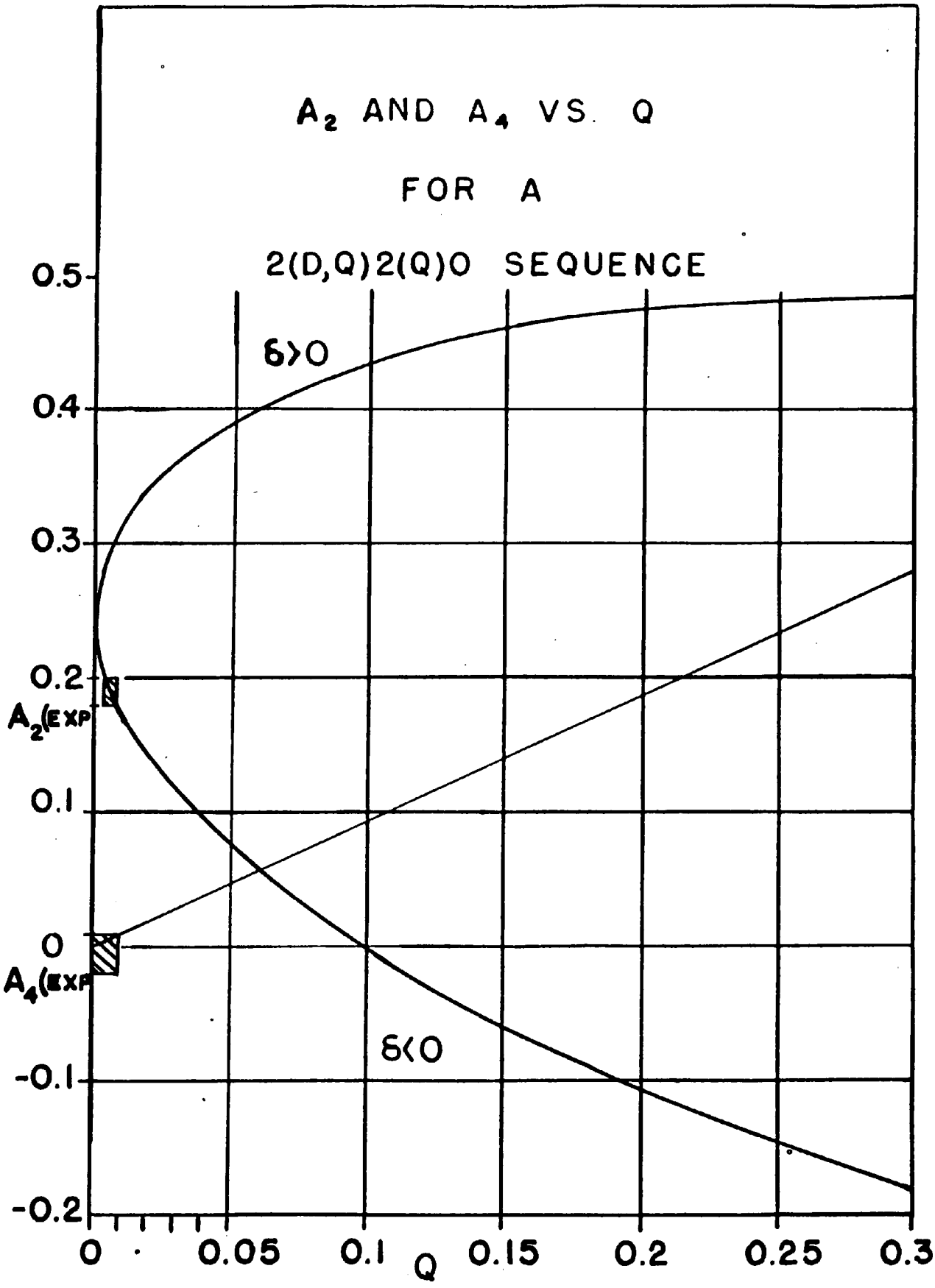


Figure 24. A_2 and A_4 Vs. Q for a 2(D,Q)2(Q)0 Sequence.

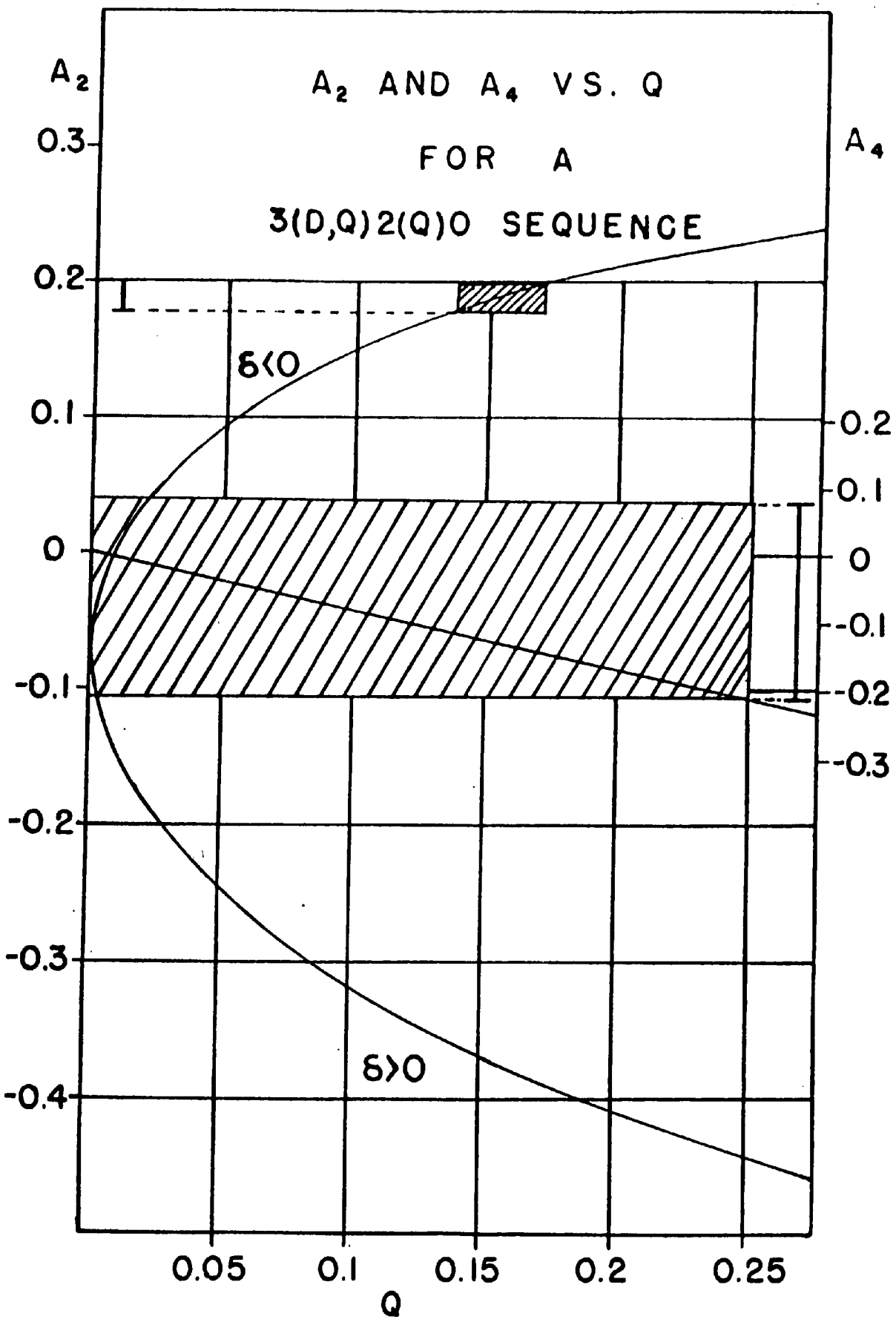


Figure 25. A_2 and A_4 Vs. Q for a 3(D,Q)2(Q)0 Sequence.

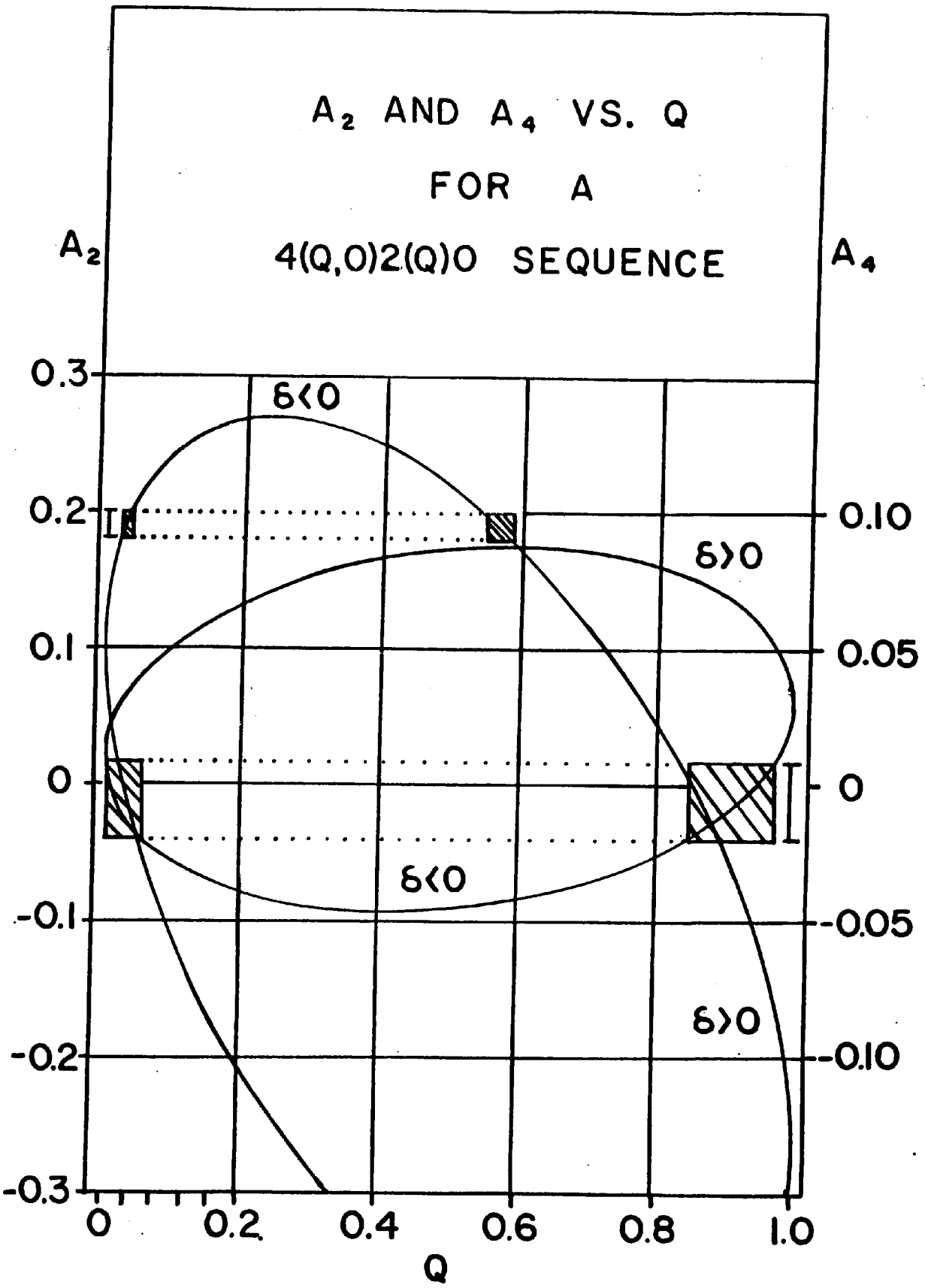


Figure 26. A_2 and A_4 Vs. Q for a 4(Q,0)2(Q)0 Sequence.

TABLE IV

MIXTURE CONTENT OF HIGHER ORDER POLE RADIATION FOR THE 1.277 MEV GAMMA RAY FOR VARIOUS SPIN SEQUENCES

Spin Sequence	Higher Order Content	Percentage of Higher Order Content
2(D,Q)2(Q)0	Q	0.5 ± 0.25%
3(D,Q)2(Q)0	Q	15 ± 2%
4(Q,0)2(Q)0	0	2.5 ± 1.5%

Directional Correlation of 0.593 Mev-1.007 Mev Gamma Rays

One discriminator was set on the 1 Mev peak, while the other was set on the 0.593 Mev peak. The correlation function is

$$W(\theta) = 1 + (0.047 \pm 0.016)P_2 + (0.005 \pm 0.023)P_4$$

The experimental points along with the least squares curve are shown in Figure 27.

This correlation had to be corrected for Compton radiation produced from the 0.725 Mev gamma which is in coincidence with the 0.998 Mev gamma. This was found to contribute about 25% of the total number of true coincidences. When the subtraction was carried out, the resultant correlation function was isotropic within the errors of the coefficients.

$$W(\theta) = 1 - (0.008 \pm 0.023)P_2 + (0.011 \pm 0.032)P_4$$

No effort was taken to fit these results to a particular sequence. Even a 10% error assigned to the subtraction process changes the correlation function to the extent that the sign of the asymmetry becomes uncertain.

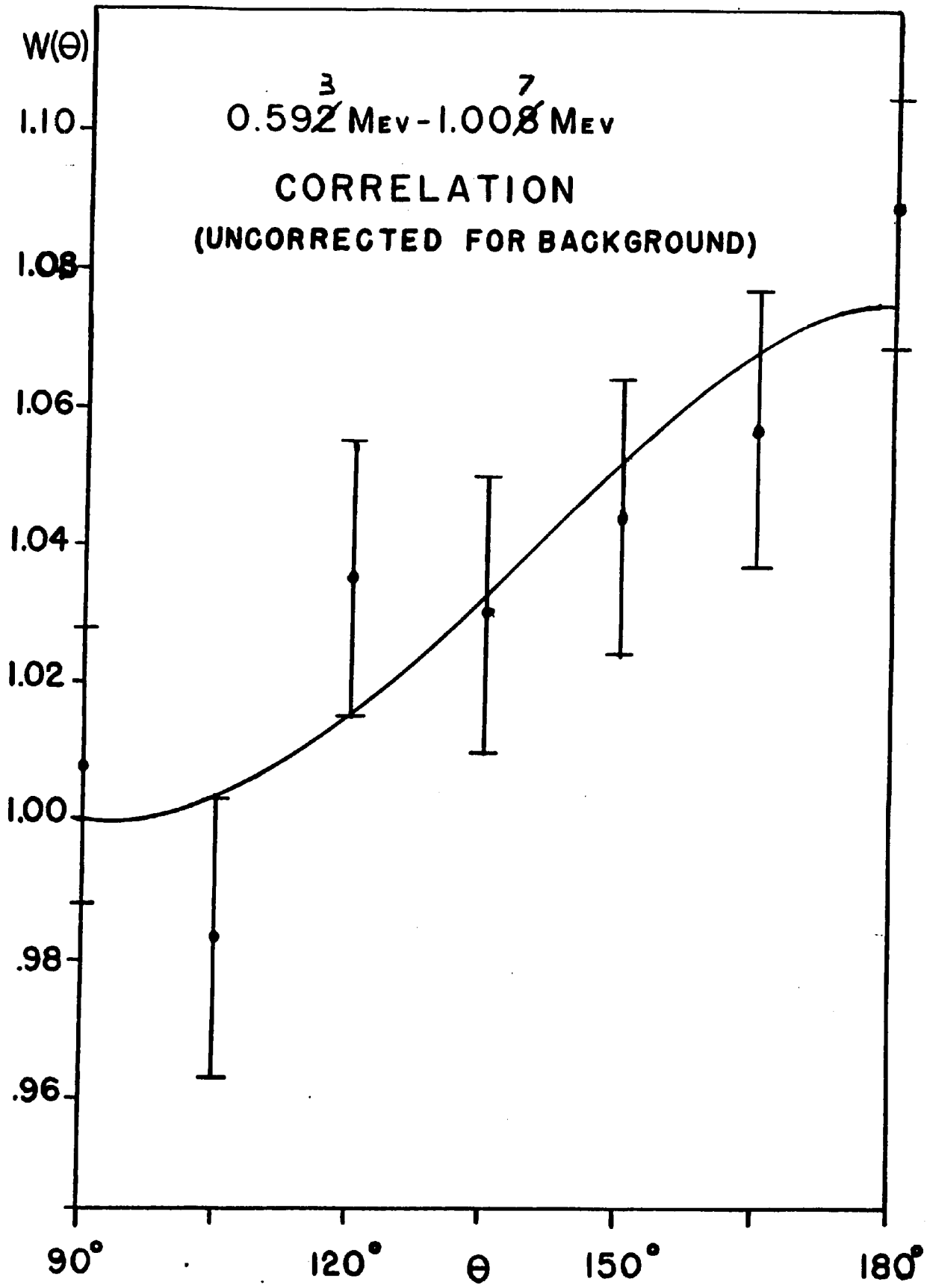


Figure 27. 0.593 Mev - 1.007 Mev Correlation in Gd^{154} - Uncorrected for Background.

Discussion

Gd^{154} may be characterized as a spheroidal nucleus, although admittedly it is on the very edge of the strongly deformed nuclei with its 64 protons and 90 neutrons. Nuclei whose equilibrium shape deviates strongly from spherical symmetry can be distinguished by two types of excitation[55-59]. These types of excitation have been described in Chapter IV. Gd^{154} is on the edge of the lower side of the rotational region. The rotational, or strong-coupling region is the region where the neutrons and protons are far away from closed shells. The shell which is of interest in this rotational region, is closed with 82 nucleons. If Equation (4.4) is assumed to hold in this case, it is found that the level at 0.371 Mev is 10% below the expected energy for the 4+ level belonging to the ground state rotational band. The 4+ character of the 0.371 Mev level is fairly certain as was seen from the correlation and conversion data.

Some of the 10% energy discrepancy between a 4+ level predicted by Equation (4.4) and that observed for the 0.371 Mev level may be due to "vibration-rotation" interaction. This "vibration-rotation" interaction is evidenced by a vibrational energy of approximately 1 Mev. This is the magnitude of energy that is observed for the third excited state in Gd^{154}. From conversion data, quantum numbers (2,2,+) and (2,3,+) were assigned to the 0.998 Mev and 1.130 Mev levels respectively. The quantum numbers refer respectively to K, I, and π. Using the experimental relative intensities, it is possible to compare the experimental reduced transition ratio (using the expressions of Chapter IV) with the theoretical values.

The relative intensities which are used to compute the experimental reduced transition ratios which appear in Tables V, VII and VIII, are those reported by Juliano and Stephens[64]. The errors on the experimental reduced transition ratios were obtained assuming the intensities of the gamma transitions correct to within 10%[64].

TABLE V

COMPARISON OF THE INTENSITIES OF THE TRANSITIONS FROM THE THIRD EXCITED STATE TO THE SECOND AND FIRST EXCITED STATES, $B(2 \rightarrow I_F)$, WITH THE INTENSITY OF THE TRANSITION FROM THE THIRD EXCITED STATE TO THE GROUND STATE, $B(2 \rightarrow 0)$, FOR VARIOUS VALUES OF K_i

Final State I_F	Experimental $\frac{B(2\rightarrow I_F)}{B(2\rightarrow 0)}$	Theoretical $K_i=0$	$B(2\rightarrow I_F)/B(2\rightarrow 0)$ $K_i=1$	$K_i=2$
2^+ (123 kev)	1.94 ± 0.27	1.43	0.357	1.43
4^+ (371 kev)	not observed	2.57	1.14	.071

It is seen that a spin of 2 and K value of 2 will fit the 0.998 Mev level very well. The theoretical reduced transition probability divided by the experimental value is equal to $74 \pm 12\%$. This may be considered as a rather good agreement with experimental data.

The conversion data[64] for a few of the gamma rays in Gd^{154} is given in Table VI. These conversion coefficients are reported to be good to within 20-30 percent.

TABLE VI

GAMMA-RAY ABUNDANCES, CONVERSION COEFFICIENTS, AND MULTIPOLARITY ASSIGNMENTS

E_γ	γ-ray abs.abun.	αK(Exp.)	αK(E1)*	αK(E2)	αK(M1)	αK(M2)	Probable Multipolarity
0.123	0.35	--					E2
0.248	--	--	--	--	--	--	E2
0.593	0.04	--	--	--	--	--	--
0.694	< 0.03	> 2.9×10^{-2}					M2 or higher
0.706	< 0.03	--	1.9×10^{-3}	4.9×10^{-3}	9×10^{-3}	2.4×10^{-2}	--
0.725	0.21	2.8×10^{-3}					E1,E2
0.759	< 0.03	> 5×10^{-3}					M1,E2,or higher
0.875	0.13	5.8×10^{-3}	1.4×10^{-3}	3.3×10^{-3}	5.8×10^{-3}	1.5×10^{-2}	M1
0.998	0.14	2.1×10^{-3}	1.1×10^{-3}	2.4×10^{-3}	4.2×10^{-3}	1.0×10^{-2}	E2
1.007	0.17	4.4×10^{-3}					M1
1.277	0.42	1.7×10^{-3}	7×10^{-4}	1.5×10^{-3}	2.4×10^{-3}	5.7×10^{-3}	M1,E2,M1-E2
~1.6	0.03	--	--	--	--	--	--

* Theoretical K-conversion coefficients of Sliv, Reference 68.

A comparison between theoretical and experimental reduced transition ratios has been carried out for the gamma rays originating from the level at 1.130 Mev. The results are shown in Table VII.

TABLE VII

COMPARISON OF THE INTENSITY OF THE TRANSITION FROM THE FOURTH EXCITED STATE TO THE SECOND EXCITED STATE, $B(3 \rightarrow 4)$, WITH THE INTENSITY OF THE TRANSITION FROM THE FOURTH EXCITED STATE TO THE FIRST EXCITED STATE, $B(3 \rightarrow 2)$, FOR VARIOUS VALUES OF K_1

Final State I_F	Experimental $\frac{B(3 \rightarrow I_F)}{B(3 \rightarrow 2)}$	Theoretical $K_1 = 0$	$B(3 \rightarrow I_F)/B(3 \rightarrow 2)$ $K_1=1$	$K_1=2$
4+ (371 kev)	0.85 ± 0.12	$B(3 \rightarrow 4) = 0$ $B(3 \rightarrow 2) = 0$	2.50	.40

Here again it appears that a value of K = 2 is most consistent with the experimental data. The rather high experimental value compared to the theoretical value is not surprising considering the lack of information on the 759 kev gamma ray.

In all the above calculations it was assumed that all transitions occurring were L = 2 type radiation.

Of the four gamma rays which have been under consideration, the 0.998 Mev gamma ray certainly appears to be of E2 character which would demand an assignment of 2+ to the 0.998 Mev level. The conversion data also support an E2 character to the 0.759 Mev gamma ray, and although both the 0.875 Mev and 1.007 Mev gamma rays appear, from conversion data, to be closer to M1 type radiation, the experimental conversion coefficients would have to be changed by less than a factor of 2

in both cases to make them compatible with E2 radiation. If K is considered a good quantum number, L = 1 radiation is forbidden with a resultant increase of E2 radiation. It thus appears that the 0.998 Mev and 1.130 Mev levels may be considered to be members of a second rotational band which is due to a vibration-rotation interaction of approximately 1 Mev. This band would be a γ-vibrational band with K = 2, I = 2, 3, and even parity. The energy difference of 0.132 Mev between these two levels is very close to the 0.123 Mev separation of the first excited state from the ground state. This would imply a value for the moment of inertia for this second band close to the ground state moment of inertia. The transition from the 1.130 Mev level to the 0.998 Mev level is calculated to be too weak to be observed. This transition has not been found. The state at 0.998 Mev could possibly be assigned a spin of 1, although the conversion data does not seem to fit either an M1 or E1 as well as it does an E2. Based on the observed intensities of the gamma rays originating from the level at 1.130 Mev, the spin assignment of 3 to the 1.130 Mev level seems to be favored. The conversion data is in best agreement with a positive parity assignment. The assignment of 2+ to the 0.998 Mev level and 3+ to the 1.130 Mev level might be expected from the systematics in this rotational region. A few other deformed nuclei in this region have been found to exhibit two states lying approximately 1 Mev above the ground state and having the same energy separation as exists between the first excited state and the ground state. The classification of these two states has been made as 2+, 3+, respectively in the order of increasing energy. The possibility of spins of 2 or 4 to the 1.130 Mev level cannot be

completely eliminated. Due to the contamination of Eu^{152} which was present in the source used in the correlation study, the directional correlation of the 1.007 Mev-0.123 Mev gamma rays was not attempted. If this correlation were done with a "pure" source of Eu^{154}, a more unique assignment of quantum numbers to the 1.007 Mev level might be made.

The correlation data is consistent with spins of 2, 3, and 4, for the 1.400 Mev state. The results are given in Table IV. A 4- interpretation is not in agreement with the conversion data. A 4+ interpretation would require an E2-M3 mixture. This would require an M3 transition probability greatly enhanced over the single particle estimate. Such a mixture, while not common, cannot be eliminated completely.

It appears that the level at 1.400 Mev is in best agreement with the directional correlation data, the observed intensities, and the conversion data, if spins of 2 or 3 are considered for this level. The directional correlation results, Table IV, show that with either the assignment of I = 2 or 3 to the 1.400 Mev level, the 1.277 Mev gamma ray is mainly dipole radiation (less than 17% quadrupole). If the most probable assignment of K and I to this state is given as (2, 2) or (3, 3), it is seen that in either case dipole radiation should be K forbidden for the 1.277 Mev gamma ray. It appears that there is at least a partial breakdown of K as being a good quantum number.

From the correlation data, it has been shown that spins of 2, 3, and 4 should be considered as possibilities for the 1.723 Mev

level, Tables II and III. Spins and K values of (2, 2) and (3, 3) and (4, 4) are in agreement with the experimental data. This is shown in the following table.

TABLE VIII

COMPARISON OF THE INTENSITY OF THE RADIATION FROM THE 1.723 MEV LEVEL TO THE 0.998 MEV LEVEL WITH THAT TO THE 1.130 MEV LEVEL, ASSUMING VARIOUS VALUES OF K AND I FOR THE 1.723 MEV LEVEL. THE TRANSITIONS WERE ASSUMED TO BE EITHER BOTH DIPOLE OR BOTH QUADRUPOLE RADIATION

K_i	I_i	L_1, L_2	Theoretical $\frac{B(I_i \rightarrow 2)}{B(I_i \rightarrow 3)}$	Experimental $\frac{B(I_i \rightarrow 2)}{B(I_i \rightarrow 3)}$
4	4	2 2	1.79	1.91 ± 0.27
3	3	1 1	2.86	2.86 ± 0.40
3	3	2 2	.86	1.91 ± 0.27
3	4	2 2	7.14	1.91 ± 0.27
2	4	2 2	.45	1.91 ± 0.27
2	3	2 2	∞	1.91 ± 0.27
2	3	1 1	.71	2.86 ± 0.40
2	2	1 1	2.00	2.86 ± 0.40
2	2	2 2	.57	1.91 ± 0.27

The correlation data show that in order for spin 4 to be assigned to the level at 1.723 Mev, an appreciable octupole content would have to be included in the 0.725 Mev radiation. This is not in agreement with the conversion data which shows the 0.725 Mev radiation to be either E1 or E2. With a spin 2 or 3 for this level, K can be no

larger than 2 or 3 respectively. Dipole radiation to the levels at 0.998 Mev and 1.130 Mev is not K forbidden. Dipole radiation is expected to predominate. This is confirmed from the correlation results, Table III. Since the conversion data on the 0.725 Mev radiation favors either E1 or E2 over that of M1 or M2, the negative parity seems to be favored for the 1.723 Mev level. This requires the "unfavored" mixture between E1 and M2. For a 2- assignment to this level, the mixture will be (99.7% E1-0.3%M2) for the 0.725 Mev gamma ray. The 3- assignment requires a mixture of (78.5%E1- 21.5%M2) for the 0.725 Mev gamma ray.

From the high log ft values, it appears that K forbiddenness is of great importance. It has been predicted that Eu^{154} has (3, 3, -) for the quantum numbers describing the ground state.[63,64] Recently, the ground state has been measured to be 3[69]. This could account for the lack of a beta transition to the (0, 0, +) member and low percentages to the other two members of the K = 0 band. The log ft values get smaller and the percentages of the beta transitions get larger for the higher excited states. A value of K = 2 for the 1.130 Mev and 0.998 Mev levels is in good agreement with this. The beta data gives a percentage of 42% to the 1.400 Mev level, and 28% to the 1.723 Mev level. This suggests a K value of 2 or larger for these states, and, therefore, agrees with the possible assignments that have been listed for these two levels. If the negative parity is maintained for either of these states, the level might be interpreted as lying in an octupole vibration band.

It has been pointed out by Juliano and Stevens[64] that K forbiddenness could explain the high log ft values to the ground state rotational band members as Δ K would be equal to 3. Hence, so far as K

is a good quantum number, these transitions would be second or higher forbidden. However, such is not the case for the beta transitions leading to the higher excited states. The values of Δ I and Δ K for these transitions indicate that the beta transitions should be either allowed or first forbidden. Although the log ft values do get smaller for these higher excited states, the smallest log ft value observed is around 9, instead of 7 or less. The quantum number K appears to be a good quantum number for some of the data obtained on this radioactive nucleus, for some of the data there seems to be at least a partial breakdown of the K selection rules.

CHAPTER VI

DIRECTIONAL CORRELATION OF THE GAMMA RAYS IN W^{182}

Introduction

The decay of Ta^{182} has been the subject of a number of investigations.[70-78] The mode of decay of this isotope has been extensively investigated by Murray, Boehm, Marmier, and Dumond.[75] It is the work of this group which is the basis of the present study. The decay scheme proposed by Murray et al. is shown in Figure 28. Murray et al. were able to measure internal conversion coefficients for a number of the gamma transitions occuring in W^{182}. These conversion coefficients along with the gamma intensities and predicted multipolarities of the gamma rays are presented in Table IX. Theoretical conversion curves for M1, M2, M3, E1, E2, and E3, based on the tables of Rose, are given in Figures 29 and 30. The experimental values of α_k for the various gamma rays obtained by Murray et al., are plotted on these curves.

Alaga, Alder, Bohr, and Mottelson[55] assumed the decay scheme of W^{182} proposed by Murray et al. With the aid of this decay scheme and the information on the multipolarities of the gamma rays which was obtained by Murray et al., Alaga et al., were able to classify the gamma transitions and the excited states of W^{182} by the theory for deformed nuclei (Chapter IV). They were able to place the energy levels into three rotational bands, with the possibility of the start of a fourth band. The quantum numbers (K, I, Π) listed in Figure 28 are those given by Alaga et al. In general the spin values (I) are in agreement with those values given by Murray et al. In a few cases the intensities of

TABLE IX

DATA FOR TRANSITIONS IN W^{182}

Initial and Final Energy Levels	γ-ray Energy (kev)	γ-ray Intensity	Internal Conversion Coefficients αK	αLI	αLII	αLIII	αTotal	Multi-polarity
			Transitions in W^{182}					
ED	33.36±0.01	Weak	--	--	--	--	--	(E1)
HG	42.71±0.01	Weak	--	--	--	--	--	(E1)
KJ	65.71±0.01	7.5	--	2.8	0.4	0.23	4.0	M1(+E2)
FD	67.74±0.01	85	--	0.17	0.07	0.07	0.31	E1
HF	84.67±0.02	5	--	1.8	0.6	0.5	(8)	M1(+E2)
BA	100.09±0.02	40	1.5	0.13	1.45	1.35	5.0	E2
JH	113.66±0.02	7.5	1.7	0.4	0.07	--	2.2	M1
KI	116.40±0.02	1.7	--	--	--	--	--	--
HD	152.41±0.03	35	0.07	--	--	--	0.07	E1
JG	156.37±0.04	11.5	Small	--	--	--	--	(E1)
KH	179.36±0.05	16	0.41	0.17		0.05	0.58	M1+E2
JF	198.31±0.06	7.5	0.24	--	0.11	0.07	0.36	E2
KG	222.05±0.07	35	0.06	0.01	--	--	0.07	E1
CB	229.27±0.08	20	0.16	--	0.05	0.03	0.24	E2
KF	264.09±0.10	22	0.11	--	0.04	0.02	0.17	E2
EC	927 ±1	--	--	--	--	--	--	(E3)
FC	960 ±1	--	--	--	--	--	--	(E3)
GC	1003 ±1	--	--		K/L=7.0		0.006	(M1+E2)
DB	1122 ±1	100	0.005		K/L=6.7		0.006	M1+E2
EB	1155 ±1	6.5	0.004	--	--	--	0.005	(M2)
FB	1189 ±1	45	0.006		K/L=6.5		0.007	M2+E3
DA	1222 ±1	95	0.003		K/L=6.0		0.0035	E2
GB	1231 ±1	50	0.003	--	--	--	0.0035	E2
FA	1289 ±1	--	--		K/L=6.6		--	(M2)
HA	1375 ±2	--	--	--	--	--	--	(E3)
IA	1437 ±4	--	--	--	--	--	--	--
KB	1454 ±4	--	--	--	--	--	--	(M2+E3)

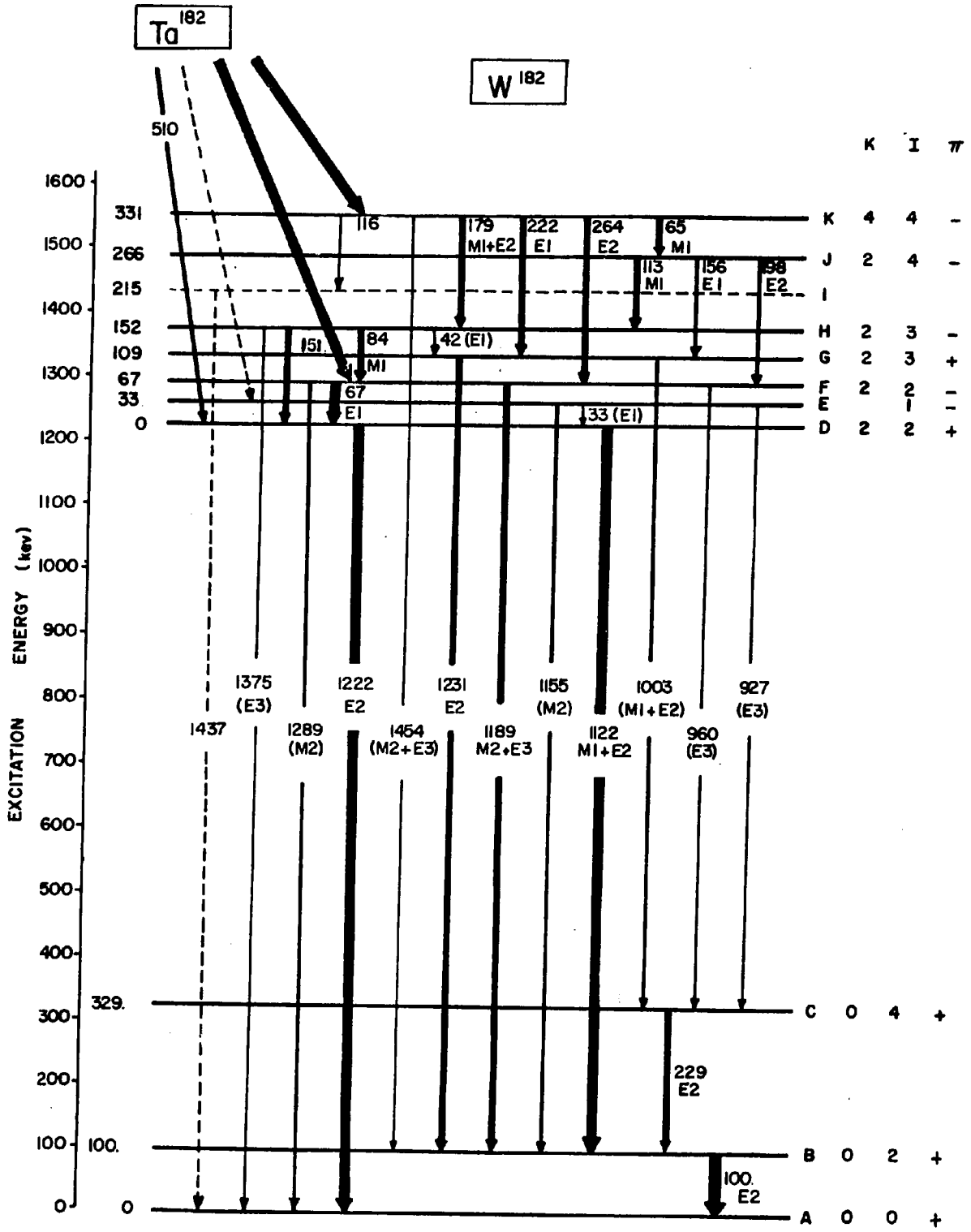


Figure 28. Decay Scheme of Ta^{182}

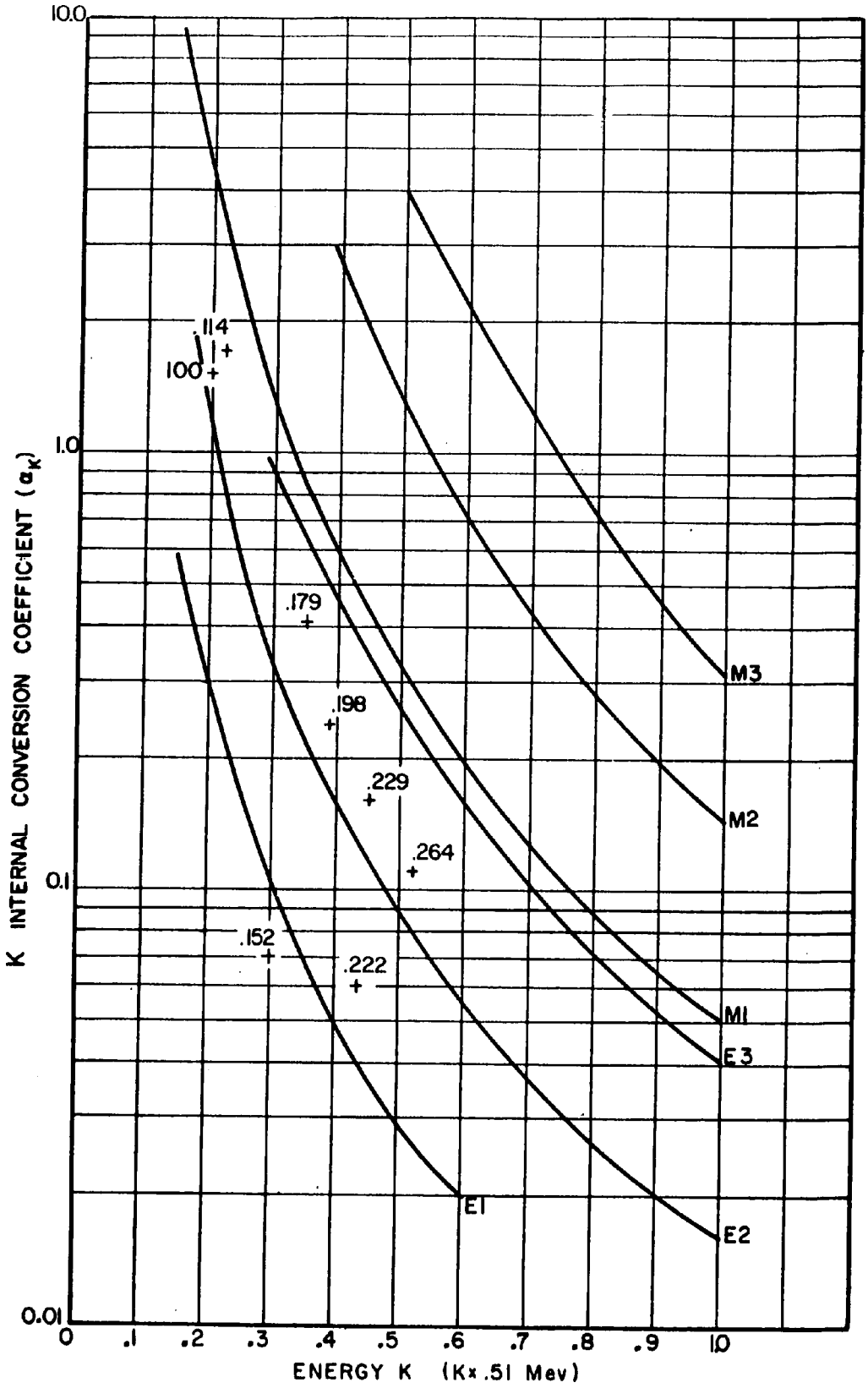


Figure 29. Comparison of Theoretical (Curves) and Experimental K-Shell Internal Conversion Coefficients for E1,E2, E3,M1,M2 and M3 Transitions in W^{182} (Crosses).

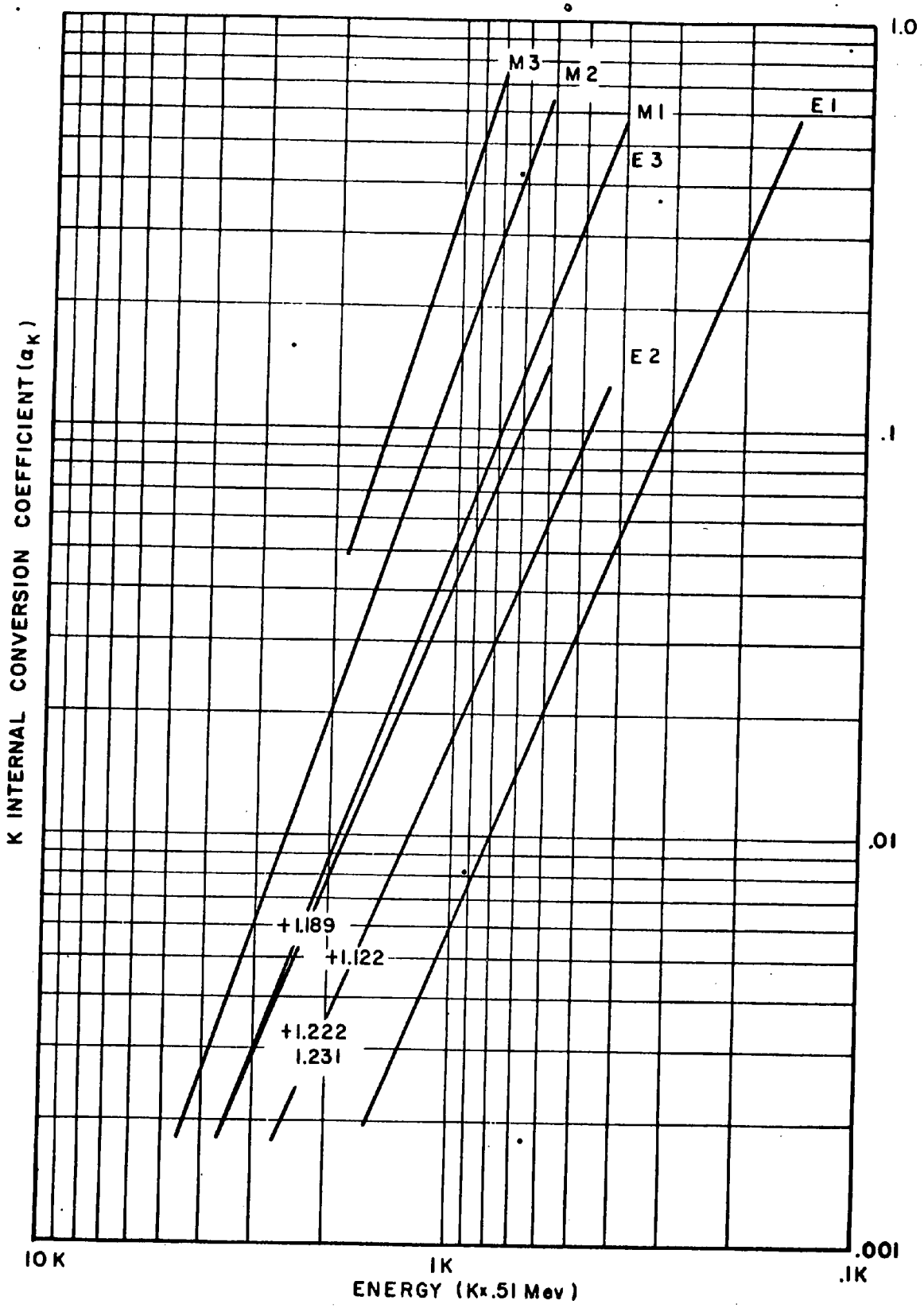


Figure 30. Comparison of Theoretical (Curves) and Experimental K-Shell Internal Conversion Coefficients for E1,E2, E3,M1,M2 and M3 Transitions in W^{182} (Crosses).

the gamma rays originating from a member of one rotational band to members of another rotational band are in agreement with those predicted by the reduced transition probabilities given by Alaga et al. (Chapter IV.) These will be discussed later in greater detail.

An investigation of this complicated decay scheme of W^{182} was undertaken using angular correlation techniques. From these measurements, along with the work of the previous investigators, it was hoped that more definite assignments of spins to the excited states of W^{182} could be made. In the cases where the gamma rays do not appear to be pure transitions, an analysis of the mixture content of the gamma rays was attempted.

Results

The scintillation gamma spectrum of W^{182} is given in Figure 31. The angular correlation results are given in Table X. These results have been interpreted, with the aid of conversion data and intensities of the gamma rays, in terms of the Collective Model for deformed muclei.

Directional Correlation of 1.222 Mev-0.068 Mev Gamma Rays

One discriminator was set integrally on the 1.222 Mev peak, while the other discriminator was set with a narrow window on the 0.068 Mev peak. The base line of the discriminator which accepted the 1.222 Mev gamma ray was set high on the 1.222 Mev peak to keep the interference from the 1.122 Mev radiation to a minimum. The result of this measurement yields $W(\theta) = 1 + (0.164 \pm 0.013) P_2 - (0.026 \pm 0.020) P_4$ The correlation curve and the experimental points are shown in Figure 32.

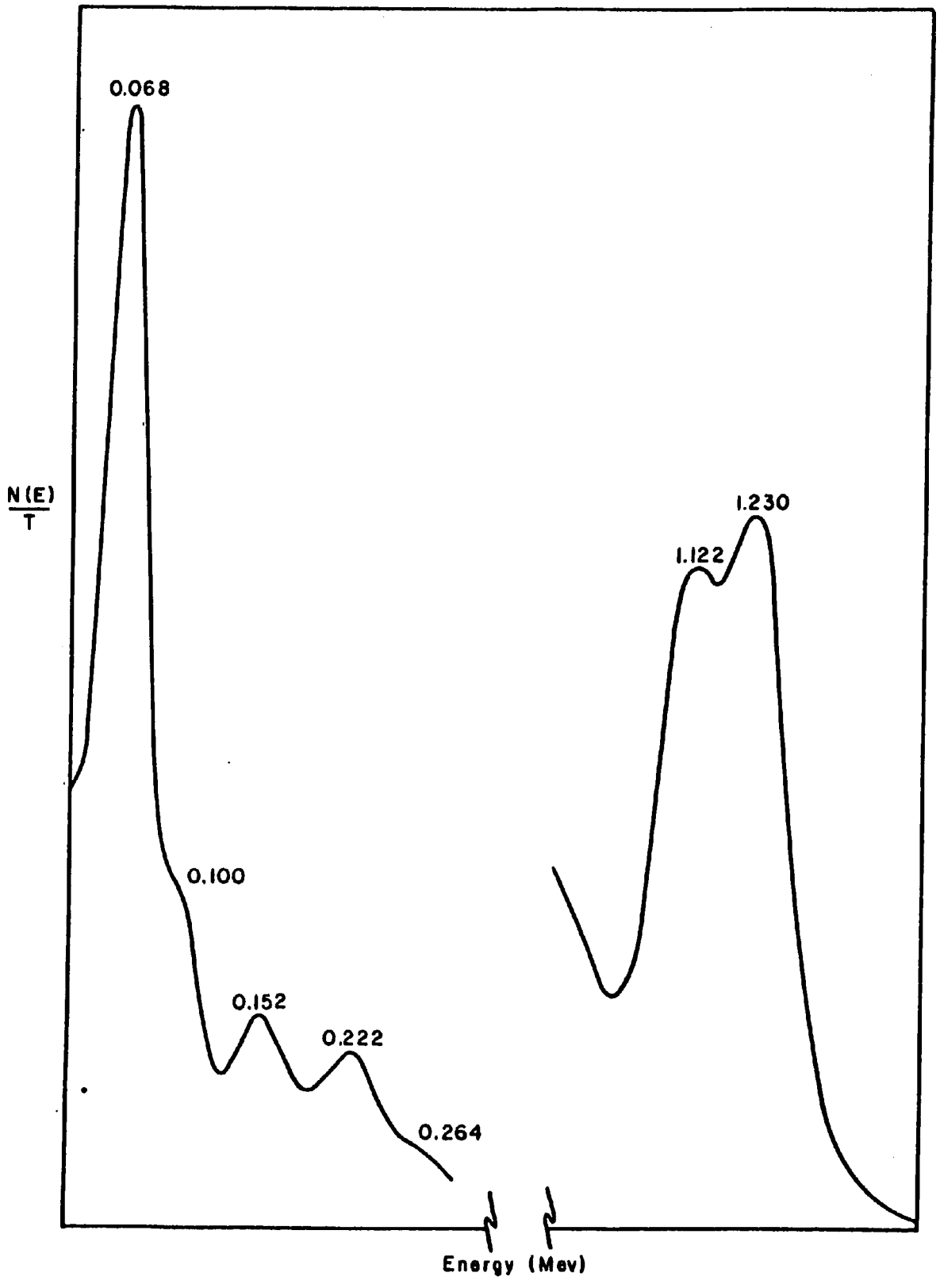


Figure 31. Scintillation Spectrum of Gamma Rays in W^{182}.

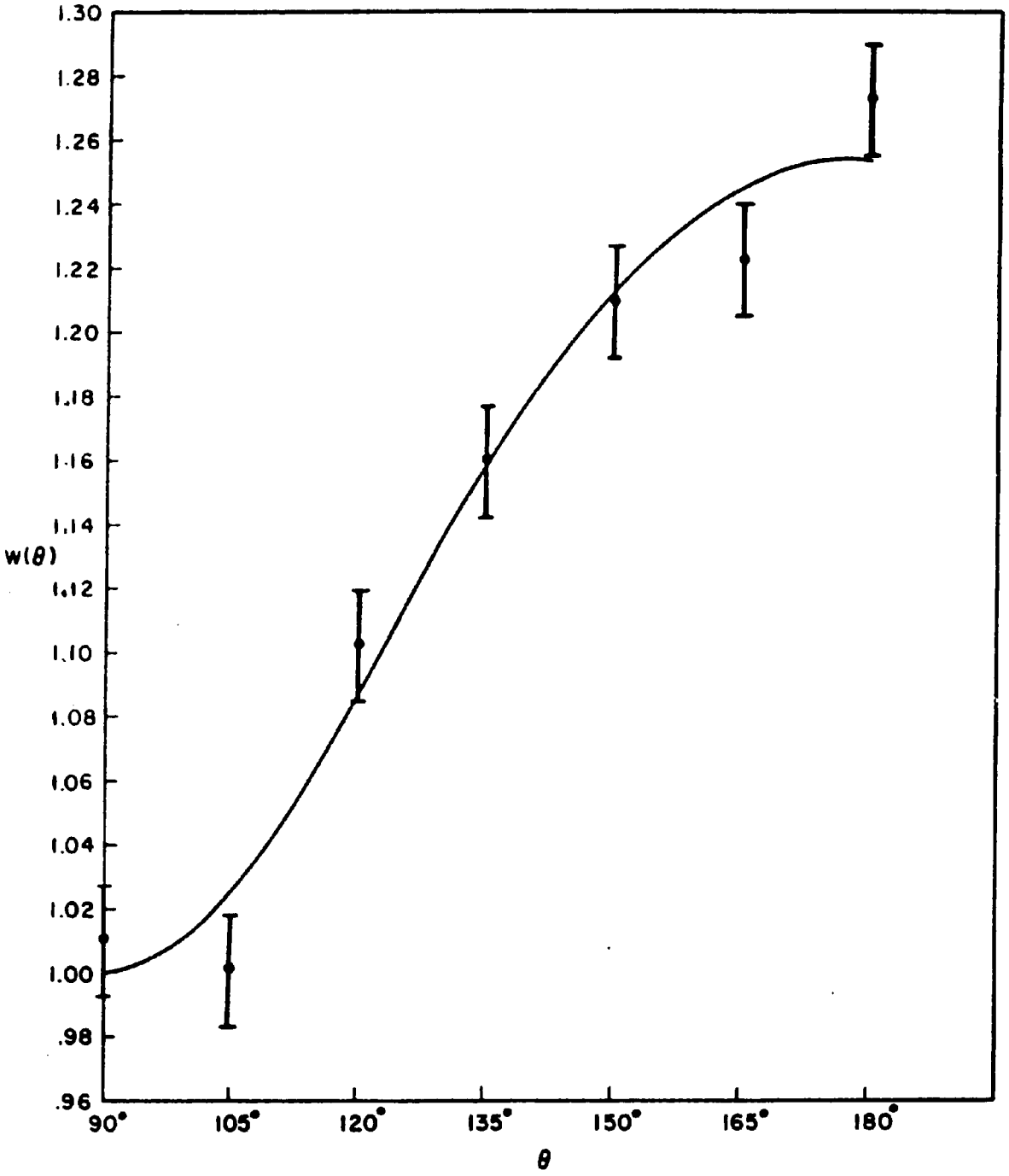


Figure 32. 1.222 Mev - 0.068 Mev Correlation in W^{182}.

TABLE X

DIRECTIONAL CORRELATION RESULTS

(Gamma Transitions Involved)	$A_2 \pm \epsilon_2$	$A_4 \pm \epsilon_4$
1.222 Mev - 0.068 Mev	+0.164 ± 0.013	-0.026 ± 0.020
1.222 Mev - 0.264 Mev	+0.076 ± 0.035	+0.016 ± 0.055
1.231 Mev - 0.222 Mev	-0.012 ± 0.014	-0.001 ± 0.020
1.122 Mev - 0.152 Mev	-0.010 ± 0.014	+0.013 ± 0.019
1.222 Mev - 0.152 Mev	-0.037 ± 0.012	+0.003 ± 0.018
(1.222 + 1.122)Mev - 0.152 Mev	-0.024 ± 0.012	-0.004 ± 0.017
1.231 Mev - 0.100 Mev	+0.037 ± 0.012	-0.002 ± 0.018
Before Background Subtraction (0.222 + 0.229)Mev - 0.100 Mev	+0.027 ± 0.011	+0.027 ± 0.016
After Background Subtraction (0.222 + 0.229)Mev - 0.100 Mev	+0.034 ± 0.024	+0.013 ± 0.035
0.222 Mev - 0.100 Mev	-0.005 ± 0.038	+0.015 ± 0.055

If a spin of 2 is considered for level D as has been proposed by Murray et al., and Alaga et al., the correlation results show that level F can only be assigned spin 3. When the experimental values of A_2 and A_4 are plotted on the mixture curve (Figure 33) for the sequence 3(D,Q)2(Q)0 the mixture in the 0.068 Mev gamma ray is (89 ± 1% D, 11 ± 1% Q). This is in fair agreement with the E1 assignment for the 0.068 Mev gamma ray which was made on the basis of the conversion data. When level D is

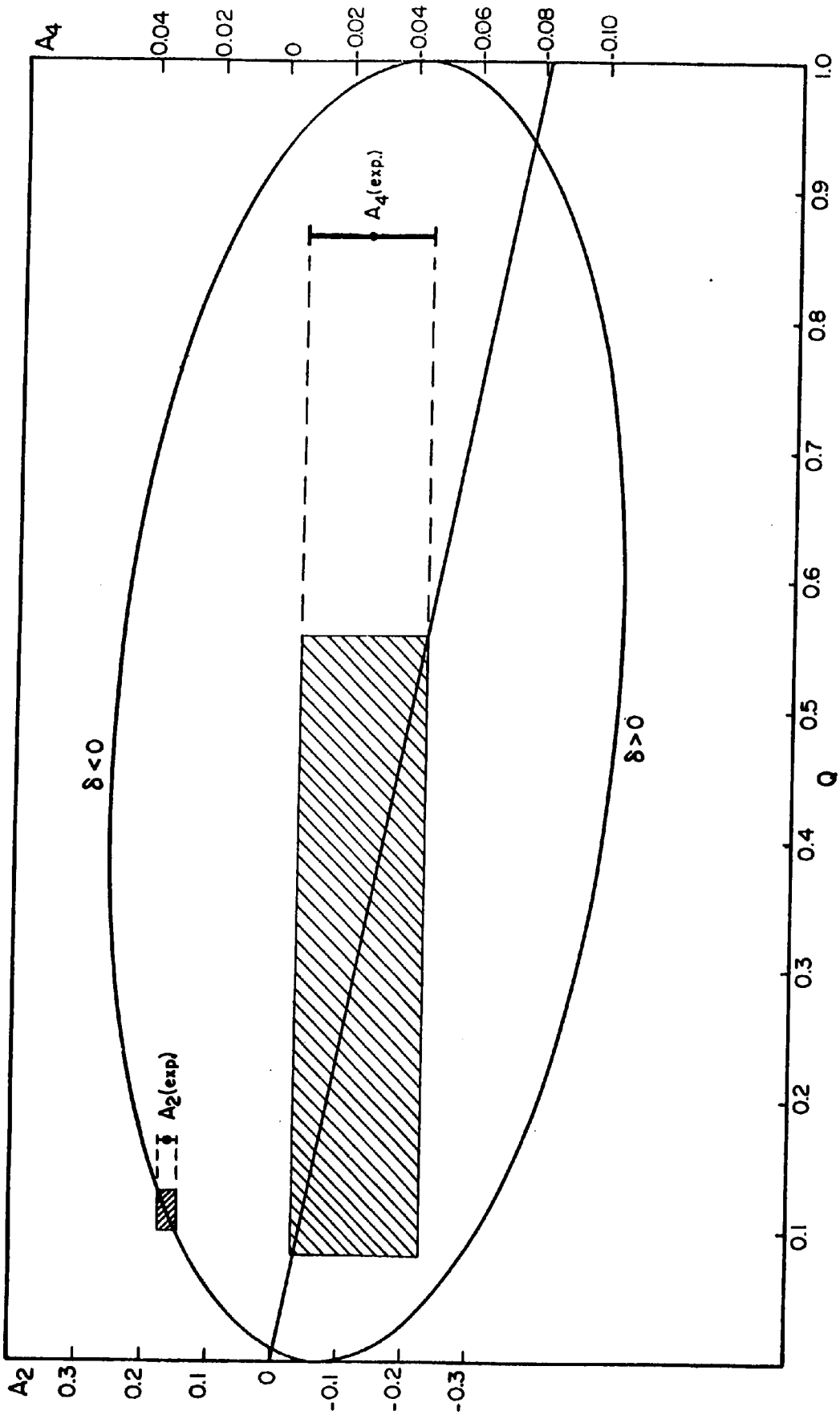


Figure 33. A_2 and A_4 Vs. Q for a 3(D,Q)2(Q)0 Sequence.

assigned spin 2, the correlation data is not in agreement for level F to be assigned either spins 1 or 2. However, if the error on the experimental value of A_4 were twice as large as was found, a spin of 2 would be in agreement with the correlation data. In this case the 0.068 Mev gamma ray would consist of a quadrupole mixture of approximately 1%. Since there is a quadrupole transition observed from state F to the ground state (spin 0), neither spin 0 nor spin 4 is considered as a possibility for state F.

The consideration of level D as a spin 2 state is in agreement with the conversion data which shows the 1.222 Mev radiation to be more like E2 than either M1 or E1. A spin of 3 for level D would be in complete disagreement with the observed intensities for the gamma rays originating from this level. If level D is assigned spin 3, the 1.222 Mev gamma transition would be octupole in character. A strong transition from state D to state C would be expected. Such a transition has not been observed. The following "pure" cascades connecting states F, D, and A are listed in Table XI for the case in which state D is considered as spin 1.

TABLE XI

"PURE" CASCADES CONNECTING STATES F, D, AND A - D IS CONSIDERED AS SPIN 1

Sequence	A_2
1(D)1(D)0	-0.250
2(D)1(D)0	+0.050
3(Q)1(D)0	-0.071

None of these spin sequences is consistent with the correlation data. If spin 1 is assigned to state D and mixtures are considered for the 0.068 Mev gamma ray, a spin of 1 to state F results in the following quadrupole content for the 0.068 Mev radiation. 8-9%Q or 91-92%Q. An assignment of spin 2 to level F under the same circumstances results in the following quadrupole content for the 0.068 Mev radiation. 3%Q or 99%Q.

Interference

The channel which accepted the 0.068 Mev gamma ray undoubtedly accepted some X-rays which are produced by the low energy gamma rays that are strongly converted. The coincidences between these X-rays and the 1.222 Mev gamma rays add a symmetric component to the correlation function. The observed value of A_2 would be less than the "true" value, therefore making the anisotropy of the correlation function less than the "true" value.

Directional Correlation of 0.152 Mev - 1.222 Mev Gamma Rays

One discriminator was set integrally on the 1.222 Mev gamma ray, while the second discriminator was set with a narrow window on the 0.152 Mev gamma ray. Again the base line of the discriminator selecting the 1.222 Mev gamma ray was set high on the 1.222 Mev peak to prevent other high energy radiations from interfering. The result of this correlation corrected for solid angle is

$$W(\theta) = 1 - (0.037 \pm 0.012) P_2 + (0.003 \pm 0.018) P_4$$

The least squares curve and the experimental points are shown in Figure 34.

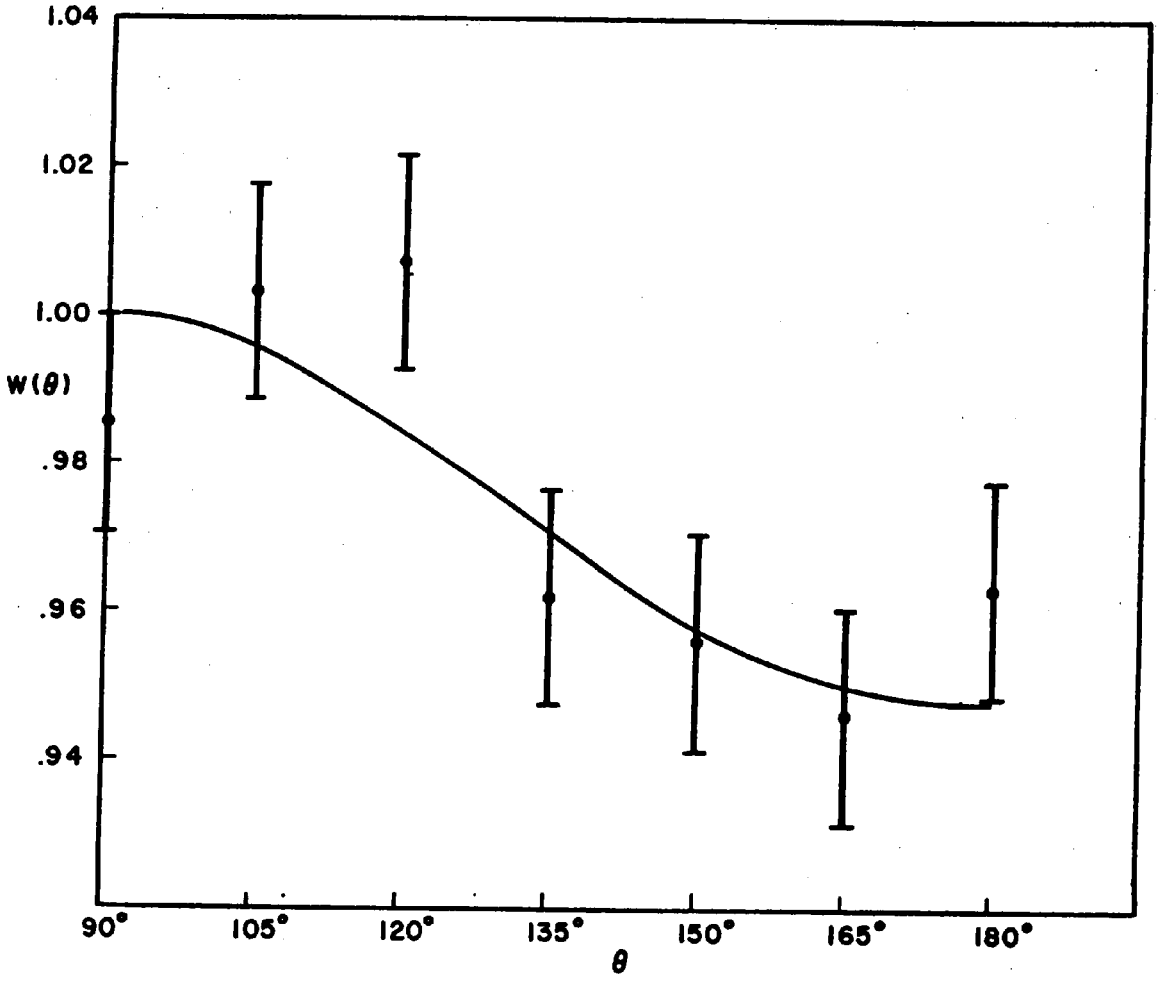


Figure 34. 0.152 Mev - 1.222 Mev Correlation in W^{182}.

When level D is assigned a spin of 2, the datum from the 0.152 Mev - 1.222 Mev correlation measurement shows that only an assignment of spin 3 can be made to level H. The experimental values of A_2 and A_4 plotted on a mixture curve for a 3(D,Q)2(Q)0. (Figure 35) sequence shows the quadrupole content of the 0.152 Mev gamma ray to be less than 0.5%. This is in agreement with the work of Murray et al., which showed the 0.152 Mev radiation to be E1. The sequences 1(D,Q)2(Q)0, 2(D,Q)2(Q)0, are inconsistent with the correlation data. If a spin of 4 is considered for level H, the correlation results for a 4(Q)2(Q)0 sequence should be observed. [A_2 = +0.102 and A_4 = +0.009.] This is in disagreement with the observed values of A_2 and A_4. If however level D is assigned spin 1 instead of spin 2, then level H is consistent with the correlation data with an assignment of either spin 1 or 2. In either case the 0.152 Mev radiation could be nearly all dipole or nearly all quadrupole.

Directional Correlation of 0.152 Mev - 1.122 Mev Gamma Rays

One discriminator was set differentially with a narrow window on the 1.122 Mev peak, while the other discriminator was set differentially with a narrow window on the 0.152 Mev peak. The result of this correlation corrected for solid angle is

$$W(\theta) = 1 - (0.010 \pm 0.014) P_2 + (0.013 \pm 0.019) P_4$$

There is a possibility of interference from the strong peak at 1.222 Mev gamma ray. This effect is thought to be small. The results of the combined correlation of the (1.222 Mev, 1.122 Mev - 0.152 Mev) gamma rays also support this assumption.

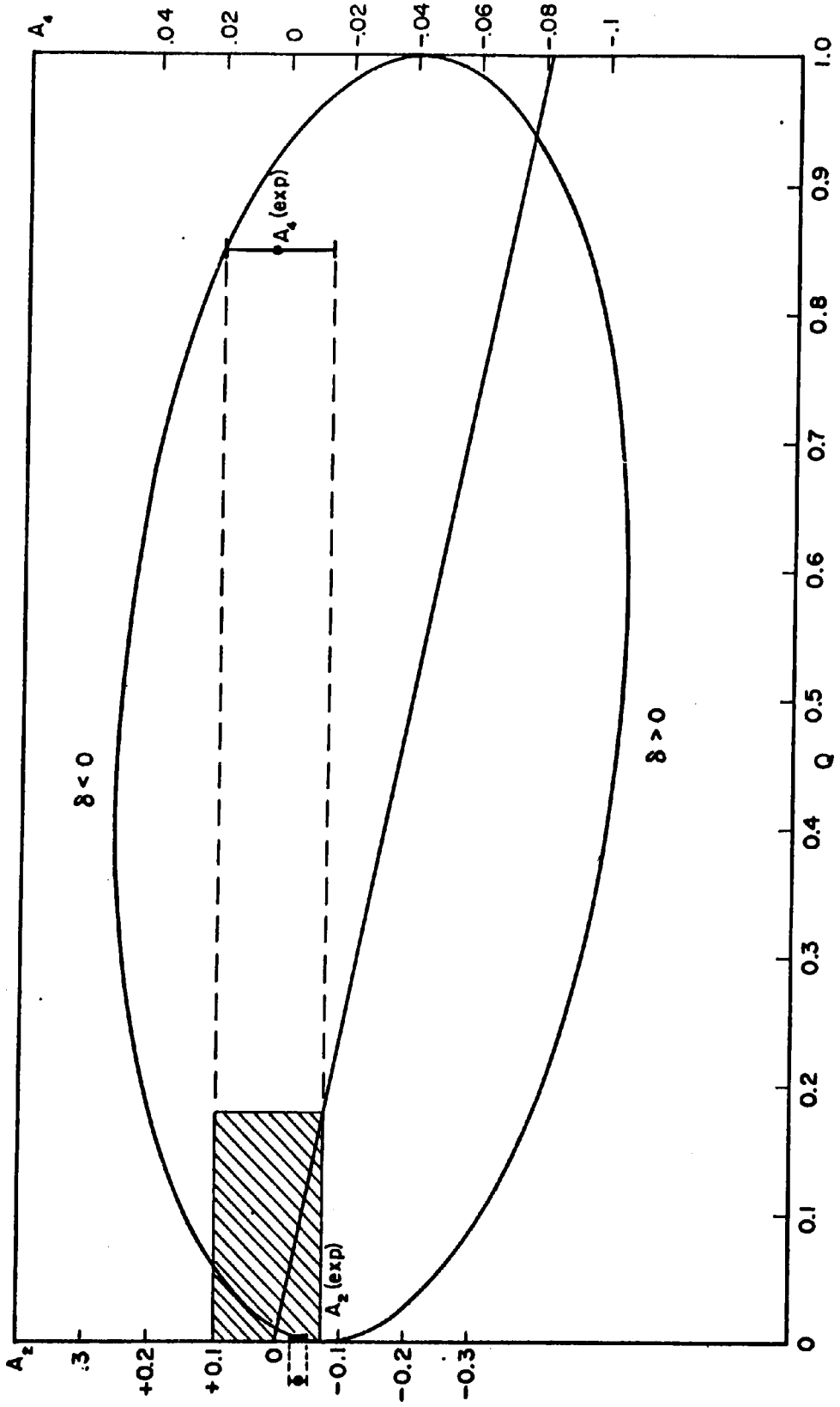


Figure 35. A_2 and A_4 Vs. Q for a 3(D,Q)2(Q)0 Sequence.

Level D has been assigned spin 2 and level H assigned spin 3 as the best possible choices. The spin of state B is undoubtedly 2. This assignment to state B is in agreement with the systematics in this region of the periodic table, and with the E2 character of the 0.100 Mev radiation. The spin sequence involving the 0.152 Mev - 1.122 Mev gamma rays may be written as 3(D,Q)2(D,Q)2. Such double mixture problems can lead to very ambiguous results, especially when the experimental coefficients A_2 and A_4 are small. The complexity of the problem is reduced if the mixture in one of the transitions is known. In this case, the mixture in the 0.152 Mev gamma ray has been determined to be <0.5% quadrupole. The first transition is, therefore, essentially pure dipole and the sequence can be written as 3(D)2(D,Q)2. This sequence is calculated and the experimental values of A_2 and A_4 plotted on the curve. This is shown in Figure 36. The quadrupole content of 3-11% or 94-99% is determined for the 1.122 Mev gamma ray.

Directional Correlation of 0.152 Mev - (1.122 - 1.222) Mev Gamma Rays

One discriminator was set on the 0.152 Mev in an identical manner as used in the two previous correlations involving the 0.152 Mev gamma ray. The window of the discriminator which was used to select the high energy radiation was placed symmetrically across the two high energy peaks. The correlation function for this arrangement corrected for solid angle is

$$W(\theta) = 1 - (0.024 \pm 0.012)P_2 - (0.004 \pm 0.017)P_4$$

Because of the symmetrical setting of the discriminator selecting the high energy radiation, and because the intensities of the

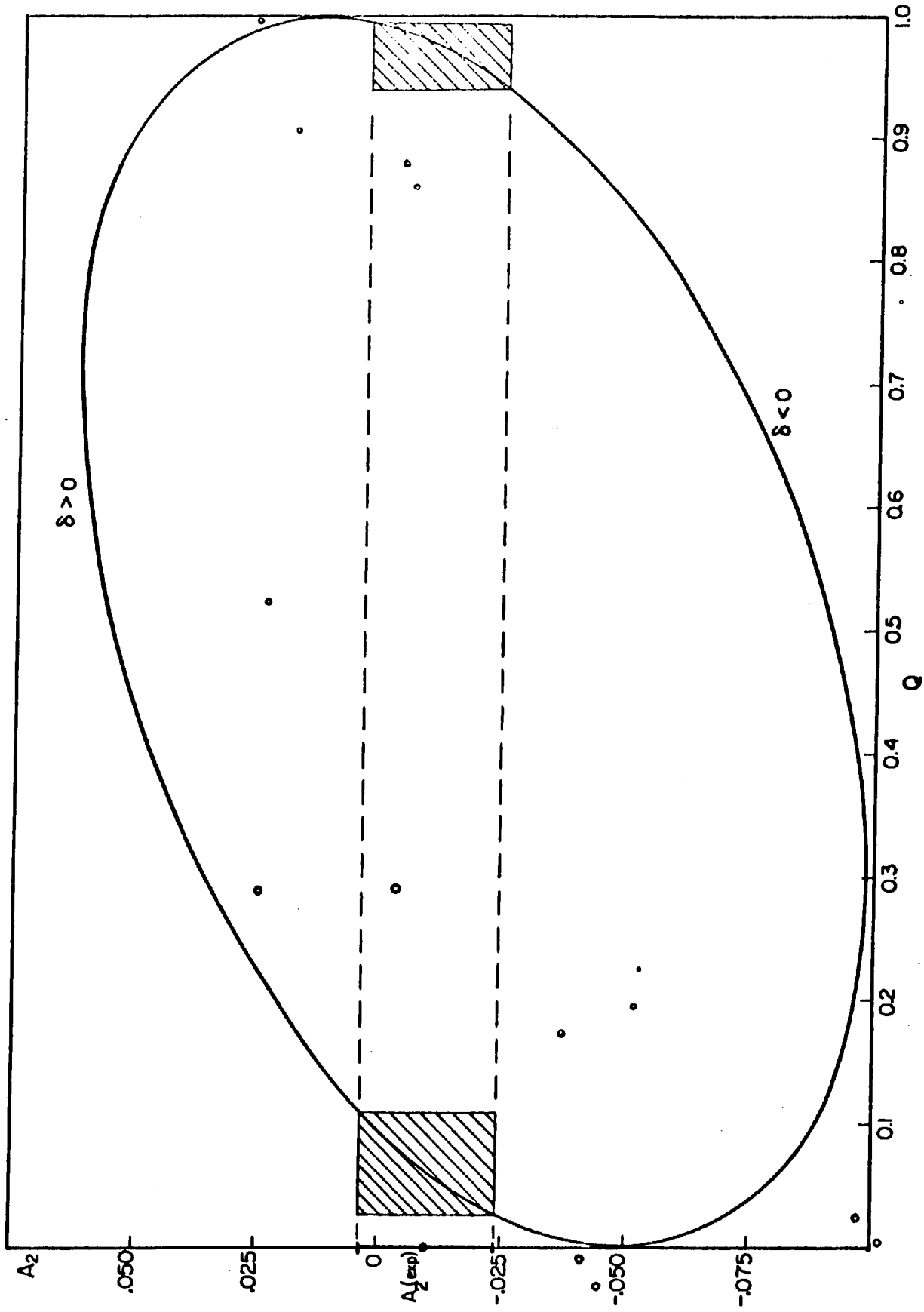


Figure 36. A_2 and A_4 Vs. Q for a 3(D)2(D,Q)2 Sequence.

1.122 Mev and 1.222 Mev gamma rays are approximately the same (Table IX), the above correlation function is considered to be made up of 50% (0.152 Mev - 1.222 Mev) correlation and 50% (0.152 Mev - 1.122 Mev) correlation. If 50% of each of the separate correlations is considered, the combined correlation result is

$$W(\theta) = 1 - (0.023 \pm 0.009)P_2 + (0.008 \pm 0.013)P_4$$

This is in good agreement with the above correlation function which was measured as the sum of these two separate correlation function.

On the basis of these results it appears that the interference from the 1.222 Mev in the (1.122 Mev - 0.152) correlation is not important. The results of the (1.122 Mev - 0.152 Mev) correlation are therefore assumed to be fairly reliable.

Directional Correlation of 0.264 Mev - 1.222 Mev Gamma Rays

One discriminator was set high on the 0.264 Mev peak with a wide window. The other discriminator was set integrally on the high side of the 1.222 Mev peak. The result of this 1-3 correlation, corrected for solid angle is

$$W(\theta) = 1 + (0.076 \pm 0.035)P_2 + (0.016 \pm 0.055)P_4$$

The least squares curve and the experimental points are given in Figure 37.

A. The following discussion concerning the possible spin assignments for state K is based on the assignment of spin 2 for states F and D. The 0.068 Mev gamma ray is nearly pure dipole ($\sim$1) % quadrupole.

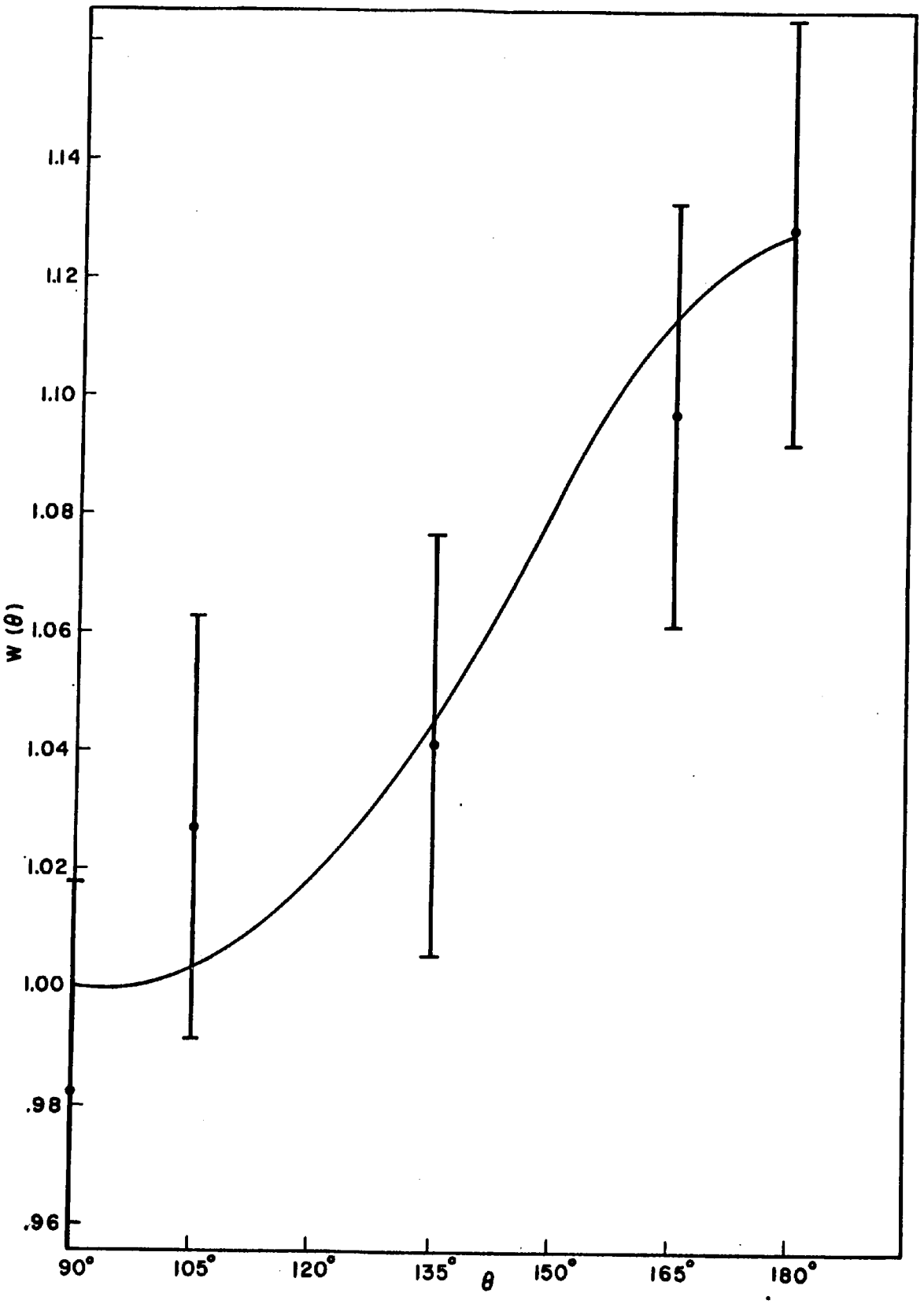


Figure 37. 0.264 Mev - 1.222 Mev Correlation in W^{182}.

Assignment of Spin 5 to Level K: The following sequence for the 1-3 correlation involving levels K, F, D, and A can be formed 5(0)2(D)2(Q)0. The resultant coefficients A_2 and A_4 are $A_2 = +0.893$; $A_4 = +0.003$. The A_2 coefficient is ten times larger than the experimental A_2 and therefore spin 5 is not in agreement with the experimental data. The octupole character for the 0.264 Mev gamma ray would also be in disagreement with the conversion data.

Assignment of Spin 4 to Level K: The sequence 4(Q)2(D)2(Q)0 is in agreement with the correlation data. In this case the theoretical values of A_2 and A_4 are $A_2 = +0.051$; $A_4 = +0.006$. The coefficients for the sequence 4(Q)2(Q)2(Q)0 are $A_2 = -0.022$; $A_4 = -0.002$ which are not in agreement with experimental results. This sequence calls for quadrupole radiation for the 0.068 Mev gamma ray. This would be in disagreement with the conversion data, and therefore the sequence 4(Q)2(Q)2(Q)0 would not be expected to be consistent with the correlation data.

Assignment of Spin 3 to Level K: The sequence 3(D,Q)2(D,Q)2(Q)0 is analyzed for a quadrupole content of 1% in the unobserved 0.068 Mev transition. The sequence then takes the following form 3(D,Q)2(.99D, .01Q)2(Q)0. This sequence is shown in Figure 38.

A spin of 3 to this level is in agreement with the correlation data. However, since the quadrupole content for the 0.264 Mev radiation is determined to be 10^{+10}_{-6}% or 77^{+9}_{-16}%, the results of the spin assignment of 3 to the level K are inconclusive.

Assignment of Spin 2 to Level K: The sequence 2(D,Q)2(D,Q)2(Q)0 is analyzed for a quadrupole content of 1% in the unobserved 0.068 Mev radiation. The sequence then takes the form 2(D,Q)2(.99D, .01Q)2(Q)0.

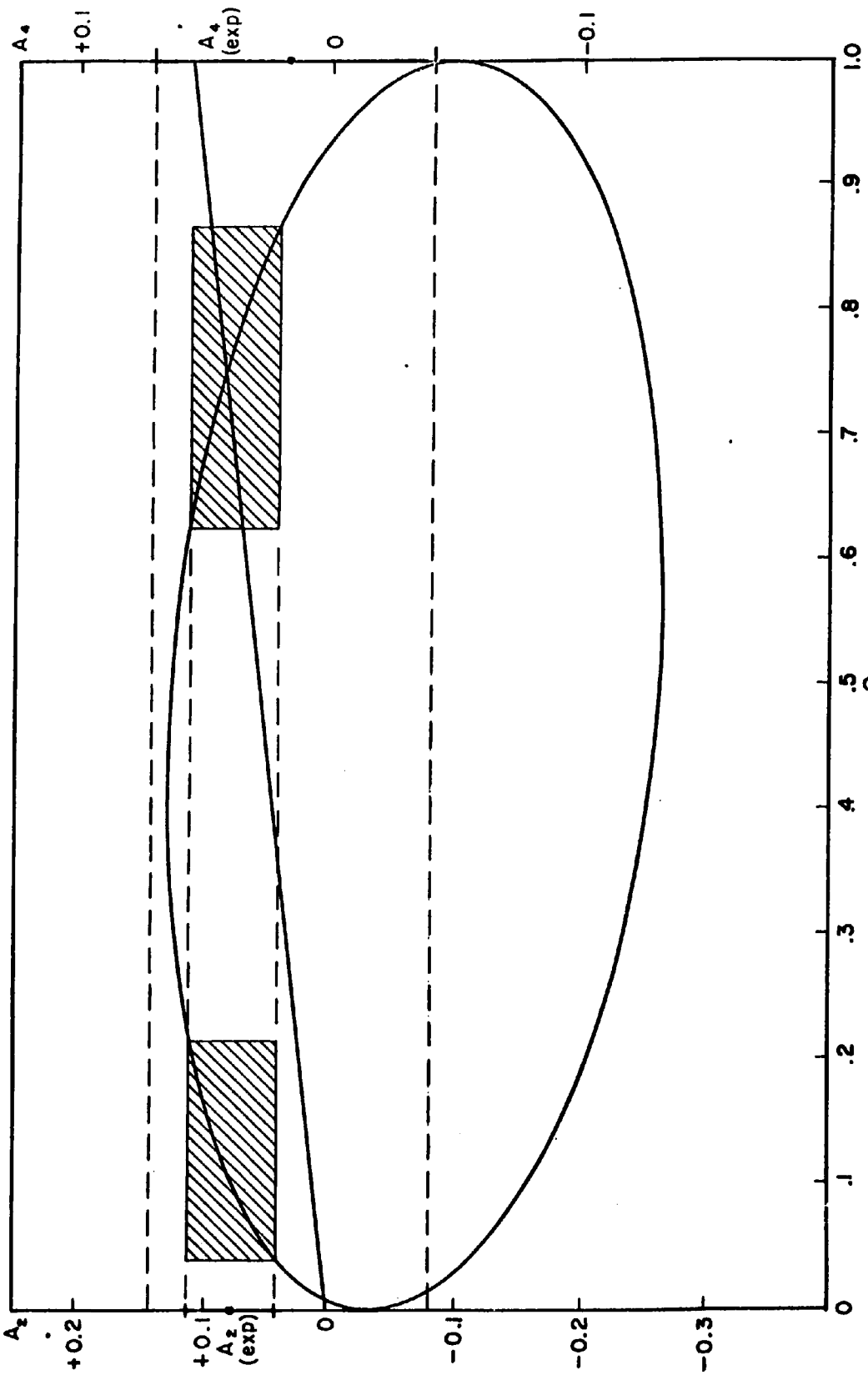


Figure 38. A_2 and A_4 Vs. Q for a 3(D,Q)2(.99D .01Q)2(Q)0 Sequence.

When the experimental values of A_2 and A_4 are plotted on the mixture curve representing the above sequence, no value of quadrupole mixture can be found which is consistent with the correlation data. Therefore a spin of 2 to the K level is not given further consideration.

Due to the transition, (although weak), from level K to level B, and the absence of a transition to level A, spins lower than 2 were not considered.

B. Level F is assigned spin 3 with a 10% quadrupole content for the 0.068 Mev radiation. Table XII gives the values of A_2 and A_4, or the quadrupole content of the 0.264 Mev gamma ray, which are obtained when the experimental values of A_2 and A_4 are plotted on the mixture curves for various assignments of spin to state K.

TABLE XII

VALUES OF A_2 AND A_4, OR THE QUADRUPOLE CONTENT OF THE 0.264 MEV GAMMA RAY, OBTAINED FOR VARIOUS SPIN ASSIGNMENTS TO STATE K

Sequence	Percent of Quadrupole Content	A_2	A_4
5(Q)3(.9D, .1Q)2(Q)0		+0.092	+0.007
4(D,Q)3(.9D, .1Q)2(Q)0	$5.5\ ^{+3.0}_{-2.5}$		
3(D,Q)3(.9D, .1Q)2(Q)0	$7.5\ ^{+2.5}_{-3.0}$		
2(D,Q)3(.9D, .1Q)2(Q)0	$7.0\ ^{+2.5}_{-1.5}$		

The assignment of spin 5 to state K is in agreement with the correlation results. With the assignment of spin 4,3, or 2 to state K, the 0.264 Mev gamma ray is found to be mainly dipole radiation. This is not in agreement with the quadrupole assignment for the 0.264 Mev gamma ray made on the basis of the conversion data.

Directional Correlation of 1.231 Mev - 0.222 Mev Gamma Rays

The discriminators were adjusted so that one accepted the 1.231 Mev gamma ray, while the second discriminator accepted only the 0.222 Mev gamma ray. The result of this correlation corrected for solid angle showed an isotropic function

$$W(\theta) = 1 - (0.012 \pm 0.014)P_2 - (0.001 \pm 0.020)P_4$$

Murray et. al. found the 1.231 Mev gamma ray to be E2 and the 0.222 Mev gamma ray to be E1. If these assignments are assumed to be correct, and in addition if spins of 4, 3, and 2 are assumed for states K, G, and B respectively, the values of A_2 and A_4 can be calculated for a 4(D)3(Q)2 cascade. The results are $A_2 = -0.018$: $A_4 = 0$.

These coefficients are in good agreement with the coefficients obtained in this correlation. The results of this experiment are also in agreement with the conversion data. However, the experimental coefficients are small and since mixture in both transitions is possible, nearly any spin sequence with appropriate mixture in the transitions will give results which are in agreement with experimental results.

Directional Correlation of 1.231 Mev - 0.100 Mev Gamma Rays

One discriminator was adjusted integrally to accept the 1.231 Mev gamma ray. The other discriminator was set with a narrow window on

the 0.100 Mev peak. The result of this correlation corrected for solid angle is

$$W(\theta) = 1 + (0.037 \pm 0.012)P_2 - (0.002 \pm 0.018)P_4$$

The least squares curve and the experimental points are shown in Figure 39.

The experimental coefficients A_2 and A_4 are plotted on the mixture curve 3(D,Q)2(Q)0. Figure 40 gives a quadrupole content of $2 \pm 0.5\%$ for the 1.231 Mev radiation. This mixture is in disagreement with the conversion data which gives the multipolarity of the 1.231 Mev gamma ray as E2. With an error on the A_4 term approximately three times as large as was found, it would be possible to obtain an appreciable quadrupole content (approximately 90% quadrupole).

A spin of 4 for level G might be considered, but the coefficients for a "basic" 4-2-0 sequence are not in agreement with the observed results.

Spins of 1 and 2 for level G are not in agreement with the correlation results. With errors twice as large on the A_4 either sequence 1(D,Q)2(Q)0, 2(D,Q)2(Q)0, would be in agreement with the correlation data. In either sequence the amount of quadrupole mixture in the 1.231 Mev would be between 5-8%. With these sequences errors 2 or 3 times as large on the A_4 term would not lead to a large quadrupole content. It therefore appears that level G should be assigned spin 3.

There is the possibility the (1.231 Mev - 0.100 Mev) correlation has been contaminated by the strongly positive correlation which was obtained for the (1.222 - 0.068 Mev) cascade.

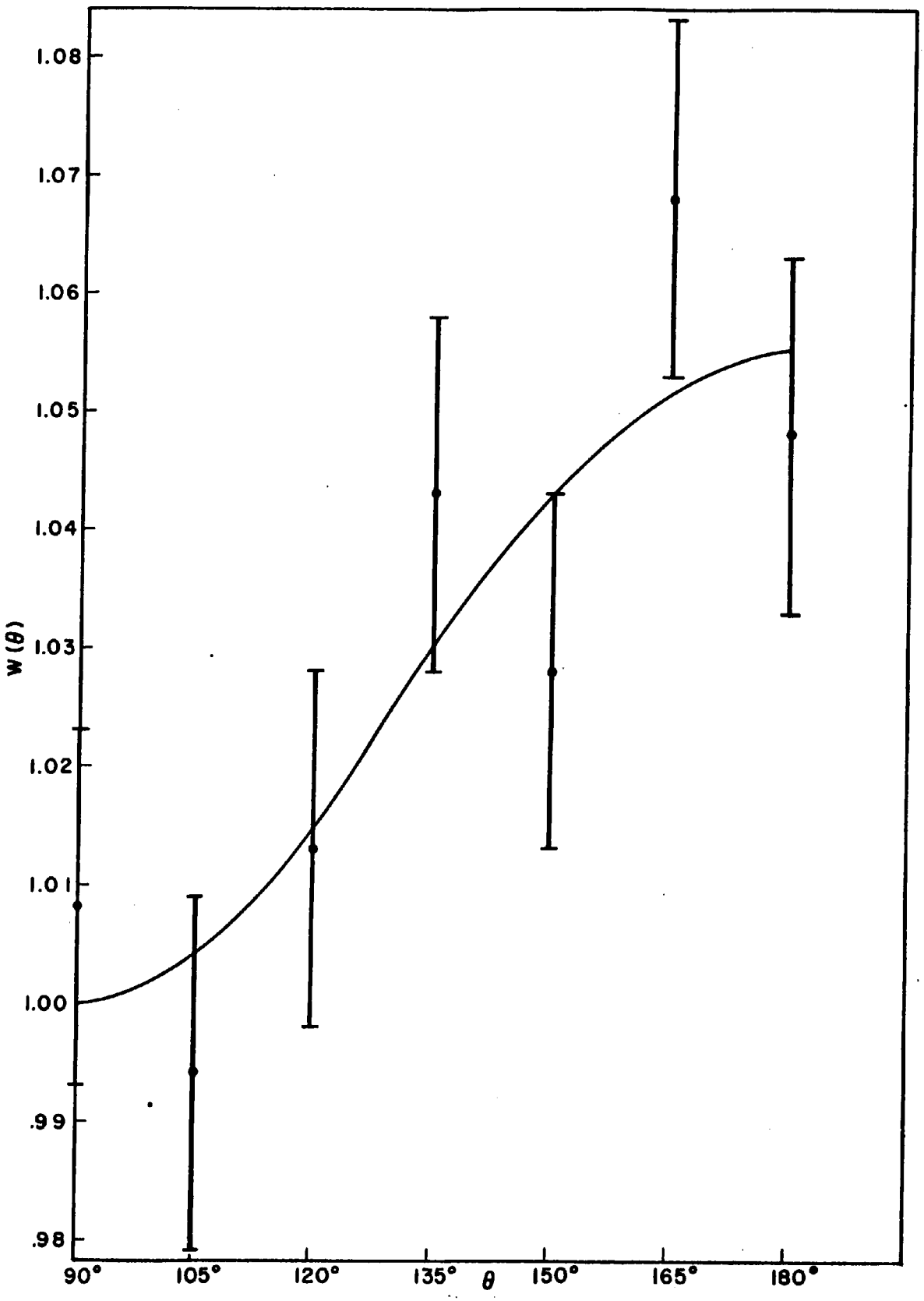


Figure 39. 1.231 Mev - 0.100 Mev Correlation in W^{182}.

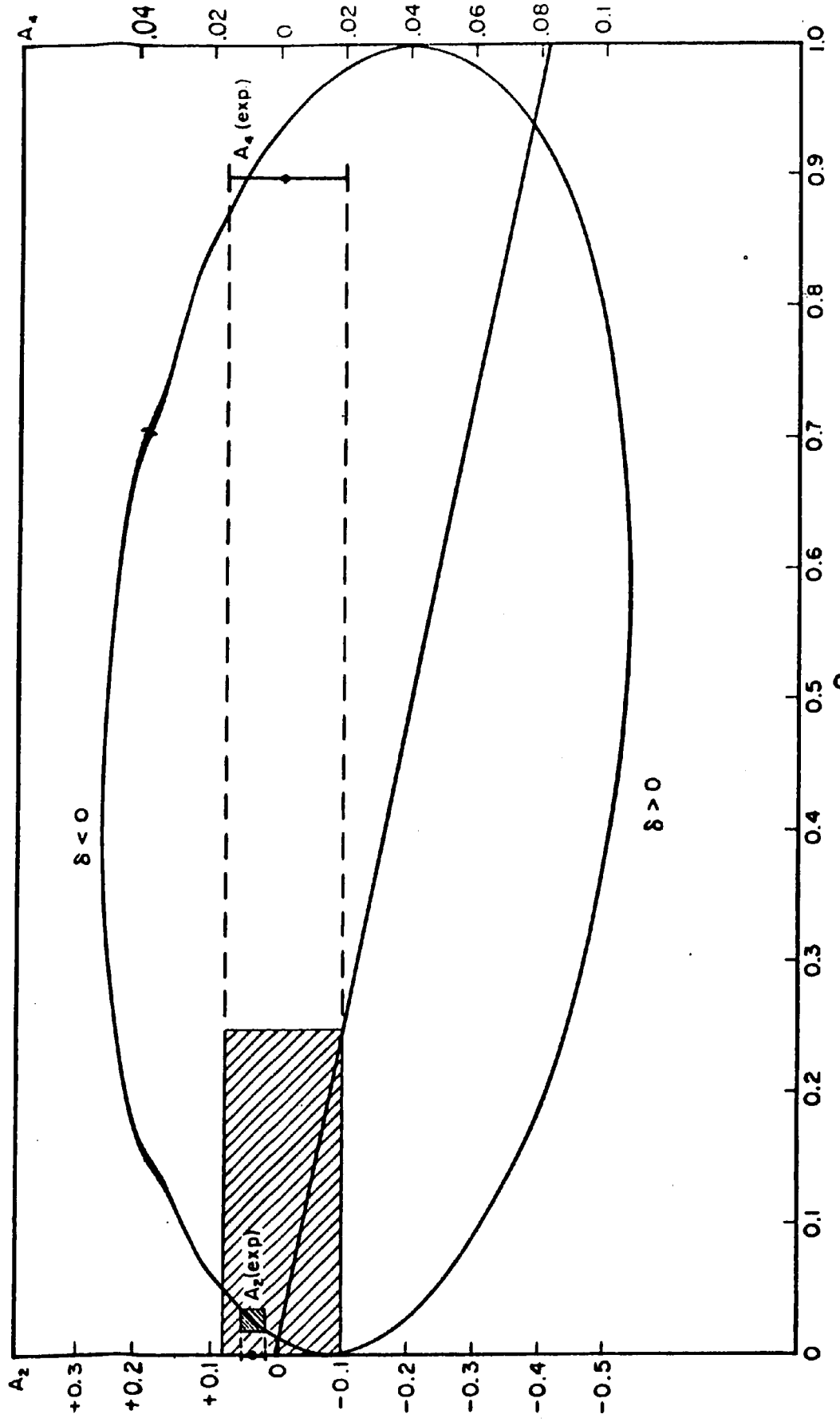


Figure 40. A_2 and A_4 Vs. Q for a 3(D,Q)2(Q)0 Sequence.

Directional Correlation of 0.222 Mev - 0.100 Gamma Rays

One discriminator was set with a narrow window on the 0.222 Mev peak. The second discriminator was set with a narrow window on the 0.100 Mev peak. The result of this correlation corrected for solid angle is

$$W(\theta) = 1 + (0.027 \pm 0.011)P_2 + (0.027 \pm 0.016)P_4$$

Correction was made for the Compton background by first keeping one discriminator on the 0.100 Mev peak and moving the second discriminator out to approximately 0.300 Mev. The counts that were collected in the channel that was setting on the 0.100 Mev peak were normalized to the number of counts collected in this channel in the original set up. The coincidence count was then adjusted by the same factor, and these normalized coincidences were subtracted from the total number of coincidences in the original set up. This was all done at 90°.

One discriminator was moved back to the 0.222 Mev peak, while the other discriminator was set at approximately 0.300 Mev. The same normalizing procedure as given above was carried out, and the coincidence counts subtracted from the total coincidences which were obtained in the original set up at 90°.

The result of these subtractions yields

$$W(\theta) = 1 + (0.034 \pm 0.024)P_2 + (0.013 \pm 0.035)P_4$$

This (0.222 Mev - 0.100 Mev) correlation also contains coincidences from the (0.229 Mev - 0.100 Mev) cascade. The 0.222 Mev and 0.229 Mev gamma rays are of equal intensity so it was assumed the correlation function which was measured contained 50% of the (0.229 Mev - 0.100 Mev)

correlation. After subtracting out this amount from the above correlation function, the resulting correlation function corrected for background and solid angle is

$$W(\theta) = 1 - (0.005 \pm 0.038)P_2 + (0.015 \pm 0.055)P_4$$

Since the coefficients of A_2 and A_4 are small and since the quadrupole content of the unobserved (1.231 Mev) radiation is not known with certainty, no interpretation of this 1-3 correlation was attempted.

Discussion

Interesting observations may be made with regard to the beta transitions from Ta^{182} to the excited states of W^{182}. There are no beta transitions observed from Ta^{182} to states A, B, and C in W^{182}. However, there are strong beta transitions to states F and K, although these beta transitions are much lower in energy than the transitions to states A, B, and C would be. For a given spin value the transitions to the higher excited states would be expected to proceed with probabilities much less than for the higher energy transitions.

Other interesting observations concern the gamma transitions occurring from states D, F, and G. These transitions are either pure quadrupole, or have a large quadrupole content, although dipole radiation is allowed (equation 1.5). The absence of an E2 transition of 893 kev from level D to the 4+ state at 329 kev seems unusual. It is concerning such observations (relative transition rates to various members of a nuclear rotational band) that the model for deformed nuclei makes precise predictions.

W^{182} with its 74 protons and 108 neutrons is expected to exhibit properties of deformed nuclei. Both the neutrons and protons are far away from the shell which closes with 82 particles.

The transition probability formulas of Chapter IV might be expected to be appropriate. The experiment transition probability ratios which appear in the next section (Tables XIII, XIV, and XV) are based on the relative intensities of the gamma rays obtained by Murray et al.

Considerations of Reduced Transition Probabilities

TABLE XIII

COMPARISON OF THE INTENSITIES OF TRANSITIONS FROM THE THIRD EXCITED STATE TO THE SECOND AND FIRST EXCITED STATES, $[B(2\rightarrow I_f)]$, WITH THE INTENSITY OF THE TRANSITION FROM THE THIRD EXCITED STATE TO THE GROUND STATE, $[B(2\rightarrow 0)]$, FOR VARIOUS VALUES OF K_i-E2 RADIATIONS HAVE BEEN ASSUMED FOR ALL THE TRANSITIONS.

Final State I_f	Experimental $\frac{B(2\rightarrow I_f)}{B(2\rightarrow 0)}$	Theoretical $B(2\rightarrow I_f) / B(2\rightarrow 0)$ $K_i = 0$	$K_i = 1$	$K_i = 2$
2+ 100 kev	1.61 ± 0.34	1.43	0.36	1.43
4+ 330 kev	not observed	2.57	1.14	0.07

TABLE XIV

COMPARISON OF THE INTENSITY OF THE TRANSITION FROM LEVEL G TO LEVEL C, [B(3→4)], WITH THE INTENSITY OF THE TRANSITION FROM LEVEL G TO LEVEL B, [B(3→2)], FOR VARIOUS VALUES OF K_i. E2 RADIATIONS HAVE BEEN ASSUMED FOR ALL THE TRANSITIONS.

Final State I_f	Experimental $\frac{B(3\rightarrow I_f)}{B(3\rightarrow 2)}$	Theoretical $K_i = 0$	$B(3\rightarrow I_f) / B(3\rightarrow 2)$ $K_i = 1$	$K_i = 2$
4+		B(3 4) = 0		
330 kev	0.48	B(3 2) = 0	2.50	0.40

If the quantum numbers for state D are now considered as I = K = 1, the reduced transition probability ratio becomes

$$\frac{B(1\rightarrow 2)}{B(1\rightarrow 0)} = 0.50 \qquad \text{(L = 1 Transitions)}$$

This is to be compared with the experimental ratio of 1.36

If I = 1, K = 0 for this state, the theoretical ratio would be equal to 2.00.

If level G is assumed to be spin 2 the reduced transition probability ratio $B(2\rightarrow 4) / B(2\rightarrow 2)$ for given values of K is given in Table XV. E2 transitions have been assumed for all the transitions.

TABLE XV

COMPARISON OF THE INTENSITY OF THE TRANSITION FROM LEVEL G TO LEVEL C, [B(2→4)], WITH THE INTENSITY OF THE TRANSITION FROM LEVEL G TO LEVEL B, [B(2→2)], FOR VARIOUS VALUES OF K_i. E2 RADIATIONS HAVE BEEN ASSUMED FOR ALL THE TRANSITIONS.

Final State I_f	Experimental $\frac{B(2\rightarrow I_f)}{B(2\rightarrow 2)}$	Theoretical $B(2\rightarrow 4) / B(2\rightarrow 2)$ $K_i = 0$	$K_i = 1$	$K_i = 2$
4+				
330 kev	≈ 0	1.80	3.20	0.05

The conversion data of Murray et al., show the 100 kev transition from states B to A to be E2, resulting in a 2+ assignment to state B (all even-even nuclei have ground state spin 0). Level C being assigned 4+ is in agreement with the E2 assignment which was made on the basis of the conversion data. If the energy separation between the ground state and first excited state is used to compute the next excited state (4+) according to Equation (4.4), the 4+ level is found to occur at 333.3 kev. This is in good agreement with the observed value of 329.4 kev. Therefore, it appears that the ground state and first two excited states make up the "ground state rotational band."

On the basis of the conversion data, the level at 1.222 Mev (state D) is assigned spin 2.

When spin 2 is assigned to level D, the value of K = 2 is in best agreement with the transition probability ratios.

Level G, was found from correlation results to have most probable spin of 3. The energy separation of 110 kev between levels G and D

is approximately the same separation as is found between the first excited state and the ground state. Also since levels G and D appear to be characterized best by spins of 3 and 2 respectively, it appears that these two levels belong to a second rotational band with K = 2. Since the 1.222 Mev gamma ray appears to be E2 radiation, the positive parity assignment is made to level D. (In a rotational band the parity of all levels is the same, therefore, the parity of level G is also positive.) This band may represent a "γ vibrational band" which was mentioned in Chapter IV.

Spins of 2 or 3 have been found, from the correlation results, as the most probable assignments for level F. The spin of 3 is in best agreement with the correlation results. However, as was mentioned earlier, the experimental value of A_4 would not have to be changed a great deal in order for spin 2 to be in agreement with the correlation results. In this latter case the 0.068 Mev transition between levels F and D would be nearly pure dipole ($\sim$ 1% quadrupole). The assignment of spin 2 to level F is in best agreement with the conversion coefficient measurements. The correlation results give the spin assignment of 3 to level H. The 0.152 Mev gamma ray between levels H and D was found to be mainly dipole radiation ($<$ 0.5% quadrupole). The energy separation of 85 kev between levels H and F is only about 15% different than the 100 kev separation between levels A and B. Therefore, it appears that levels F and H may belong to a third rotational band. Since both the 0.152 Mev and 0.068 Mev gamma rays have been assigned as E1 transitions on the basis of the conversion coefficients, negative parity is assigned to both levels F

and H. Alaga et al., assigned a K value of 2 to these states. Using the observed separation of 85 Kev between states H and F, the next excited state in this band is found at 141.7 kev above state F (equation 4.4).

State J is 114 kev above level F and was therefore assigned by the previous investigators as the 4-member of the same band F and G belong to. Since the parity of this band is negative, the possibility exists that this band is an octupole vibrational band (chapter IV).

There were no directional correlation measurements carried out which involved level J. This was due to the fact that there would have been too great an influence from other correlations to arrive at any reliable results.

Murray et al. assigned the spin and parity as 4 - to state K, with an E2 assignment for the 0.264 Mev gamma ray. Alaga et al. assigned a K value of 4 to this state. The correlation datum is in agreement with the assignment of spin 4 to state K. The 0.264 Mev gamma would be "pure" quadrupole radiation. The correlation data also shows that spins of 3 and 5 could be assigned to state K.

Conclusions

The results of directional correlation measurements are in agreement with the mutlipolarities of the gamma rays which were determined by Murray et al. on the basis of conversion coefficient measurements. There is only one case where there is disagreement. Murray et al. listed the 1.231 Mev gamma ray as an E2 transition. From the correlation data the 1.231 Mev gamma ray appears to be mainly dipole radiation

($2 \pm 0.5\%$ Q). However, it has been mentioned that the error of A_4 would only have to be made larger by a factor of 2 or 3 in order to have the mixture curve show an appreciable quadrupole content ($\sim 90\%$ Q). The correlation data is also in agreement with the spins given to the excited states by Alaga et al., on the basis of the collective model for spheroidal nuclei. The only exception to this is the spin assignment found from correlation results for level F. This has been discussed above. In W^{182} there exists a ground state rotational band (K = 0) with three members. Two "rotational - vibrational" bands also appear. There are two members of the K = 2 even parity band, and three members of the K = 2 odd parity band. The even parity band might be classified as a γ vibrational band (quadrupole - vibration). The odd parity band might be classified as an "octupole" vibrational band.

The highest excited state had been given the quantum numbers (4, 4, -). The correlation data is in agreement with this, but also is in agreement with the assignment of spin of 3 or 5 to this state.

These higher excited states which have been classified as vibrational states can equally well be purely "particle excitation" levels.

The most definite evidence for the vibrational character of the bands would be life-time measurements of the levels. If the lifetimes were found to be substantially shorter than predicted by the individual particle lifetime formulas, this would constitute strong evidence for some vibrational character for the levels. Such measurements by ordinary electronic techniques seems impossible, as the expected lifetimes are so short. The theoretical calculated mean lifetimes for an E2 transition

from the (2, 3 +) state at 1.331 Mev; single proton transition to the (0, 2 +) state at 0.100 Mev would be approximately 10^{-12} seconds. The same transition if considered as a single phonon (vibrational transition) would have a mean lifetime of 10^{-14} seconds.

Alaga et al., in their discussion of the decay scheme of Ta^{182} cite as possible evidence for the γ - vibrational character of the band at 1.222 Mev the fact that the rotational moment of inertia for the band is slightly ($\sim$ 10%) smaller than that for the ground state rotational band, where as a particle - excitation level generally has a greater rotational moment of inertia.

Speculation might arise as to why no K = 0 bands associated with quadrupole and octupole vibrations are observed in the decay of Ta^{182}, while there are observed bands with K = 2. Murray et al. labeled level E as having spin and parity value of 1-. This state may be a K = 0 state. Such a state has been found in Sm^{152}. From the proposed decay scheme it seems reasonable to assign I = K = 2 or 3 to the ground state of Ta^{182}. [The ground state of Eu^{154} was found to be a (3, 3, -) state.](69) The beta transitions leading to the ground state rotational band members would then be expected to be weak and the log ft values high. Higher lying states with low spin and K = 0 would also be populated very weakly by beta transitions, so that radiations from such states probably would have been too weak to be observed. Similar arguments apply when the possible population of high - lying K = 0 states by gamma radiation from the K = 2 bands is considered. For instance, a hypothetical (0, 1, -) state around 1 Mev excitation energy might be fed by dipole or quadrupole

radiation from the higher excited states. The dipole radiation would be very weak due to K - forbiddenness and the quadrupole radiations to this state would be reduced owing to the competition for the quadrupole radiations by the ground state rotational band. The same type of arguments apply when other members of the high - lying K = 0 bands are considered.

BIBLIOGRAPHY

1. Reines, F. and Cowan Jr., C. L., Physics Today, August (1957).
2. Hamilton, D. R., Phys. Rev., 50, 122 (1940).
3. Brady, E. L. and Deutsch, M., Phys. Rev. 72, 870 (1947).
4. Brady, E. L. and Deutsch, M., Phys. Rev. 74, 154 (1948).
5. Brady, E. L. and Deutsch, M., Phys. Rev. 78, 558 (1950).
6. Deutsch, M. and Metzger, F., Phys. Rev. 74, 1542 (1948).
7. Metzer F. and Deutsch, M., Phys. Rev. 78, 551 (1950).
8. Condon, E. U. and Shortley, G. H., The Theory of Atomic Spectra (Cambridge), 1951.
9. Blatt, J. M. and Weisskoff, V. F., Theoretical Nuclear Physics (John Wiley and Sons, Inc.), 1952.
10. Frauenfelder, H., Beta and Gamma Ray Spectroscopy, edited by K. Siegbahn, (North-Holland Publishing Co.), 1955.
11. Biedenharn, L. C. and Rose, M. E., Rev. Mod. Phys. 25, 729 (1953).
12. Falkoff, D. L. and Uhlenbeck, G. E., Phys. Rev. 79, 323 (1950).
13. Falkoff, D. L. and Uhlenbeck, G. E., Phys. Rev. 79, 334 (1950).
14. Falkoff, D. L., Doctoral Dissertation, University of Michigan (1948), unpublished.
15. Goertzel, G., Phys. Rev. 70, 897 (1946).
16. Gardner, J. W., Proc. Phys. Soc. (London) A62, 763(1949).
17. Ling, D. S., and Falkoff, D. L., Phys. Rev. 76, 1639 (1949).
18. Racah, G., Phys. Rev. 84, 910 (1951).
19. Fano, U., Phys. Rev. 90, 577 (1953); National Bureau of Standards Report 1214.
20. Lloyd, S. P., Phys. Rev. 85, 904 (1952).
21. Alder, K., Helv. Phys. Acta. 25, 235 (1952).

22. de Groot, S. R., Physica 18, 1201 (1952).

23. Coester, F., and Jauch, J. M. Helv. Phys. Acta 26, 3 (1953).

24. Coester, F., Phys. Rev. 93, 1304 (1954).

25. Abragam, A. and Pound, R. V., Phys. Rev. 89, 1306 (1953).

26. Pound, R. V., and Abragam A., Phys. Rev. 90, 993 (1953).

27. Abragam, A. and Pound, R. V., Phys. Rev. 92, 943 (1953).

28. Coester, F., Phys. Rev. 93, 1304 (1954).

29. Abragam, A. and Pound, R. V., Phys. Rev. 89, 1306 (1953).

30. Pound, R. V. and Abragam, A., Phys. Rev. 90, 993 (1953).

31. Hemmig, W. and Steffen, R. M., Phys. Rev. 92, 832 (1953).

32. Simon, A., Oak Ridge National Laboratory Report 1718 (1954).

33. Simon, A., VanderSluis, J. H. and Biedenharn, L. C., Oak Ridge National Laboratory Report 1679 (1954).

34. Biedenharn, L. C. and Rose, M. E., Rev. Mod. Phys. 25, 746 (1953).

35. Ferentz, H. and Rosezweig, N., Argonne National Laboratory Report 5324 (1954).

36. Coester, F., Argonne National Laboratory Report 5316 (1954).

37. Biedenharn, L. C., Arfken, G. B. and Rose, M. E., Phys. Rev. 83, 586 (1951).

38. Arfken, G. B., Biedenharn, L. C. and Rose, M. E., Phys. Rev. 86, 761 (1952).

39. Satchler, G. R., Phys. Rev. 94, 1304 (1954).

40. Rose, M. E., Phys. Rev. 91, 610 (1953).

41. Schiff, L. I., Phys. Rev. 50, 88 (1936).

42. Frankel, S., Phys. Rev. 83, 673 (1951).

43. Church, E. L. and Kraushaar, J. J., Phys. Rev. 88, 419 (1952).

44. Lawson, Jr., J. L. and Frauenfelder, H., Phys. Rev. 91, 649 (1953)

45. Howland, P. R. and Kreger, W. E., Phys. Rev. 95, 407 (1952).

46. Davisson, C. M. and Evans, R. D., Rev. Mod. Phys. 24, 79 (1952).

47. Arns, R. G., Private communication.

48. Morton, G. A., Nucleonics 10, No. 3 (1952).

49. Kelly, W. H., Thesis, University of Michigan (1955) unpublished.

50. Moskowitz, S. and Racker, J., Pulse Techniques (Prentice Hall Inc.) 1953.

51. Garwin, R. L., Rev. Sci. Instr. 21, 569 (1950).

52. Garwin, R. L., Rev. Sci. Instr. 24, 618 (1953).

53. Stewart, M. G., Thesis, University of Michigan (1955) unpublished.

54. Scharenberg, R. P., Thesis, University of Michigan (1955) unpublished.

55. Alaga, G., Alder, K., Bohr, A. and Mottelson, B. R., Kgl. Danske Uidenskab Selskab, Mat-fys. Medd. 29, No. 9 (1955).

56. Bohr, A., Rotational States of Atomic Nuclei, (Ejnar Munksgaard, Copenhagen), 1954.

57. Alder, K., Bohr, A., Huus, T., Mottelson, B. R. and Winther, A., Revs. Modern Phys. 28, 432 (1956).

58. Moszkowski, S. A., Handbuch der Physik, vol XXXIX.

59. Bohr, A. and Mottelson, B. R. Kgl. Danske Videnskab Selskab, Mat-fys. Medd. 27, No. 16 (1953).

60. Nathan, O., Nuclear Physics 4, No. 1 (1957).

61. Rasmussen, J. O., Stephens Jr., F. S., Strominger, D. and Aström, B., Phys. Rev. 99, 47 (1955).

62. Bohr, A., Mottelson, B. R., Beta and Gamma Ray Spectroscopy, edited by K. Siegbahn, (North-Holland Publishing Co.), 1955.

63. Cork, J. M., Brice, M. K., Helmer, R. G. and Sarasan, D. E., Phys. Rev. 107, 1621 (1957).

64. Juliano, J. O. and Stephens Jr., F. S., Phys. Rev. 108, 341 (1957)

65. Grodzins, L., (private communication) as reported by Cork et. al.(63)

66. Ofer, S., Nuclear Physics 4, No. 3 (1957).

67. Lide, R. W., (private communication).

68. Sliv, L. A. and Band, I. M., Coefficients of Internal Conversion of Gamma Radiation Part I, K-Shell, Lenigrad Physics - Technical Inst., 1956.

69. Abraham, M., Kedzie, R. and Jeffries, C. D., Phys. Rev. 108, 58(1957).

70. Muller, D. E., Hoyt, H. C., Klein, D. J. and Dumond, J. W. M., Phys. Rev. 88, 775 (1952).

71. Cork, J. M., Childs, W. J., Branyan, C. E., Rutledge, W. C. and Stoddard, A. E., Phys. Rev. 81, 642 (1951).

72. Mihelich, J. W., Phys. Rev. 95, 626 (1954).

73. Fowler, C. M., Kruse, H. W., Keshishian, V., Klotz, R. J. and Mellor, G. P., Phys. Rev. 94, 1082 (1954).

74. Dumond, J. W. M., Hoyt, H. C., Marmier, P. E. and Murray, J. J., Phys. Rev. 92, 202 (1953).

75. Murray, J. J., Boehm, F., Marmier, P. E. and Dumond, J. W. M., Phys. Rev. 97, 1007 (1955).

76. Sumbaev, O. I., Soviet Physics JETP 5, 170 (1957).

77. Bäckström, Arkiv-Fysik 10, 387 (1956).

78. Boehm, F., Marmier, P. E. and Dumond, J. W. M., Phys. Rev. 95, 864 (1954).